Localization of plasmid DNA in living *Streptomyces lividans* mycelium

Dissertation

der Mathematisch-Naturwissenschaftlichen Fakultät

der Eberhard-Karls-Universität Tübingen

zur Erlangung des Grades eines

Doktors der Naturwissenschaften

(Dr. rer. nat.)

vorgelegt von

Linkon Paul

aus Chattogram, Bangladesch

Tübingen

2024

Gedruckt mit Genehmigung der Mathematisch-Naturwissenschaftlichen Fakultät der Eberhard-Karls-Universität Tübingen.

Tag der mündlichen Qualifikation:	22.11.2024
Dekan:	Prof. Dr. Thilo Stehle
1. Berichterstatter/-in:	Dr. rer. nat. Günther Muth
2. Berichterstatter/-in:	Prof. Dr. rer. nat. Heike Brötz-Oesterhelt

To my supervisor, all the teachers and parents

Declaration

I declare that this dissertation, entitled “Localization of plasmid DNA in living *Streptomyces lividans* mycelium” is my own work and all the sources I have used had been indicated or noted in the list of references.

Table of Contents

A. Zusammenfassung

Das Gram-positive Bodenbakterium *Streptomyces* wächst durch apikale Spitzenverlängerung und bildet ein mehrfach verzweigtes Myzel. Diese Wachstumsform stellt ein Problem für die richtige Verteilung des genetischen Materials, d.h. des Chromosoms und der Plasmide, dar. Bislang war die Position eines Plasmids in einem myzelialen Organismus nicht bestimmt worden.

Um die Lokalisierung des *single-copy* Plasmids SCP2 im lebenden *S. lividans*-Myzel im Vergleich zu der des Chromosoms zu klären, wurde ein fluoreszierendes Repressor-Operator-System (FROS) eingesetzt. Ein aus 120 Bindungsstellen bestehender *tetO*-Array wurde in ein bifunktionelles SCP2-Derivat (SCP2tetO) eingefügt oder in den zentralen Teil (nt. 5327700) des *S. lividans*-Chromosoms integriert. Die Integration eines Gens, das für ein TetR-mCherry-Fusionsprotein kodiert, führte zu hellen Fluoreszenzfoci, die die Positionen der einzelnen Kopien des Plasmids oder des mit dem *tetO*-Array markierten Bereich des Chromosoms anzeigten.

Standbilder von Hyphen und Zeitrafferaufnahmen von SCP2tetO und dem Chromosom zeigten ein sehr ähnliches Lokalisierungsmuster, wobei die spitzennahe Kopie immer der Spitze in einem konstanten Abstand von 2.21µm; ± 0.99µm (SCP2tetO) und 3.69µm; ± 2.86µm (Chromosom) folgte. Das Lokalisierungsmuster von SCP2tetO hing von dem ParAB$_{SCP2}$-Verteilungssystem ab. Die Deletion von *parA*$_{SCP2}$ reduzierte die Anzahl der sichtbaren Plasmid-Spots. Diese Spots hatten eine höhere Fluoreszenzintensität als die des Elternplasmids SCP2tetO, was darauf hindeutet, dass sich die Plasmidkopien nach der Replikation in Abwesenheit von *parA*$_{SCP2}$ nicht trennen konnten. Darüber hinaus schien ParAB$_{SCP2}$ für die Verankerung von SCP2tetO an Verzweigungsstellen und Hyphenspitzen erforderlich zu sein, da SCP2tetOΔ*parA* nur sehr selten an Verzweigungsstellen und Spitzen nachgewiesen wurde.

Das FROS-System ermöglichte auch die Beobachtung des konjugativen SCP2tetO-Transfers und der Mobilisierung von chromosomaler DNA in einen Empfängerstamm, der für eGFP und das TetRmcherry-Fusionsprotein kodiert. Diese Studien legen nahe, dass der Winkel der Hyphenkontaktstelle für den konjugativen Transfer wichtig ist. Ein Plasmidtransfer wurde nur beobachtet, wenn Spender- und Empfängerhyphen in

einem Winkel von über 59° aufeinander trafen, während bei einem Winkel von unter 27.5° kein Transfer beobachtet wurde.

Mit Hilfe von FROS wurde der konjugative Transfer von chromosomaler DNA und ihre Etablierung und anschließende Ausbreitung im Empfängermyzel sichtbar gemacht. Dies ist der erste Bericht, der den konjugativen Transfer von chromosomaler DNA durch Fluoreszenzbildgebung zeigt.

B. Summary

The Gram-positive soil bacterium *Streptomyces* grows by apical tip extension, forming a multiply branched mycelium. This mode of growth poses a problem for the proper distribution of the genetic material, i.e. the chromosome and plasmids. So far, the position of a plasmid has not been determined in a mycelial organism.

To elucidate the localization of the single copy number plasmid SCP2 in living *S. lividans* mycelium in comparison with that of the chromosome, a fluorescent repressor operator system (FROS) was applied. A *tetO* array consisting of 120 binding sites was inserted into a bifunctional SCP2 derivative (SCP2tetO) or integrated into the central part (nt. 5327700) of the *S. lividans* chromosome. Integration of a gene encoding a TetR-mCherry fusion protein resulted in bright fluorescence foci, indicating the positions of individual copies of the plasmid or the chromosomal region, marked with the *tetO* array.

Still-images of hyphae and time-lapse imaging of SCP2tetO and the chromosome revealed a very similar localization pattern, with the tip-proximal copy always following the tip at a constant distance of 2.21µm; ± 0.99µm (SCP2tetO) and 3.69µm; ± 2.86µm (chromosome). The localization pattern of SCP2tetO depended on the $ParAB_{SCP2}$ partitioning system. Deletion of $parA_{SCP2}$ reduced the number of visible plasmid spots. These spots had a higher fluorescence intensity compared to those of the parent plasmid SCP2tetO, suggesting that, following replication, the plasmid copies could not separate in the absence of $ParA_{SCP2}$. In addition, $ParAB_{SCP2}$ seemed to be required to anchor SCP2tetO to branching sites and hyphal tips, since SCP2tetOΔ*parA* was detected only very rarely at branching sites and tips.

The FROS system also allowed observation of conjugative SCP2tetO transfer and the mobilization of chromosomal DNA to a recipient strain, encoding eGFP and the TetRmcherry fusion protein. These studies suggested that the angle of the hyphal contact site was important for conjugative transfer. Plasmid transfer was only observed if donor and recipient hyphae hit each other at an angle above 59 °, while no transfer was observed when the angle was below 27.5 °.

Using FROS the conjugative transfer of chromosomal DNA and its establishment and subsequent spreading in the recipient mycelium was visualized. This is the first report demonstrating the conjugative transfer of chromosomal DNA by fluorescence imaging.

1. Introduction

The earth emanated a delightful and natural fragrance. On a woodland walk or composting, we notice a pleasant earthy scent. These olfactory experiences are not only enjoyable, but also provide us with information about the ecological systems in which we live in. On the other side, when individuals seeking medical treatment for e.g. bronchitis or a septic finger, antibiotics are typically prescribed by the attending physician. The common feature of these subjects are soil bacteria of the genus *Streptomyces*, which do not only produce the earthy smelling geosmin (Gust et al., 2003), but also synthesize the majority of the antibiotics used across the world.

Streptomycetes are soil-dwelling bacteria, that have gained the interest of the scientific community for a duration exceeding one century as a result of its noteworthy ability to generate an extensive assortment of biologically active molecules, which have saved millions of lives and revolutionized the practice of medicine.

1.1 The diversity of *Streptomyces* species: antibiotic factory

Streptomyces is one of the most substantial bacterial genera in existence, which can be found almost everywhere, including the deep oceans and high mountains (Ribeiro da Cunha et al., 2019; Sarmiento-Vizcaíno et al., 2018; Waksman et al., 2010), although the majority of streptomycetes investigated to date have been isolated from terrestrial habitats (Encheva-Malinova et al., 2014; Hotta et al., 1980; Lam, 2006). The genus *Streptomyces* belongs to the Actinobacteria that have a wide range of G+C content, with streptomycetes having over 70% G+C, corynebacteria having 54%, and the pathogen *Tropheryma whipplei* which has less than 50% G+C (Chater & Chandra, 2006). The first genome of a *Streptomyces* species, *Streptomyces coelicolor*, was sequenced in 2002 (Bentley et al., 2002), revealing a complex genome of about 8 million base pairs and over 7,000 protein-coding genes. Since then, the genomes of more than 150 *Streptomyces* species (validly published names at http://www.bacterio.net) have been sequenced and analysed, revealing a remarkable diversity of genomic architectures, metabolic pathways, and regulatory networks. It is noteworthy that *Streptomyces* produces 39% of the overall microbial metabolites. Specifically, within the class Streptomycetales, this genus alone has been found to contribute to almost 80% of the bioactive molecules synthesized (Bérdy, 2012).

Throughout history, the identification of influential bioactive secondary metabolites such as antibiotics, anticancer drugs, immunosuppressive drugs, and other biologically active substances has been markedly facilitated by *Streptomyces* derived from environmental sources (Bérdy, 2005; Cragg et al., 2011; Mann, 2001; Strohl, 2004). Streptomycin, the first antibiotic discovered from *Streptomyces*, was isolated in 1943 and proved effective against tuberculosis and other bacterial infections (Woodruff, 2014). Since then, many other antibiotics, such as tetracycline (Petković et al., 2006), Bleomycin (Kong et al., 2018), Chloramphenicol (Brock, 1961), Nystatin (Hazen & Brown, 1950) have been identified from *Streptomyces* species, and some of them remain essential drugs for treating human and animal diseases. Moreover, some *Streptomyces* strains can produce secondary metabolites with novel bioactivities that are being investigated for their potential as anticancer agents, immunosuppressants, or insecticides.

Besides secondary metabolites, *Streptomyces* is also a prolific source of enzymes, pigments, flavour compounds, and other biologically active molecules that have a wide range of applications in biotechnology and ecology. For example, some *Streptomyces* enzymes can break down plant cell walls and release sugars that can be used as feedstocks for biofuels and other renewable chemicals (Itoh et al., 2002).

Another important aspect of *Streptomyces* genomics is the presence of a large number of mobile genetic elements, such as plasmids, transposons, and bacteriophages, that can transfer and rearrange genetic information between strains and species. These elements can confer new metabolic capabilities, and can contribute to the evolution of new *Streptomyces* lineages with distinct ecological niches

1.2 Developmental biology of *Streptomyces*: The life cycle

Each *Streptomyces* species has a unique combination of genetic traits that determine its metabolic capabilities, environmental preferences, and ecological roles. Investigating the genetics of *Streptomyces* has gained significant importance due to their intricate life cycle. These bacteria have a complex life cycle that involves the formation of filamentous structures called hyphae, which can grow up to several millimeters in length and give rise to spores (Figure 1.1).

(a) (b) (c)

Figure 1.1: *Streptomyces* strains growing for two days on LB agar (a) and on R5 agar for 8 days (b, c). Due to the excessive production of the blue pigmented antibiotic actinorhodin, *S. coelicolor* M145 (a, left and right) and the surrounding medium is stained blue, while *Streptomyces lividans* redstrep 1.7 (a, top and bottom) appears yellowish. After longer incubation on R5 plates, both strains produce grey pigmented spores (b, *S. coelicolor*; c, *S. lividans* redstrep 1.7).

Throughout the process of colony growth from a spore, there is a notable escalation in colonial complexity (Champness, 1994; Chater, 1993; Chater & Losick, 1997; Hodgson et al., 1992). With each replication of the chromosomes in the initially aseptated germ tube, the germ tube emerges from the unigenomic spore following a proper germination trigger, and its cell wall expands primarily at the tip (Chater & Losick, 1997). After a few DNA replication cycles, the potentially disastrously rising rate of tip extension stabilizes when new tips form through lateral branching as more chromosome doublings take place. In shortly, a typical *Streptomyces* spore will

germinate under ideal conditions and produce one or two germ tubes **(**Figure 1.2**)**. After that, they extend their tips and form a network of branched filaments called the substrate mycelium (vegetative phase) (Chater, 1984). As they age, aerial multinucleated mycelium is generated, which then experiences synchronous cell division, resulting in the creation of monoploid compartments, each of which differentiates into spores (reproductive sporulation phase) (Barka et al., 2015; Chater, 1993).

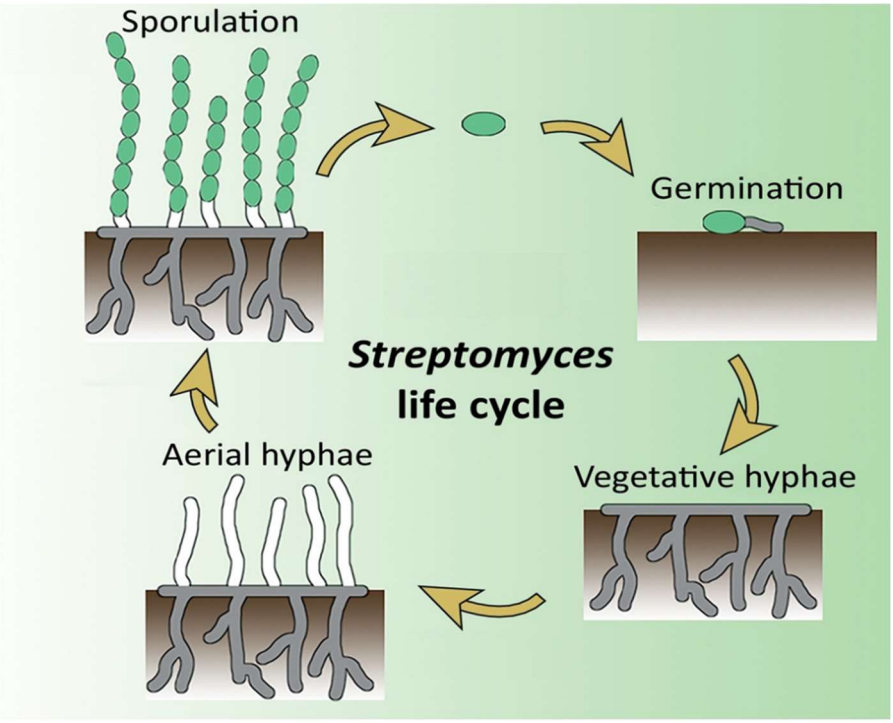

Figure 1.2: The Life cycle of *Streptomyces*. Modified from (Jones & Elliot, 2017), Trends in Microbiology, Volume 25, Issue 7, Pages 522-531

1.3 Plasmids in *Streptomyces*: Diversity and Function

Plasmids are extrachromosomal DNA molecules that can replicate independently from the host chromosome and usually carry genes that confer selective advantages, such as antibiotic resistance or metabolic diversification. In *Streptomyces*, plasmids are common and diverse, ranging in size from 5 to 600 kb. Beside circular plasmids, also linear plasmids have been described. The linear plasmids, e.g. the 17 kb pSLA2 from *S. rochei*, replicate from a centrally located replication origin, and only the synthesis of the very last 280 bp at the ends is primed by terminal proteins, called telomerases

(Chang & Cohen, 1994) (Vogelmann et al., 2011). Except for the giant linear plasmids, like SCP1, that have been shown to encode antibiotic biosynthetic pathways (Kinashi, 2011), typical *Streptomyces* plasmids only encode functions involved in replication, stability and conjugative plasmid transfer, but do not carry resistance genes (Vogelmann et al., 2011). The analysis of sequencing data revealed that plasmids present in Actinobacteria exhibit a mean G+C content of 64.5% (Shintani et al., 2015).

S. coelicolor A3(2), the genetically best studied *Streptomyces* species (Hopwood), possesses three extrachromosomal elements, SCP1, SCP2, and SLP1. SCP1 is a 350 kb linear plasmid, encoding methylenomycin biosynthesis (Kinashi et al., 1987).

The circular 30 kb SCP2 was the first plasmid isolated from a *Streptomyces* species (Schrempf et al. 79, Bibb et al., 81). It is a single-copy number plasmid that replicates via a Theta mechanism, which involves bidirectional replication from an origin to produce a new copy (Haug et al., 2003).

SLP1 (Bibb et al., 1981) belongs to the class of integrative conjugative elements (ICE). These elements typically reside in the host chromosome, but can excise from the chromosome and autonomously replicate. Following conjugative transfer into a new host, ICEs integrate into a specific attachment site of the host chromosome by site specific recombination, mediated by phage-like *int* and *xis* genes (Carraro & Burrus, 2015; Vögtli & Cohen, 1992). The *attB* site of SLP1 overlaps a highly conserved tRNA gene, ensuring non-mutagenic integration of the ICE (Vögtli & Cohen, 1992).

In addition, *Streptomyces* strains often carry multi copy plasmids, for example the 8.9 kb pIJ101 isolated from *S. lividans* (Kieser et al., 1982; Pernodet & Guerineau, 1981). They replicate through a circular, single-stranded replication intermediate using a rolling-circle mechanism (sigma mode). A distinctive, plasmid-encoded replication protein initiates the replication process, by introducing a single-stranded brake at the nicking site within the double-stranded origin *dso* (Khan et al., 1982).

One of the most intriguing aspects of *Streptomyces* plasmids is their potential for inter-plasmid recombination and integration, which can lead to the formation of hybrid plasmids that, in case of giant linear plasmids carry multiple biosynthetic gene clusters and regulatory elements. This process, contributing to horizontal transfer, can result

in the emergence of new antibiotic-producing strains that are highly divergent from their parental strains and can have unique bioactivities. Another important feature of *Streptomyces* plasmid is their ability to transfer between cells via conjugation and to mobilize chromosomal DNA. This was discovered in 1950s by Sermonti (Hopwood & Sermonti, 1963; Sermonti & Spada-Sermonti, 1955, 1956), shortly following the demonstration of fertility in *E. coli* by Lederberg and Tatum (Lederberg & Tatum, 1946).

1.4 Mechanism of conjugative DNA transfer in *Streptomyces*

One of the most interesting aspects of plasmid biology is the mechanism of conjugal transfer, whereby plasmids can be transferred between different bacterial cells through a process that requires physical contact and a set of dedicated genes. In contrast to conjugation systems of other bacteria, which involves a complex plasmid encoded multi-protein type IV secretion system that secretes a single-stranded DNA (ssDNA) molecule, the transfer regions of *Streptomyces* plasmids are relatively limited in size, comprising only about 3-5 kb (Kataoka et al., 1991; Kieser et al., 1982; Reuther et al., 2006; Servn-Gonzlez et al., 1995). Conjugation in the *Streptomyces* genus was likewise elucidated.

Sequencing of the minimal transfer region of plasmid pIJ101 identified a single *tra* gene (Hopwood, 2006; Kendall & Cohen, 1988). The deduced Tra protein had low sequence similarity to the FtsK and SpoIIIE proteins, which are involved in chromosome segregation during cell division and sporulation (Begg et al., 1995; D. J. Sherratt et al., 2010; Wu et al., 1995). Moreover, the lack of conjugative relaxase genes (Hopwood, 2006) and the discovery that the presence of the *SalI* restriction enzyme, which cleaves incoming double-stranded DNA (dsDNA) but does not cut ssDNA, strongly influences conjugative DNA transfer in *Streptomyces*, demonstrated that dsDNA is transferred during *Streptomyces* conjugation (Possoz et al., 2001). The purified DNA translocase TraB of the *S. venezuelae* plasmid pSVH1 was shown to assemble to hexameric rings in artificial membranes and form characteristic pores (Vogelmann et al., 2011). In vitro, TraB also forms higher aggregates (Amado et al., 2019). TraB is a DNA-specific ATPase that interacts with peptidoglycan and that binds to a specific plasmid region, called cis acting locus of transfer (*clt*) by recognizing series of 8-bp repeats (Franco et al., 2003; Vogelmann et al., 2011).

As an adaptation to the mycelial growth of *Streptomyces*, plasmids are transferred in a two-step process. Following the initial conjugative plasmid transfer by TraB, the plasmid can spread within the recipient hyphae, thereby colonizing the recipient mycelium. This intramycelial spreading across septal cross walls, depends on a set of *spd* genes in addition to *traB* (Thoma et al., 2015).

Imaging of conjugative plasmid transfer by fluorescence microscopy (Figure 1.3.) revealed that the plasmid becomes transferred between the lateral walls, not involving a complete fusion of the hyphae (Thoma & Muth, 2016).

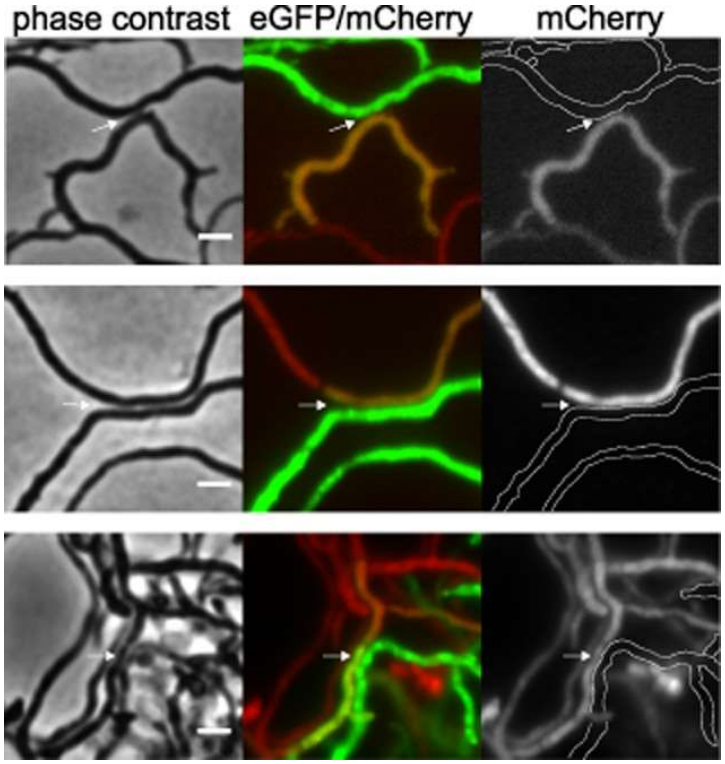

Figure 1.3: Imaging of conjugative plasmid transfer in living *S. lividans* mycelium. When a plasmid pLT303ΔSpd carrying donor (green) hyphae hits the *S. lividans* T7-mCherry recipient (red) it bends and grows for a while next to the recipient. At the contact sites plasmid transfer takes place via the lateral walls (white arrows). Transfer does not involve complete fusion of the donor and recipient hyphae, which would result in the diffusion of mCherry from the recipient to the donor. The donor hyphae's location in the mCherry channel is denoted by dashed lines. 2 µm scale bar (Thoma et al., 2016)

1.5 Plasmid SCP2: in this research study

SCP2 (31 kb) is a single copy number, circular plasmid from *Streptomyces coelicolor* (Lydiate et al., 1985). SCP2 has been used as a molecular tool for the genetic manipulation of *Streptomyces* species due to its ability to replicate stably, even when carrying large inserts (Hopwood et al., 1985).

The complete nucleotide sequence of the 31 317 bp SCP2 was determined. 34 candidate proteins ranging in length from 31 to 710 amino acids were identified by the examination of sequence, the majority of which did not resemble any known proteins (Haug et al., 2003).

Deletion analysis identified a 1.6 kb replication region, consisting of a 650 bp non-coding region and two genes, *repI* and *repII*, encoding small proteins of 161 and 131 aa. The previously identified “stability” region was shown to encode three proteins. MrpA belonging to the lambda integrase family of site-specific recombinases probably represents a dimer resolution system. ParA and ParB constitute a typical partitioning system with the ATPase ParA and the ParB DNA-binding protein (Haug et al., 2003). Such partitioning systems are well studied in unicellular bacteria. They had been developed to actively transport the replicated chromosomes or plasmids to the cell poles via a “diffusion ratchet mechanism” (D. Sherratt, 2013) to ensure proper segregation to the daughter cell after division.

ParB multimers bind to a specific sequence close to the origin of replication. ParA is an ATPase and binds non-specifically to DNA (ParA-ATP). Interaction of DNA-bound ParA with ParB results in ATP hydrolysis, which releases ParA (together with *ori*-bound ParB) from the DNA. Released *ori*-bound ParB binds again to ParA bound to DNA. By sequential repetitions of this cycle, the ParB-bound *ori* moves to the cell pole following the ParA gradient.

This system is used in bacteria not only for partitioning of the chromosome but also many low copy number plasmids encode their own ParAB plasmid partitioning system (Brooks & Hwang, 2017).

1.6 Methods to detect the position of specific DNA fragments in viable cells

Understanding the dynamics of the genetic material requires methodology to specifically localize DNA sequences within a living cell without interfering with its viability. For this purpose, the Fluorescence Reporter and Operator System (FROS) was developed (Tsukamoto et al., 2000). This is a fluorescence microscopy technique, which is based on the use of two components.

First, a gene fusion, encoding an autofluorescence protein and a repressor protein (FR), that can bind to a certain DNA-fragment in a highly specific manner. In the absence of the binding site, FR cannot bind to DNA, resulting in a uniform faint fluorescence throughout the whole cell, when observed by fluorescence microscopy.

Second, an “operator” DNA sequence, which contains multiple binding sites of the repressor. When this operator array is integrated into the genomic region of interest, multiple copies of FR will bind. This results in the production of a strong fluorescent signal that exactly localizes the position of the operator sequence within the cell.

The Fluorescence Reporter and Operator System is highly sensitive and specific, making it a valuable tool for researchers working with complex biological systems. Additionally, it is a non-invasive method that does not require destructive sampling, making it suitable for longitudinal studies and real-time monitoring of cellular processes. Based on different repressor proteins and their cognate operator sequences different FROS systems have been developed. Widely used systems are the LacI/*lac*-System (Robinett et al., 1996), the TetR/*tetO*-System (Lau et al., 2003) and the ParB/*parS*-System (Li & Austin, 2002)

FROS methods had been widely used to analyze elementary cell processes such as DNA replication, chromosome folding and segregation, or to determine *in vivo* genetic copy numbers by measuring fluorescence intensities. Apart from this, FROS can be used to track the localization and mobility of small circular DNA molecules during transfection or viral infections in the mammalian nucleus (Mearini et al., 2004).

The low-copy number conjugative plasmid R388 was localized in living *E. coli* cells with the GFP-ParB/*parS* system. Each plasmid molecule was localized as a bright green spot in the cell.

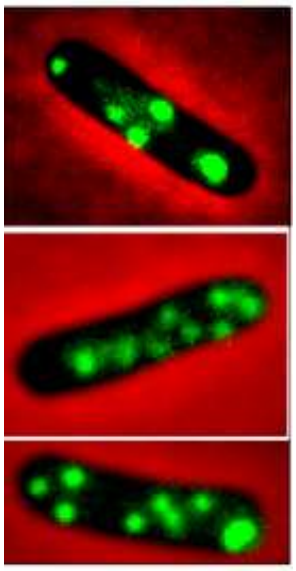

Figure 1.4: Localization of plasmid R388 and derivatives in living *E. coli* cells using a parS/GFP-ParB system. This figure modified from (Guynet et al., 2011), PLoS Genetics, May 2011.

The TetR-FROS system was used to study the distribution of chromosomes in *S. coelicolor* during spore germination and branching. An array of 120 tandem *tetO* repeats was integrated into the *S. coelicolor* chromosome approximately 29 kb from the *oriC* region (Kois-Ostrowska et al., 2016). By time-lapse microscopy it was shown that during spore germination and branching, ParA anchors the *oriC* region of one of the multiple chromosomal copies to the new hyphal tip through interaction with the apical polarisome. The positioning of the *oriC* region to the hyphal tip is required for the elongation of hyphal tube (Figure 1.6).

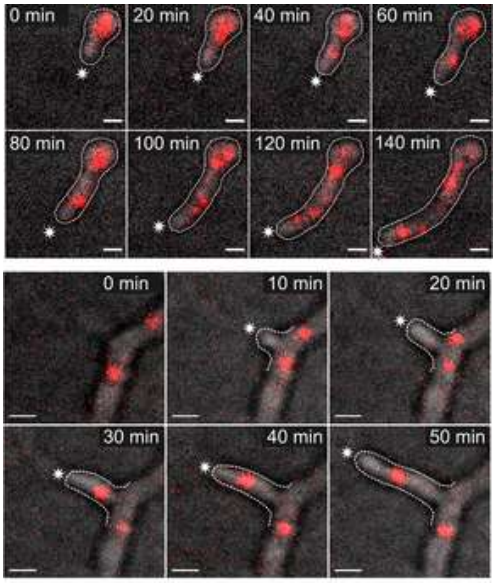

Figure 1.5: Time-lapse snapshots of FROS complexes indicating the position of the *oriC* region during germination (top panels) and branch formation (bottom panels) in *S. coelicolor*. The images are the overlay of TetR-mCherry fluorescence and differential interference contrast (DIC) image (grey), scale bar 1 µm. Image is taken from (Kois-Ostrowska et al., 2016).

1.7 Aim of this study

So far, nothing is known about the position and distribution of plasmids in a mycelial organism. It has not been studied before, whether plasmids follow the extending tips and how plasmids enter into new branches. Moreover, it is unclear, how a plasmid is transferred to the recipient hyphae during conjugation, how it spreads in the recipient mycelium and whether the plasmid ParAB partitioning system is involved in plasmid movement. Since plasmid transfer is frequently associated with the transfer of chromosomal DNA, the chromosome has to be simultaneously transported to the recipient during conjugation. The kinetics of plasmid transfer and chromosome transfer is waiting for its elucidation. These questions should be addressed by imaging the positions of plasmids and chromosomes during vegetative growth and during mating.

2. Materials and Methods

2.1 Materials

Table 2.1.1: Bacterial strain(s)

Bacterial strain(s)	Description	Reference or source
***E. coli* strain(s)**		
NovaBlue	*recA1, endA1, gyrA96, thi-1, hsdR17 (r_{K12}^- ,m_{K12}^+) supE44, relA1, lac [F', proAB, lacI^q , lacZ*∆M15, Tn*10 (Tet^R)*	Novagen
E. coli Stellar™	*E. coli* HST08, ultra-competent cells, prepared by Inoue method	Clonetech
E. coli ET12567/pUZ8002	methylation-deficient *E. coli* strain containing pUZ8002, F-, *dam::*Tn*9, dcm-6, hsdM, hsdR, lacY1*, Cam^R; pUZ8002 is a RK2 derivative (Kan^R) with a defective *oriT* used for *Streptomyces* (intergeneric) conjugation	(MacNeil, et al., 1992)
***Streptomyces* strain(s)**		
Streptomyces lividans TK54	*his-2, leu-2, spc-1*	Hopwood et al. 1983
Streptomyces lividans TK64	Plasmid free	Hopwood et al. 1983
Streptomyces lividans JT46	*pro-2, str-6, rec-46*, SLP2$^-$, SLP3$^-$	Tsai JF, Chen CW, 1987
Streptomyces lividans JT46::tetRmCherry	*pro-2, str-6*, ::pMS83-tetRmCherry	L. Thoma et al., 2016
Streptomyces lividans Red.Strep 1.7	Δact, Δcda, Δred, Δcpk, Δmel	(Novakova et al., 2018)
Streptomyces coelicolor M145	Wild type, SCP1$^-$, SCP2$^-$	Kieser et al. 2000

Streptomyces coelicolor M1146	SCP1$^-$, SCP2$^-$, Δact, Δcda, Δred, Δcpk	Gomez-Escribano und Bibb 2011

* Apra^R = apramycin resistance, Cam^R = chloramphenicol resistance, Kan^R = kanamycin resistance, Tet^R = tetracycline resistance, Thio^R = thiostrepton resistance

Table 2.1.2: Plasmids and Vectors

Plasmid/Vector	**Description**	**Reference**
pIJ303	pIJ101, conjugative, Thio^R	Kieser et al. 1982
pIJ903 tetOK	Low-copy, SCP2* Derivat, pIJ903, [*tetO*]n=120 , *aac(3)IV, aphII*	L. Thoma et al., 2016
pLT190	pGM190 derivative, *aphII*	L. Thoma and G. Muth (unpublished)
pRM43	*aphII, egfp, int*$_{\Phi C31}$	G. Muth (unpublished)
pRM43mCherry	*aphII, mcherry*, *int*$_{\Phi C31}$	G. Muth (unpublished)
pGM190	*E. coli-Streptomyces* shuttle vector derived from pSG5, *tipA* promoter, *tsr, aphII*	(Wohlleben, et al., 2009)
pSCP2-tetO	Low-copy, SCP2* derivative, [*tetO*]n=120, *aphII*	L. Thoma et al., 2016
pSCP2-tetO ΔparA	Low-copy, SCP2* derivative, [*tetO*]n=120, *aphII*	This study

Table 2.1.3: Growth media (liquid and solid) and composition

All following compositions refer to 1L of medium

Medium	Composition(s)	Reference
2xYT-Medium	16g Tryptone 10g Yeast extract 5g NaCl	Kieser et al. 2000
LB-Medium	10g Tryptone 5g Yeast extract 5g NaCl Solid medium: added 15g/l Agar	modified after Sambrook and Russell, 2001
TSB-medium	30g TSB powder	Bacto™ Tryptic Soy Broth Soybean-Casein Digest Medium, ready for use; Becton, Dickinson and company
MS	20g Mannitol 20g Soy flour (fat reduced) Solid medium: added 16g/l Agar	Hobbs et al. 1989
MS with $MgCl_2$	20g Mannitol 20g Soy flour (fat reduced) 2g $MgCl_2$ Solid media: added 16g/l Agar	Hobbs et al. 1989 (modified)
S-Medium	4g Peptone 4g Yeast extract 4g K_2HPO_4 2g KH_2PO_4 10g Glycine 800ml $H_2O_{deion.}$ Separately autoclaved	Okanishi et al. 1974 (modified)

	10g Glucose 0,5g $MgSO_4*7H_2O$ 200ml $H_2O_{deion.}$ Separately autoclaved and added to the medium	
R5-Medium	103g Saccharose 10g Glucose 5g Yeast extract 10.12g $MgCl_2* 6H_2O$ 5.73g TES 0.25g K_2SO_4 0.1g Casamino acid 2ml Trace elements solution Solid medium: Added 18g/l Agar fill up to 950ml with dH_2O and adjust pH to 7.2 before autoclaving Separately autoclaved 20ml 1M $CaCl_2$ 10ml 0,54% (w/v) KH_2PO_4 20ml 20% (w/v) L-Proline Separately autoclaved in each case and added to the medium.	Kieser et al. 2000
R5-Media with $CuCl_2$	103g Saccharose 10g Glucose 5g Yeast extract 10.12g $MgCl_2$ 5.73g TES 0.25g K_2SO_4 0.1g Casamino acid 2ml Trace elements solution Solid medium: Added 18g/l Agar	Kieser et al. 2000 (modified)

	fill up to 950ml with dH_2O and adjust pH to 7.2 before autoclaving Separately autoclaved 20ml 1M $CaCl_2$ 10ml 0,54% (w/v) KH_2PO_4 20ml 20% (w/v) L-Proline 100µl 20 mM $CuCl_2$	
Trace elements solution	200mg $FeCl_3 * 6H_2O$ 40mg $ZnCl_2$ 10mg $CuCl_2 * 2H_2O$ 10mg $MnCl_2 * 4H_2O$ 10mg $(NH_4)_6Mo_7O_{24} * 4H_2O$ 10mg $Na_2B_4O_7 * 10H_2O$	Okanishi et al. 1974
Minimal medium (MM)	0.5g L-asparagine 0.5g K_2HPO 4 0.2g $MgSO_4.7H_2O$ 0.01g $FeSO_4.7H_2O$ 10g Agarose pH 7.0-7.2 1000 ml Distilled water, dispense 200 ml into 250 ml Erlenmeyer flasks, At the time of use, re-melt the medium and add 4 ml of a 50% solution of glucose to each flask. Supplements: 10 ml of MM agarose (for microscopy) 50µl L-Histidine (10mg/ml) 50µl L-Leucine (7.5 mg/ml) 50µl L-Proline (7.5 mg/ml)	Hopwood, 1967

Table 2.1.4: Antibiotics

Antibiotics	Stock conc.	Working conc.	Solvent	Source
Apramycin	50 mg/ml	50 µg/ml	ddH_2O	sigma
Kanamycin	50 mg/ml	50 µg/ml	ddH_2O	serva
Nalidixic acid	25 mg/ml	25 µg/ml	In 0,2M NaOH	Fluka
Zeocin	25 mg/ml	25 µg/ml	ddH_2O	
Tetracycline	15 mg/ml	15 µg/ml	50% EtOH	sigma
Thiostrepton	25 mg/ml	25 µg/ml	100% DMSO	sigma

Table 2.1.5: Buffers and solutions

Buffer	Composition(s)	Amount per 1L ddH_20
Solutions for plasmid DNA isolation		
P1	Tris EDTA RNase A pH 8.0	50mM 10mM 100µg/ml
P2	NaOH SDS	200mM 1%
P3	Ka-Acetate pH 5.5	3M
Solutions for genomic DNA isolation		
SDS	SDS ddH_2O	5%
Lysis buffer	Lysozyme added to the P1 buffer	10 mg/ml
Solutions for agarose gel electrophoresis of DNA		
TAE-buffer	Tris/HCl $C_2H_3NaO_2$ (sodium acetate) EDTA pH 7.8 (with glacial acetic acid)	40mM 10mM 1mM

1% Agarose-Gel	1 x TAE buffer Agarose	1000ml 10g
Bromophenol blue	Bromophenol blue (w/v) Glycerine (v/v)	0,04% 50%
Ethidium bromide dyebath	Ethidium bromide ddH_2O	5µg/ml

Table 2.1.6: Kits and their source

Name	**Supplier**
DNA-preparation and purification	
Qiagen® Plasmid Mini/Midi Kit	QIAGEN
PeqLab® Plasmid Mini/Midi Kit	PeqLab
MiniElute® Gel Extractio Kit	QIAGEN

GenRuler 1kB DNA Ladder was used as a size marker for agarose gel electrophoresis. This shows fragment sizes ranging from 250 to 1000 base pairs (Figure 2.1)

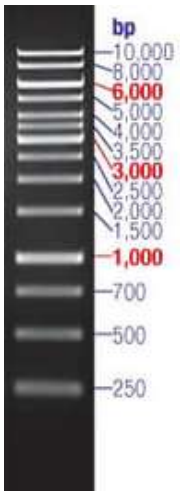

Figure 2.1: Thermo Scientific™ GeneRuler 1kb DNA Ladder. Perform sizing and approximate quantification of a wide range of double-stranded DNA on agarose gels with this mixture of individual, chromatographically purified DNA fragments. The graphic was taken from the following website and modified: https://www.fishersci.de/shop/products/fermentas-generuler-1kb-dna-ladder/11823963

Table 2.1.7: Transformation buffer solution for *E. coli* and *Streptomyces*

Solutions for transformation of *E. coli* competent cells		
Buffer	**Composition(s)**	**Amount per 1L dd$H_2$0**
$CaCl_2$-solution	$CaCl_2$ ddH_2O	100mM
Solutions for transformation of *Streptomyces*		
P-buffer for protoplast preparation (Okanishi et al.1974)	Sucrose (was dissolved in 858 ml deionized H_2O and autoclaved) Trace element solution TES (250 mM, pH 7.2) $MgCl_2$ (1M) $CaCl_2$ (250 mM) K_2SO_4 (140 mM) KH_2PO4 (40 mM) (all components have to be separately autoclaved, the buffer has to be prepared freshly before use)	103g 2ml 100ml 0.25g (10ml) 10mM (10ml) 0.05g (10ml) 25mM (10ml)
T-buffer for transformation (Thompson et al. 1982)	Sucrose $CaCl_2$ Tris-Malate (pH = 8) PEG1000 Trace element solution K_2SO_4 $MgCl_2 * 6H_2O$ KH_2PO_4 all components have to be separately autoclaved	2.5% 0.1M (10mM) 50mM 25% 2ml 0.25g 10mM 0.05g

T-buffer for transformation (Modified: Thompson et al. 1982)	Fresh P-buffer (protoplast) PEG1000 (alfa Aesar) (separately autoclaved or incubated at 60°C for 1 hour. After that filter with 0.2µm)	10 ml 3g

Both transformation buffers were used in the PEG-mediated protoplast transformation method.

Table 2.1.8: Enzymes

Enzyme	Source
Lysozyme	Serva
Restriction enzymes (10U/µg)	Thermo Fisher Scientific, New England Biolabs
RNase A	Sigma-Aldrich
T4 Ligase	Thermo Scientific
Taq-Polymerase	Genaxxon bioscience GmbH

Table 2.1.9: Chemical(s) and additive(s)

Chemical or additive	Source
Agar	Sigma-Aldrich, Roth
Agarose	Genaxxon bioscience GmbH
Bromophenol blue	Riedel-de Haen, Serva
Buffer 10X (for PCR)	QIAGEN
$CaCl_2 * 2H_2O$	Merck
Casamino acids	Difco
Cellophane membrane	ibidi
DMSO (Dimethyl sulfoxide)	Merck Millipore
EDTA	Merck
Ethanol	BDH PROLABO (VWR) , Sigma-Aldrich
Ethidium bromide	Serva, Roth
Gene frame	Thermo scientific

GeneRuler™ 1kB DNA Ladder	Thermo Scientific
GeneRuler™ DNA Ladder Mix	Fermentas
Glucose	Roth
Glycerol	Sigma, Roth
Glycine	AppliChem
Isopropanol	Normapur
KCl	Merck
$K_2HPO_4*3H_2O$	Calbiochem
K_2SO_4	Riedel-de Häen
KH_2PO_4	Roth
L-Proline	AppliChem
Tris-Maleate	Roth
Mannitol	Merck
$MgCl_2*6H_2O$	Roth
$MgSO_4*7H_2O$	Merck
Sodium acetate	Roth
Sodium chloride (NaCl)	Sigma-Aldrich
NaOH	Normapur
PEG 1000 (B22134)	Alfa Aesar
PEG 1000	Merck/Roth
Pepton (Bacto™ Peptone)	BD Biosciences
Phenol/Chloroform (Roti®-Phenol/Chloroform)	Roth
Polymer membrane- D 263 Schott glass	ibidi
Saccharose	Roth
Soy flour (low/full fat)	Henselwerk GmbH
TES	AppliChem
Tris/HCl (Trizma base)	Sigma
Tryptone (BactoTM Tryptone)	BD Biosciences
Y-PER	Thermo Scientific
Kaliumacetat	AppliChem
Yeast extract	Oxoid

2.2 Methods

2.2.0 Cultivation of bacterial strains

2.2.1 Cultivation of *Streptomyces*

Streptomyces strains culture for genomic DNA isolation was carried out in a 100 ml Erlenmeyer flask with baffle and stainless-steel spring. For the cultivation, 10-20 ml of TSB medium/ S medium/ LB medium (Table: 2.3) and 5-10 µl of spores or homogenized mycelium were used. In case of antibiotic resistant strains, the medium was supplemented with the appropriate antibiotic's concentration (described in Table 2.4). For the preparation of protoplasts, a 1 L baffled Erlenmeyer flask, equipped with 100 ml of TSB (+0.75% glycine) and a stainless-steel spring was used. After inoculation, a loose metal cap was placed on the flask. This increases the oxygen concentration and allows better growth, but at the same time the culture remains sterile. The bacteria were incubated for 1-3 days at 27°C or 29°C and 180 rpm (rounds per minute) on a rotary shaker.

To obtain spores, spores or homogenized mycelium were streaked out on a mannitol soya (MS) agar plate (with antibiotic if needed; Table 2.4)) and incubated at 29 °C. After 6-8 days, when the cultures had reached the spore stage, which in *Streptomyces* is often indicated by a greyish coloration, the spores were harvested. For this purpose, the spores were washed off the agar plate with 3 ml sterile ddH_2O and sterile cotton pads. Subsequently, the spores were transferred to an Eppendorf tube, centrifuged for 2 min at 14,000 rpm and the supernatant was completely removed. The spore pellet was resuspended in sterile 20% glycerol (1ml) and stored at -20°C or -80°C.

To determine the respective titer, serial dilutions (1:10 dilution) were prepared in ddH_20 and the 10^{-4}-10^{-6} dilutions were plated onto LB agar supplemented with the appropriate antibiotics. After 3 days of growth at 29 °C, the colonies were counted and the titer was calculated by the following formula.

- Titer (number of spores per ml) = (No of colonies * 10)/ dilutions.

2.2.2 Cultivation of *Escherichia coli*

E. coli cells were incubated overnight at 37 °C and 180 rpm as standard. Small-scale cultivation of *E. coli* was enough for plasmid isolation. For this purpose, test tubes with 5 ml of LB medium were used, with appropriate antibiotic(s). Then a single colony was picked up with a sterile toothpick and wiped on the wall of the test tube. The colony was then washed into the medium with a glass pipette. The test tube was covered with a metal cap and placed in a rotary shaker.

2.2.3 DNA isolation

The isolation of DNA was first demonstrated in 1869 by Friedrich Miescher (Dahm, 2005) and is now one of the basic techniques of molecular biology (Tan & Yiap, 2009). All centrifugation steps in the isolation of DNA were performed as standard with the Eppendorf Centrifuge 5424 (rotor FA-45-24-11) at 20,238 × g (14680 rpm).

2.2.3.1 Isolation of plasmid DNA from *E. coli* cells

The isolation of plasmid DNA from *E. coli* cells was performed by using alkaline lysis (Birnboim & Doly, 1979). An *E. coli* culture was prepared as described in 3.2, distributed to 1.5 ml Eppendorf reaction tubes and centrifuged for one minute. The supernatant was discarded and the pellet resuspended in 300 µl of precooled P1 buffer (Table 2.5). Subsequently 300 µl of P2 buffer (Table 2.5) was added, inverted several times and incubated for 5-10 minutes at room temperature. This was followed by the addition of 300 µl of pre-cooled P3 buffer (Table 2.5), brief vortexing and incubation for 5-10 minutes on ice. The mixture was then centrifuged for 10 minutes, and the supernatant (~750µl) was transferred to a new Eppendorf tube. To the supernatant, 750 µl of isopropanol was added and vortexed to precipitate the plasmid DNA. After vortexing, the mini preparation was centrifuged for 15 min and the supernatant was discarded. The pellet was then mixed with approx. 500 µl of 70% ethanol and vortexed. After that, the sample was centrifuged for five minutes. The supernatant was removed cleanly with a pipette and the pellet was dried for 5 min at 60 °C. The dry pellet was then dissolved in 50 µl of ddH_2O and stored at -20 °C for further use.

2.2.3.2 Isolation of plasmid DNA from *Streptomyces*

The isolation of plasmid DNA from *Streptomyces* was performed according to a similar principle as the isolation from *E. coli* cells.

- First, as described in 2.2.1, a *Streptomyces* culture was prepared.
- 1.5 ml of the culture was transferred to an Eppendorf tube, centrifuged for 1 min at 14,000 rpm and the supernatant was discarded.
- The pellet was then resuspended in 300 µl of P1 buffer (+5 mg/ml lysozyme) by vortexing and incubated at 37 °C for 30 minutes.
- After completion of the incubation period, P2 and P3 buffers were added as described in 2.2.3.1.
- Following centrifugation and transfer of the supernatant to a new Eppendorf tube, 100 µl of phenol/chloroform (pH = 7.5) was added to the supernatant and mixed by vigorous vortexing until the liquid showed a homogeneous milky appearance.
- The mixture was then centrifuged for 10 minutes and the supernatant was removed.
- Thereupon, as already in 2.2.3.1, an isopropanol precipitation and a washing step with 70% ethanol were performed, and then the dry pellet (60°C for 5 mins) was dissolved in 50 µl ddH_2O.
- Storage the sample at -20 °C.

2.2.3.3 Isolation of genomic DNA from *Streptomyces*

For the isolation of genomic DNA, a *Streptomyces* culture was prepared as described in 2.2.1.

- The *Streptomyces* culture was transferred to 1.5 ml Eppendorf tubes and the supernatant was removed after a centrifugation step, for one minute.
- The pellet was resuspended in 500 µl P1 buffer (+ 5 mg/ml lysozyme) by vortexing and then incubated for 30 min at 37 °C with occasional shaking.
- Then, 300 µl of 5% SDS solution and 3µl of proteinase K (30mg in 1.5 ml of TE buffer) were added and carefully mixed without vortexing.
- Following incubation for 15 minutes at room temperature, the tubes were incubated again for 15 minutes at 60 °C.

- At the end of the incubation period, 200 µl phenol/chloroform was added to the tube, mixed by vigorous vortexing until the liquid showed a homogeneous milky appearance.
- After addition of 1:10 of the volume of 3 M sodium acetate (approx. 80 µl), the samples were shortly mixed by vortexing and centrifuged for 10 minutes.
- Subsequently, the upper phase (~750µl) was carefully removed with a pipette and transferred to a new Eppendorf tube.
- 1 x the volume of 100% isopropanol (approx. 750 µl) was added, mixed and centrifuged for 15 minutes and the supernatant was removed carefully.
- The pellet was then washed with approx. 500 µl of 70% ethanol and vortexed.
- Following centrifugation for five minutes, the supernatant was discarded and ~200 µl of ddH_2O was added to the pellet.

  Note: The pellet should not dry extensively by incubation at 60°C before addition of ddH_2O.
- Finally, the remaining ethanol was evaporated by incubation at 60 °C for ~5 minutes.

2.2.4 Restriction digestion

Restriction endonucleases are enzymes isolated from bacteria that recognize specific sequences in DNA and then cut the DNA at those positions. Plasmid DNA was digested for cloning using restriction enzymes. Moreover, plasmids were isolated after transformation of *S. lividans* protoplasts or *E. coli* cells and verified in a control digestion. For the restriction digests, the approaches listed in the below Table 2.2.1. After preparation of the restriction reaction, the sample was incubated at 37 °C for 30mins.

Table 2.2.1: Composition for the restriction reaction.

Component	Amount
Plasmid DNA	7-10µl
Restriction buffer (10x)	1.5µl
Restriction enzyme	0.5µl
ddH_2O	X µl (up to 15µl)
Total	15 µl

At the end of the incubation period, 5 µl of the mixture was collected for an Agarose gel electrophoresis. If necessary, the restriction enzymes were inactivated by heat treatment at 65°C.

2.2.5 Agarose gel electrophoresis

For agarose gel electrophoresis, standard 1% agarose gels in TrisAcetate-EDTA (TAE) buffer (Table 2.1.5) were used. Samples were mixed with 3-5 µl of BPB loading buffer to increase density. The GeneRuler 1 kb DNA ladder was used as a size standard (see Figure 2.1). After application of the samples, electrophoresis was performed at 90 V for approximately 30 minutes and the agarose gel was stained in an ethidium bromide staining bath for 15-20 minutes. Gel documentation was performed using the blue/green LED transilluminator (312 nm) from NIPPON Genetics Europe.

2.2.6 Sequence analysis

Plasmid DNA was not only checked by control digestions, but also verified by sequence analysis. For this purpose, 5-10 µl of plasmid DNA (based on the DNA band in Agarose gel electrophoresis) was mixed with 5-10 µl of ddH_2O in an Eppendorf tube (total volume was 15µl). In addition, 15 µl of the 1:10 dilution (c= 0.1 pmol/µl) of the sequencing primer was pipetted into another tube. Both reaction tubes were sent to Eurofins Germany GmbH, which subsequently carried out the sequencing.

2.2.7 DNA transfer

2.2.7.1 DNA transfer into *E. coli*

Microorganisms can acquire new genetic material by conjugation, transduction and transformation. In case of conjugation the DNA is transferred directly from donor to recipient (upon contact). During transduction, the DNA is carried by bacteriophages, which infect a bacterial cell and introduces the DNA into the host. Transformation involves the uptake of naked DNA from the extracellular environment through the cell membrane. The transport of DNA by transformation occurs naturally (natural competence) or is triggered by artificial methods (artificial competence). The cell membrane permeability can be enhanced by different procedures, e. g. calcium chloride treatment. The most commonly techniques to introduce genetic material into *Streptomyces* cells are protoplast transformation and intergeneric conjugation.

2.2.7.1.1 Production of CaCl2-competent cells

(Cohen et al., 1972)

Treatment with $CaCl_2$ increases the permeability of the bacterial cell membrane for the uptake of free DNA molecules and enables transformation. Low-concentration shuttle plasmid DNA isolated from *Streptomyces* can thus be expressed in *E. coli* and isolated from it more easily.

- Inoculate a pre-culture of 20 ml LB medium with *E. coli* (XL1-blue or Novablue and Stellar) and grow overnight at 37°C and 180 rpm in an incubator shaker (Infors Multitron).
- Add 10 ml of *E. coli* (overnight culture) to ~190 ml of sterile LB medium. Incubate the culture at 37°C in an incubator shaker at 180 rpm (Infors Multitron) until OD_{578}= 0.5-0.8.
- Distribute the culture onto four 50 ml Falcon tubes.
- Centrifuge for 10 min at 5,000 rpm. Perform all following steps at 4°C.
- Discard supernatant and resuspend the pellet in 10 ml of ice-cold sterile 50 mM $CaCl_2$.
- Centrifuge the cell suspension at 4°C for 10 min at 5,000 rpm.
- Discard the supernatant and resuspend the pellet in 20 ml of ice-cold sterile 50 mM $CaCl_2$.
- Centrifuge for 10 min at 5,000 rpm and discard the supernatant

- Resuspend pellets in 2 ml $CaCl_2$ solution (+15 % glycerol).
- For long-term storage, dispense 200 µl aliquots into pre-cooled, sterile 1.5 ml Eppendorf tubes.
- Perform shock freezing of the cell aliquots in pre-cooled 100% ethanol at -70°C
- Store at -70° C until needed

2.2.7.1.2 Protocol for transformation of *E. coli* $CaCl_2$-competent cells

(Morrison, 1979)

- Thaw an aliquot (200 µl) of $CaCl_2$-competent cells on ice
- Add the plasmid DNA or the ligation reaction (max. 10 µl) to the competent cells and mix gently.
- Incubate on ice for 30 min
- Perform a 2 min heat shock at 42°C in a heating block
- Add 1 ml sterile LB medium and mix the sample by inverting.
- Incubate 60 min at 37°C.
- Centrifugate 1 min at 14,000 rpm.
- Discard the supernatant.
- Resuspend the pellet in the remaining medium and plate the suspension on agar plates containing the respective antibiotic for selection of clones carrying the transferred plasmid.
- Incubate the agar plates overnight at 37°C.

2.2.7.2 DNA transfer into *Streptomyces*

One commonly used technique to introduce DNA into *Streptomyces* is the protoplast transformation. To obtain protoplasts, the peptidoglycan of *Streptomyces* cell wall has to be degraded by lysozyme under isotonic conditions. After this treatment, the protoplasts are prepared for the polyethylene glycol (PEG)-mediated DNA-uptake

2.2.7.2.1 Protocol for the preparation of protoplasts

(Thompson et al., 1980)

- Inoculate 10-20 µl of *Streptomyces* spores into 100 ml of TSB medium + 0.7% glycine or S medium with appropriate antibiotics (if necessary) and incubate for two days at 37 °C and 180 rpm on a rotary shaker (described in: 2.2.1 cultivation of *Streptomyces*).

- Fill the culture into two 50 ml Falcon tubes.
- Centrifuge for 10 min at 4 °C and 5,000 rpm. Discard the supernatant.
- Resuspend the mycelium by shaking in 20 ml of sterile-filtered P-buffer containing 1 mg/ml lysozyme.
- Incubate the cells 15-20 min at 37°C in an incubator shaker and monitor protoplast formation by microscopy.
- Fill up to 50 ml with cold P buffer to stop lysozyme activity.
- To separate the protoplasts from mycelial residues, filter the solution trough sterile cotton.
- Centrifuge for 10 min at 4 °C and 5,000 rpm.
- Discard the supernatant gently and resuspend the pellet with 0.5ml-2ml of ice-cold sterile P-buffer
- Prepare 200 µl aliquots into pre-cold, sterile 1.5 ml microcentrifuge tubes.
- Storage at -20 °C.

2.2.7.2.2 Protocol for PEG-mediated protoplast transformation

(Kieser et al., 1982)

- Use 200 µl fresh protoplast sample or thaw protoplasts on ice.
- Add 3-5 µl DNA per aliquot and immediately add 500 µl T-buffer.
- Pipette up and down once with the pipette.
- Distribute and plate the suspension onto R5 agar plates (minimum 5-6 agar plates).
- Incubate the agar plates for 16 h at 29 °C.
- Overlay each plate with 1 ml of ddH_2O with 25 µl of the appropriate antibiotic for selection of clones containing the transferred DNA.
- Incubate the agar plates for another 3-5 days at 29 °C.

2.2.8 Mating experiments

In the mating experiments, $1x10^6$ spores of two *Streptomyces* strains, a plasmid-containing donor and a plasmid-free recipient, were plated out on R5 agar. The volume required for the $1x10^6$ spores was calculated using the following formula.

- $1x10^6$ spores (ml) = (10^6 / titer of the spore suspension)

With the respective titer of the spore suspensions, $1x10^6$ spores of donor and recipient were pipetted separately into an Eppendorf tube containing 100 µl ddH_2O, mixed and plated onto R5 agar (no antibiotic) and incubated for 7-8 days at 29 °C. Each mating was performed in triplicates. After incubation, spores were washed off with 3 ml ddH_2O, filtered through sterile cotton and transferred to an Eppendorf tube. The tube was centrifuged at 14,000 rpm for 2 min, the supernatant discarded, and the pellet resuspended in 1 ml of 20% glycerol. It was important that spore suspensions did not heat up too much during the wash-off process. The spores were handled on ice and stored at -20 °C for further used.

To determine the respective titer of donor, recipient, and transconjugants, serial dilutions (1:10 dilution) were prepared and plated onto LB agar supplemented with the appropriate antibiotics. Trans-conjugants are recipients, which have received a plasmid or chromosomal markers from the donor during mating.

From the respective titer, plasmid transfer rates and transmission rates of chromosomal markers can be calculated by dividing the transconjugant titer through the $1e*10^6$ spores (ml) = (10^6 / titer of the suspension)

2.2.9 Stability test of the SCP2-tetO and SCP2-tetOΔ*parA* plasmids.

Because the plasmids SCP2-tetO and SCP2-tetOΔ*parA* are single-copy plasmids (Thoma et al., 2016) and difficult to isolate from *Streptomyces* in good quality, the plasmids were isolated from *Streptomyces* and introduced into *E. coli* strain Novablue by transformation. The plasmids were re-isolated and checked by restriction analysis using the enzyme *MluI*, as described in Table 2.2.1., to confirm identity. After digestion each sample was mixed with 5 µl loading buffer bromophenol blue and checked by agarose gel electrophoresis. Thus, bands with the following size should be seen:

SCP2-tetO: 14008, 4775, 4001, 3753, 2805, and 1212 bp

SCP2-tetOΔ*parA*: 14008, 4775, 4060, 3753, **1887**, and 1212 bp.

To characterize the effects caused by the *parA* deletion in vegetative mycelium, the frequency of plasmid loss was determined. To ensure that the starting mycelium contains the respective plasmids, spores of JT46::pTetRmCherry(pSCP2tetO) and JT46::pTetRmCherry(pSCP2tetO Δ*parA*) were harvested from MS media containing antibiotic apramycin$^{50mg/ml}$, kanamycin$^{50mg/ml}$ and thiostreoton$^{25mg/ml}$ and used for inoculation. To analyse stability of plasmid SCP2tetO and pSCP2tetOΔ*parA* during vegetative growth, a liquid culture of *S. lividans* JT46::pTetRmCherry(pSCP2tetO) and JT46::pTetRmCherry(pSCP2tetOΔ*parA*) was grown at 29°C for 2 days on a rotary shaker in 100ml of TSB+0.7% glycine medium without any antibiotic. Then, the protocol for protoplast preparation described in method section 3.7.2.1 was followed. Freshly, prepared protoplast (100µl) then diluted with 500µl P-buffer and plated on five R5 agar plates without any antibiotics. After incubation of these plates at 29°C for 2 days, 100 single colonies were picked in parallel on LB agar and LB thiostrepton$^{25mg/ml}$ agar plates using sterile toothpicks. The number of grown colonies were counted after 2-3 days of incubation at 29°C.

2.2.10 Preparation and incubation of JT46::ptetRmCherry(SCP2-tetO) and JT46::ptetRmCherry(SCP2-tetOΔ*parA*) for fluorescence microscopy.

2.2.10.1 Obtaining the samples

S. lividans strains JT46::ptetRmCherry(SCP2-tetO) and JT46::ptetRmCherry(SCP2-tetOΔ*parA*) were grown on a cellophane membrane placed on LB agar supplemented with thiostrepton, kanamycin, and apramycin to select for the presence of intact plasmids and anhydrotetracycline, to induce transcription of *tetRmCherry*. After an incubation period of 2 days at 29°C, the grown mycelium was scraped off from the cellophane membrane with pipette tips and frozen in PBS containing 20% glycerol and stored at -20°C. Before use, the mycelium was transferred to a new Eppendorf tube containing 100 µl PBS with 20% glycerol and then homogenized (by rod-shaped steel homogenizer; supplementary data Figure 6.1).

2.2.10.2 Preparation of samples for fluorescence microscopy

To visualize plasmid and chromosome positions in living mycelium, the cultures were grown on agar plates. However, the mycelium applied for fluorescence microscopy must not contain any agar remains due to the high autofluorescence of agar. To direct growth of the *Streptomyces* mycelium in a two-dimensional plane, coverslips were inserted halfway into the agar at a 45° angle with tweezers. The cover slips had been washed with 70% ethanol and ddH_2O for sterilization purpose. The R5 agar plates were prepared thicker (~35 ml), which helps to insert half of the coverslips. For antibiotic selection, kanamycin and thiostrepton were used. About 5 to 15 µl of homogenized mycelium were pipetted onto the upper edge of coverslip, between the agar and the coverslip (Figure 2.2.1, blue arrows). To allow spore germination and vegetative growth as substrate mycelium, the plates were incubated at 29°C for 16-20 hours. After that, the coverslip with the attached mycelium was removed and the opposite site of the coverslip was cleaned with 70% ethanol and ddH_2O using lens tissue paper.

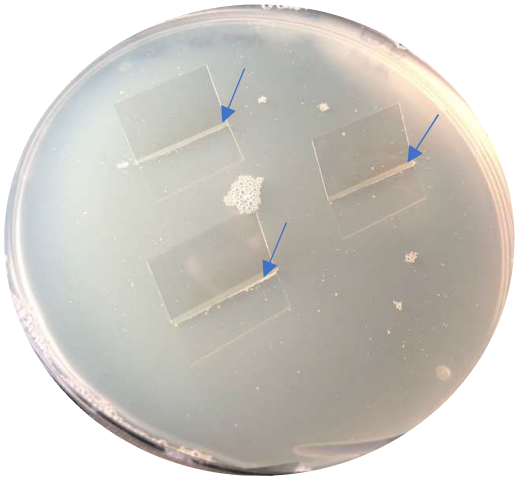

Figure 2.2.1: Sample preparation in a thicker R5 agar plate for fluorescence microscopy. Blue arrows indicate the edges of cover slip and nutrient agar media. The homogenized sample(s) were pipetted to that area.

2.2.10.3 Preparation of time-lapse microscopy

After 16-20 hours of incubation, the prepared samples were viewed under the fluorescence microscope. If a coverslip was found that fits optimally, an equivalent one was taken for processing for time-lapse microscopy. In addition, minimal medium supplemented with trace elements (described in 2.3) was prepared with 1% agarose, instead of agar and kept at 60°C.

2.2.10.4 Preparation of the microscope slide for time-lapse microscopy:

a. A microscopic micro meter metal slide (7.6 x 2.6 cm) having a round hole in the middle (Figure 2.2.2) was taken under sterile conditions.
b. The micro meter metal slide was cleaned with 70% ethanol and ddH_2O.
c. The plastic foil from a gene frame (Thermo scientific, AB-0576; 1.0 x 1.0 cm) was carefully removed without causing disassembly of the plastic cover on the other side of the gene frame.
d. The gene frame was gently attached in the middle of the metal slide by first facilitating contact on just one side, followed by guided attachment of the remaining gene frame with a sterile pipette tip (200µl). It was important to prevent air bubbles while attaching the gene frame to the metal slide. Make sure that the gene frame is tightly attached around the hole, but not blocking the hole.
e. After that, the second plastic cover from the gene frame was removed to expose the sticky side top on the gene frame.
f. Meanwhile, the polyester frame was uncovered (remove the thin plastic) using tweezers and washed with 70% ethanol and ddH_2O.
g. The polyester membrane frame was carefully attached to the surface of the sticky gene frame and fixed using a pipette tip. The tip should not stretch the polyester frame in the middle but should only be softly applied in the area of gene frame to prevent air bubbles.
h. Then a second gene frame was attached to the same position of the previous gene frame on the surface polyester membrane leaving a hole in the middle.

i. Next, 70 µl of sterile minimal agarose media (1%, kept at 60°C) were pipetted on the top of the membrane in the middle of the gene frame.
j. A sterile glass slide (washed with 70% ethanol and ddH_2O) was placed on the agarose filled gene frame and fixed for few seconds (20-30sec) avoiding formation of air bubbles.
k. Finally, the sandwiched slides were kept at least for 20 min at 4°C to allow the agarose to solidify sufficiently.

Sample preparation for microscopy slide assemble

l. The cover slip with the attached mycelium was carefully removed from the R5 agar and the opposite site was cleaned with 70% ethanol and distilled water using lens tissue paper.
m. After step k; the upper glass slide was carefully removed and any agarose medium was cut off from the outside of the gene frame with a razor blade.
n. Then, the second plastic cover from the gene frame was removed to expose the sticky side of the gene frame.
o. The cover slip with the attached mycelium has then to be placed on the agar, making sure that the mycelium was in contact to the MM medium and the cleaned side was on the top. The cover slip was hold with tweezers and slowly placed on the agar (with the help of the other hand and a sterile pipette tip) from the attaching side (outside of the medium, only in the square surface or sticky region) to the end of the cover slip. The cover slip was slowly and gently fixed to the sticky gene frame using the tip. This technique helped to prevent formation of air bubbles while attaching the cover slide to the sticky gene frame.
p. Finally, the prepared slide was transferred into a sterile Petri dish and incubated at 29°C for 4-6 hours before observation in the time-lapse fluorescence microscope.

Time-lapse fluorescence microscopy program setup

r. Appropriate objectives, filters and dichroic mirror were selected according to the experimental set-up (described in acquisition information 3.11.5).
s. Before running the sample, I tried to pre-warm (29°C) the environmental chamber. Time-lapse microscope needed time to get the optimum temperature

that depends on the room temperature as well as the heating system and the microscope.

t. Microscope software ZEISS ZEN (blue edition) Programmed for this experiment was set-up by Dr. rer. nat. Lina Thoma as described in 2.2.10.5.

u. The prepared slide was placed in the pre-warmed environmental chamber of the microscope to conduct time lapse-imaging.

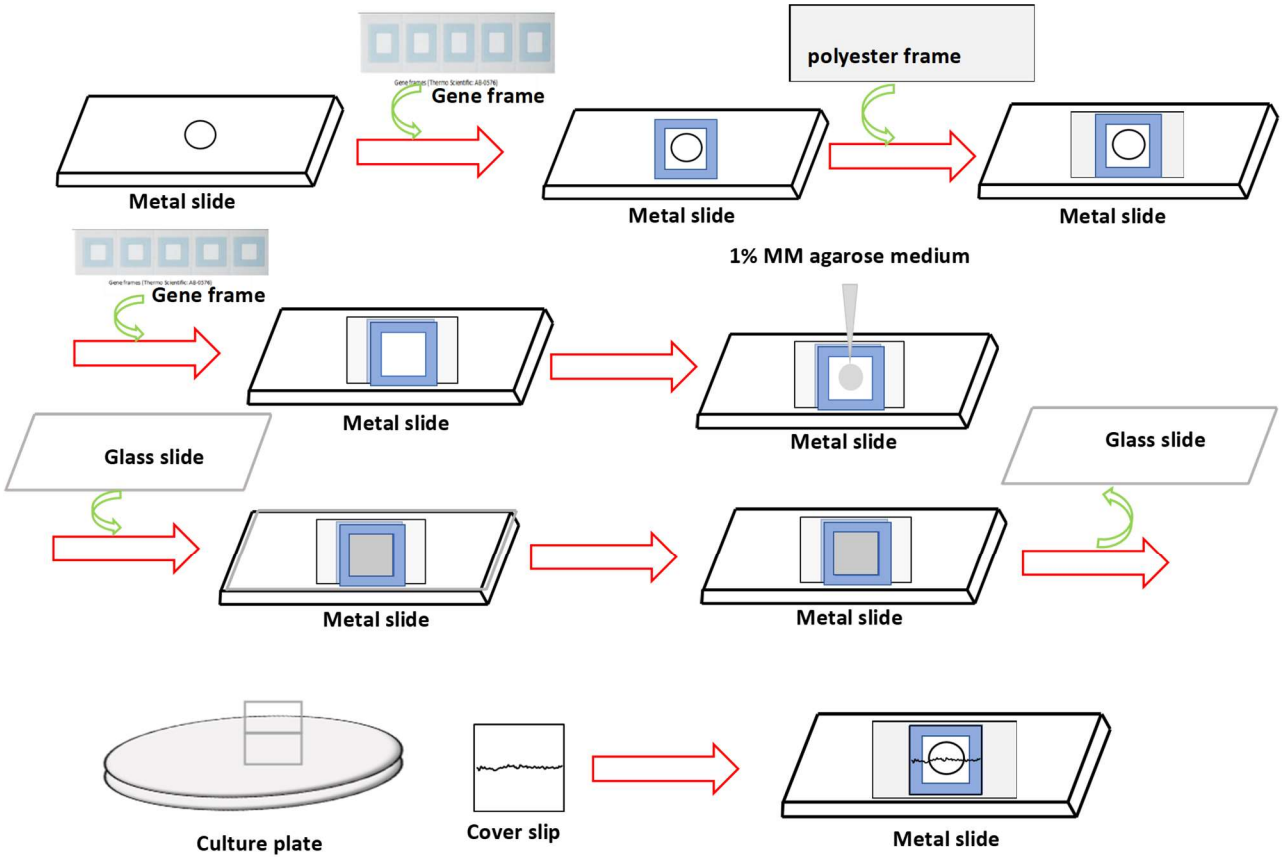

Figure 2.2.2: A step-by-step guide to microscope slide assembly for time-lapse and fluorescence microscopy.

2.2.10.5 Acquisition Information:

- Microscope: Zeiss (Axio Observer.Z1/7)
- Objective: alpha Plan-Apochromat 100x/1.46 Oil (UV) Ph3 M27
- Filters: 540 - SSO, 593 - 668,450 - 490, 500 - 550

	Channel1	**Channel2**	**Channel3**
Reflector	FCZ3_mCherry	FCZ2_eGFP	None
Beam splitter	585	495	
Filter Ex. Wavelength	540-580	450-490	
Filter Em. Wavelength	593-668	500-550	
Contrast Method	Fluorescence	Fluorescence	Phase
Light source	HXP 120V	HXP 120 V	TL Halogen Lamp
Light Source Intensity	75.00 %	30.00 %	3.50 Volt
Channel Name	mChery	eGFP	Phase
Excitation Wavelength	587	587	
Emission Wavelength	520	650	
Effective NA	1.46	1.46	1.46
Imaging Device	Hamamatsu Camera	Hamamatsu Camera	Hamamatsu Camera
Camera Adapter	1x Camera Adapter	1x Camera Adapter	1x Camera Adapter
Exposure Time	500.02 ms	125.02 ms	20.01 ms
Depth of Focus	0.87 µm	0.87 µm	0.78 µm
Binning Mode	1.1	1.1	1.1

- Image Dimensions:
  - Channels: 3 (mCherry, eGFP and Phase contrast)
  - Scaling (per pixel): 0.065µm x 0.065 µm
  - Image Size (Pixels): 27012 x 101877
  - Image Size (Scaled): 1.76 mm x 6.62 mm
  - Bit Depth: 16 Bit
  - For analysis: FIJI or ImageJ

❖ Microscope: Nikon Eclipse Ti automated

In parallel, I also used a Nikon Eclipse Ti automated microscope equipped with a perfect focus system (Nikon Instruments Europe BV, Netherlands), an Orca Flash 4.0 camera (Hamamatsu, Photonics, Japan) or Prime BSI camera (Teledyne Photometrics, United States), and CFI Plan-Apo DM 100×/1.45 Oil Ph3 objective (Nikon) or CFI Apo TIRF 100×/1.49 Oil objective (Nikon) with the external Phase Contrast (Nikon; Phaseplate PH3).

- HC Filter sets (IDEX/Semrock, USA): EGFP excitation 472 nm, emission 520 nm; Texas Red excitation 555 nm, emission 617 nm.
- For time-lapse: Software to automatically control the microscope (time series, focus stabilization, trigger for laser and bright field illumination, and positions).
- For analysis: FIJI or ImageJ

2.2.11 Measurement of hyphal contact angle

To measure the contact angle of *Streptomyces* hyphae using ImageJ or Fiji software, first the Angle tool was selected and a line was drawn along the first segment. Then, without releasing the mouse button, the cursor was dragged to the second segment and another line drawn. Upon release of the mouse button, the angle was displayed in the status bar at the bottom of the ImageJ window.

3. Results

3.1. Description of the FROS system used to localize plasmid SCP2 and the central chromosome region in *Streptomyces lividans* mycelium

Application of a TetR-based FROS system has been already described to localize chromosomal sequences of *S. coelicolor* (Kois-Ostrowska et al., 2016). In this system, the TetR-mcherry fusion protein was encoded by the integrative pMS83 plasmid (Figure 3.1), which confers hygromycin resistance. Since restriction analysis and partial sequencing of pMS83tetRmcherry showed differences to the published map and revealed the presence of *egfp*, probably included in a reduplicated DNA fragment, an improved construct (ptetRmcherry; Figure 3.2), based on pRM43 was constructed by L. Thoma (unpublished).

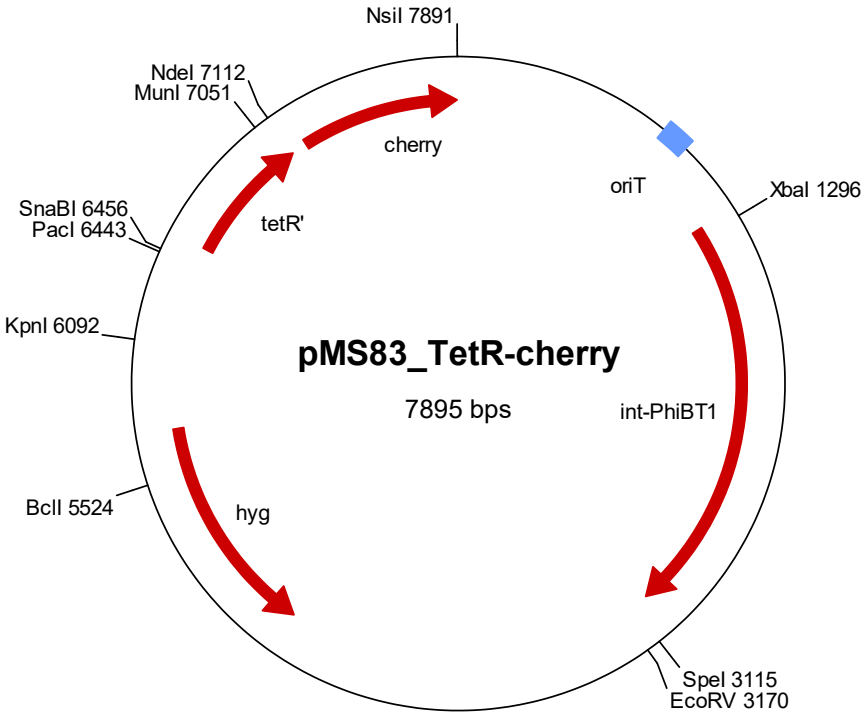

Figure 3.1: Map of pMS83tetRmcherry containing hygromycin resistant gene.

3.1.1. Expression of a codon-optimized TetRmcherry fusion gene (ptetRmcherry)

To construct ptetRmcherry, *tetR* was amplified from pMS82tetRmcherry and inserted into the *BamHI* site of pGM1192 (Muth, 2018), resulting in a translational fusion to the codon-optimized *mCherry* gene, which is under control of the strong constitutive SF14* promoter. Subsequently, the whole cassette was cut out and inserted into the integrative pRM43 (Menges et al., 2007) plasmid, yielding ptetRmcherry (Figure 3.2).

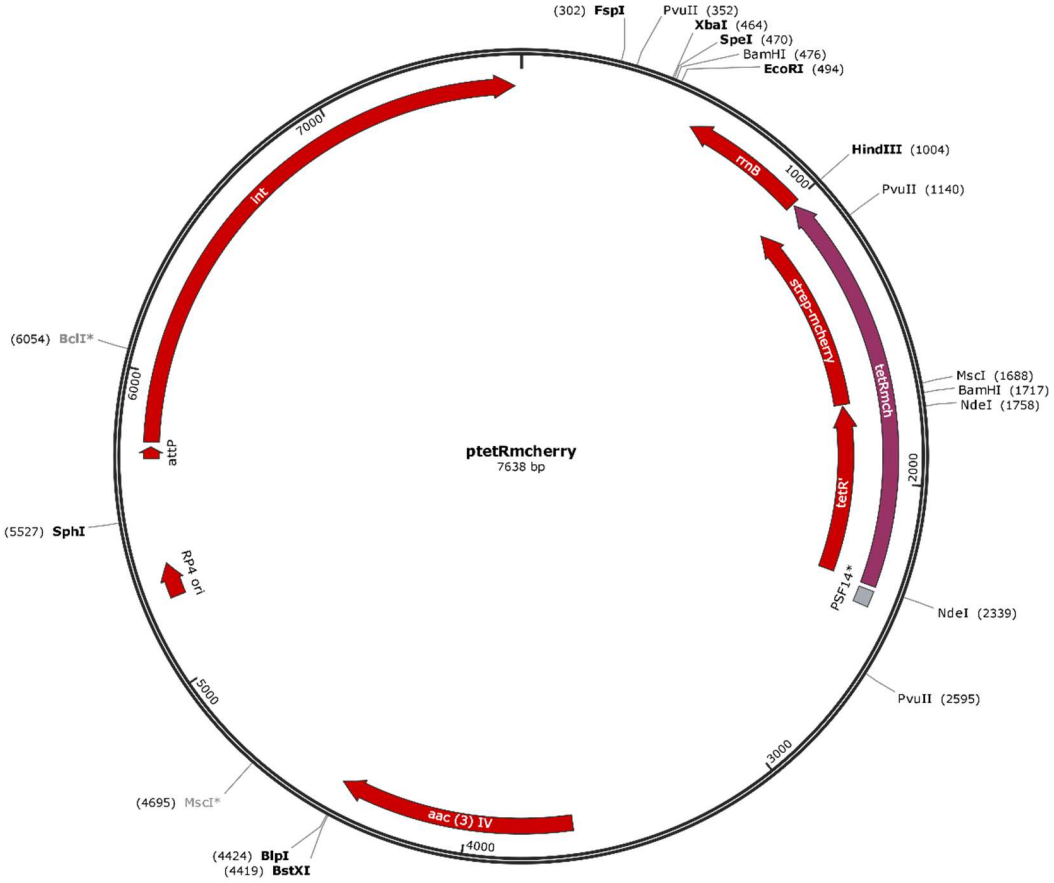

Figure 3.2: Map of ptetRmcherry.

When this plasmid was introduced into *S. lividans* and integrated into the chromosomal attachment site (SLI_4043) of the actinophage ΦC31 and when the resulting strain was observed by fluorescence microscopy, a faint non-localized red fluorescence throughout the whole mycelium was detected (Figure 3.3).

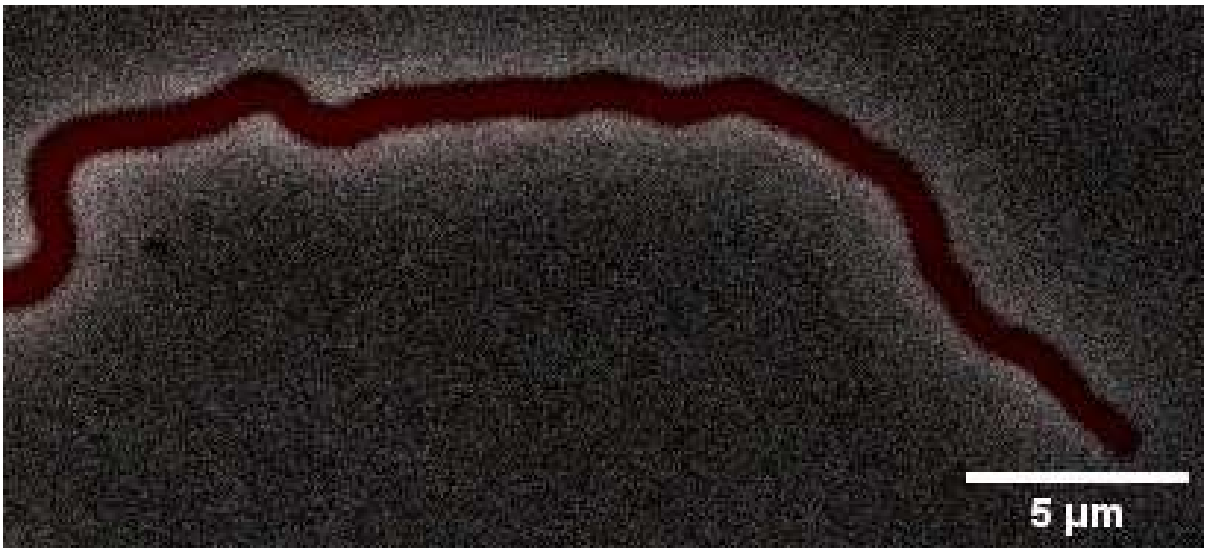

Figure 3.3: Microscopy image of *S. lividans* strain JT46::ptetRmCherry, showing faint red fluorescence in the living hyphae.

3.1.2. Labelling a bifunctional SCP2-derivative with a *tetO* array

The originally constructed SCP2 derivative pIJ903tetO contained the ColE1 replicon, as it is also present in ptetRmcherry. To avoid unwanted recombination, which would result in the integration of pIJ903tetO into the chromosome, the ColE1-part of pIJ903tetO was replaced by the CloDF replicon from pCDFduet. The resulting plasmid SCP2tetO contained a *tetO* array of 120 TetR binding sites. In addition, the *aphII* gene was inserted into the *tetO* array to enable selection (kanamycin resistance) for the presence of the *tetO* array (L. Thoma, unpublished).

Plasmid SCP2tetO was introduced into *S. lividans* JT46::pRM43tetRmcherry by PEG-mediated protoplast transformation. Observation by fluorescence microscopy showed distinct red fluorescence foci (Figure 3.4; red spots) caused by the binding of multiple TetRmcherry proteins to the *tetO* array of SCP2tetO.

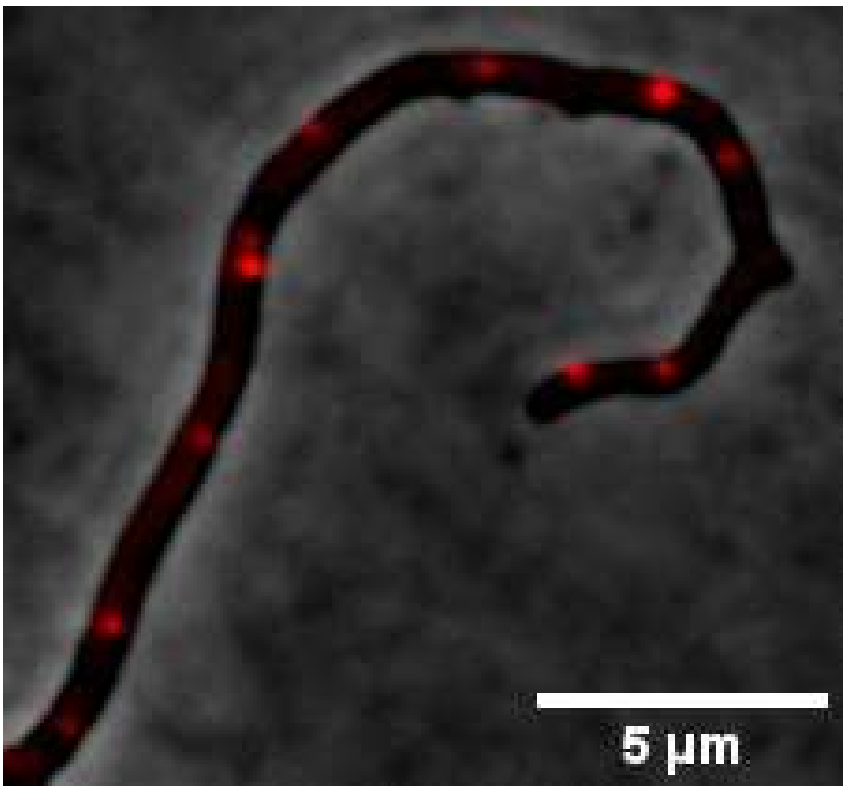

Figure 3.4: Visualization of plasmid SCP2tetO in living mycelium of *S. lividans* (strain JT46::ptetRmCherry:pSCP2tetO). Using the FROS system, the plasmid can be visualized in the living hyphae of *Streptomyces*. The red spots indicate the positons of the single copy number plasmids SCP2tetO that is bound the TetRmCherry protein.

3.1.2.1 Stability test of plasmid pSCP2tetO

To correlate the red fluorescence spots with plasmid copies, knowledge of the plasmid stability is important. The TetO array is known to cause plasmid instability. On the one hand, the *tetO* array can be deleted; in particular, the 3760 bp *XbaI* fragment was shown to suffer from deletions (R. Arndt, Bachelor thesis). On the other hand, the whole plasmid becomes eliminated, in particular during sporulation. Moreover, the binding of TetRmcherry to the *tetO* array of pSCP2tetO might interfere with the replication and stability of the plasmid. To analyse the stability of plasmid SCP2tetO during vegetative growth, a culture of *S. lividans* JT46::pTetRmCherry(pSCP2tetO) was grown for two days on a rotary shaker in TSB+0.7% glycine medium without any antibiotic. Following protoplasting of the mycelium to generate particles with a single genome and regeneration of diluted protoplasts on R5 medium, 100 single colonies were picked in parallel on LB and LB_thio25, respectively. Only 43,5% grew on thiostrepton containing agar, indicating the presence of the plasmid in these colonies.

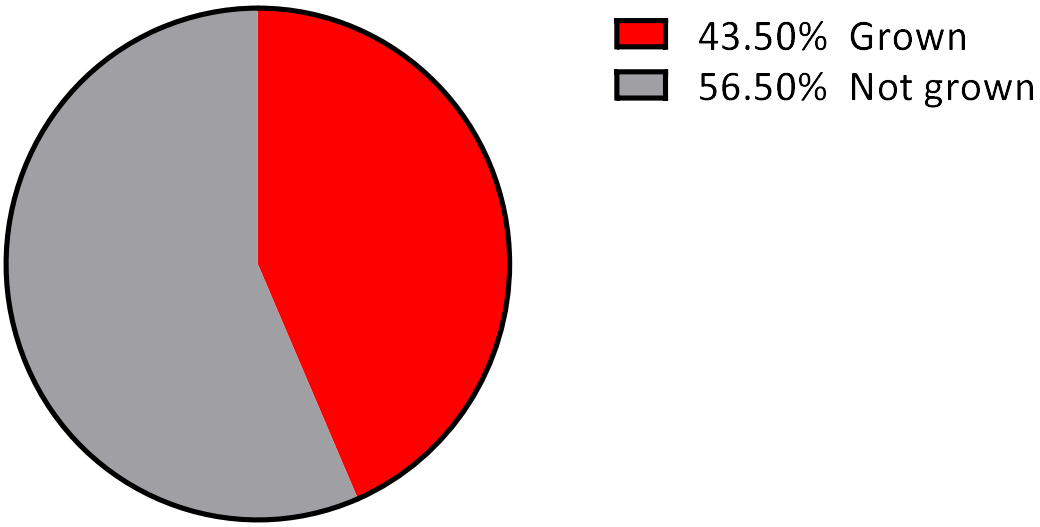

Figure 3.5: The percentage of thiostrepton-resistant (SCP2tetO-containing) and sensitive colonies derived from regenerating protoplasts is displayed in a pie chart. Percentage of plasmid loss in vegetative mycelium was calculated after the conversion of vegetative mycelium into protoplasts. Following regeneration on non-selective R5 agar, single colonies were picked in parallel on LB and LB_thio25, which indicates presence of SCP2tetO. Plasmid SCP2tetO was lost in 56.5 % of JT46::pTetRmcherry colonies. The experiment was performed in duplicate.

3.1.3. Labelling the chromosome of *S. lividans* at position SLI_5122 with a *tetO* array

To compare SCP2tetO localization data with chromosome localization, the same *tetO* array was cloned into plasmid pIJ12507, yielding pIJ12507-tetO (Figure 3.8). Plasmid pIJ12507 confers hygromycin resistance and integrates into *Streptomyces* chromosomes via the attachment site of the actinophage PhiBeta1. In *S. lividans,* the actinophage PhiBeta1 (ΦBT1) attachment site *attB* is located upstream of *SLI_5122* (nt: 5328063-5329373).

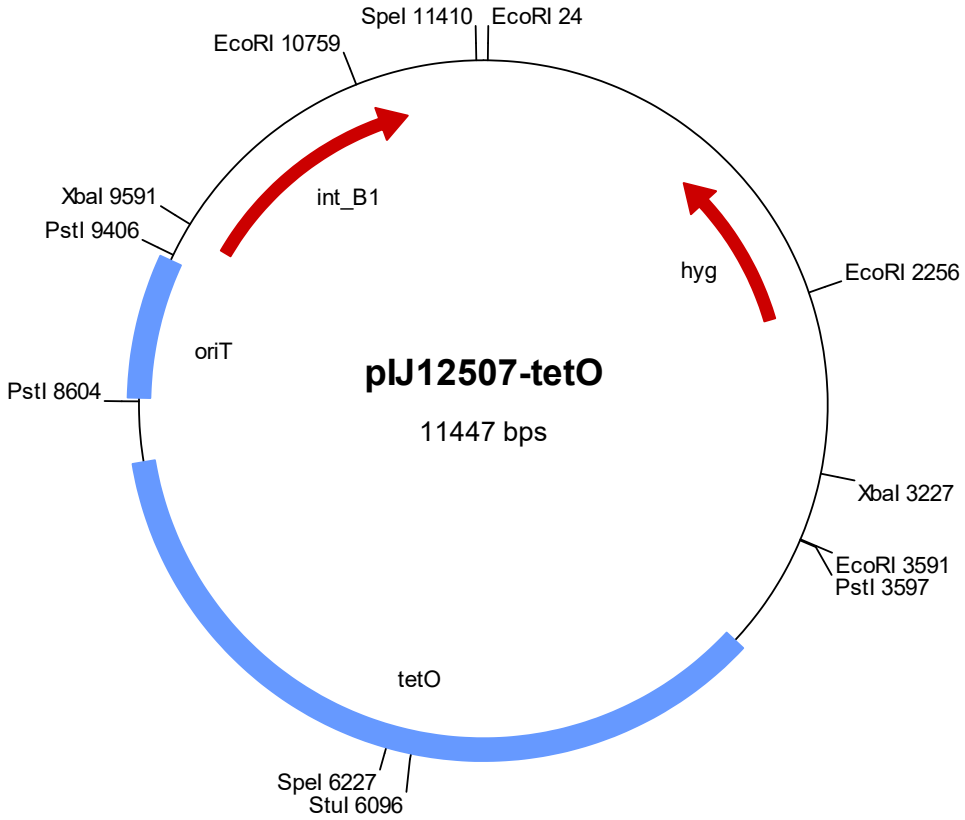

Figure 3.6: Map of pIJ12507-tetO

3.1.3.1 Localization of *Streptomyces lividans* chromosomal DNA in living mycelium

pIJ12075-tetO was introduced into *S. lividans* JT46::tetRmcherry by intergeneric conjugation and integrated into the genome. When the resulting strain JT46::tetRmcherry::pIJ12075-tetO was observed by fluorescence microscopy intense red fluorescence foci were observed, very similar to those caused by plasmid SCPtetO (Figure 3.9).

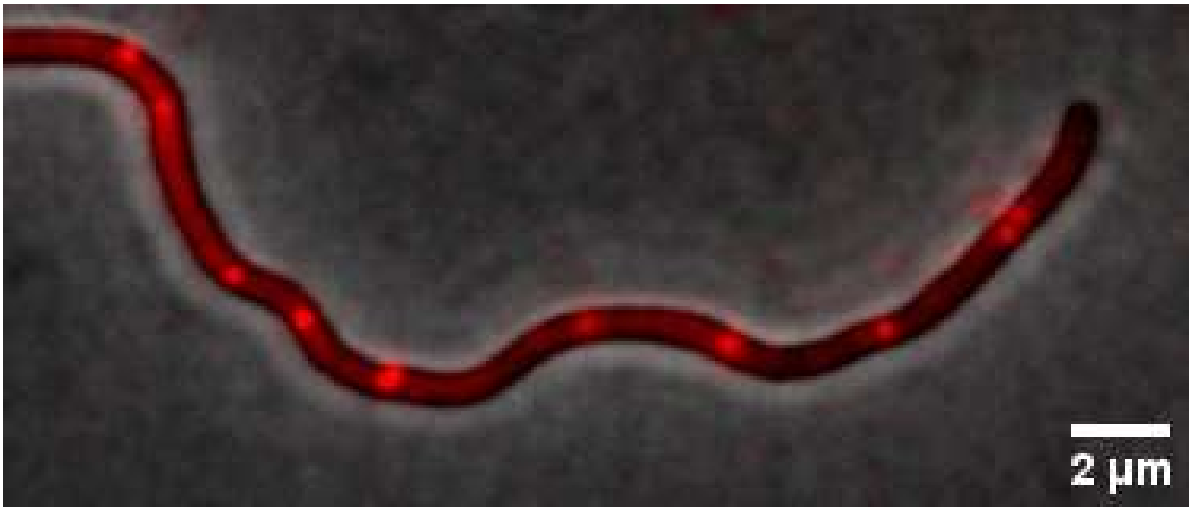

Figure 3.7: Localization of the chromosome in *S. lividans* JT46::tetRmcherry-::pIJ12507tetO mycelium. The mycelium was grown on the upper edge of a coverslip inserted at a 45° angle into R5 agar. After overnight incubation for 16-20 hours at 29°C, the mycelium samples were analysed under fluorescence microscopy using red channel (mCherry) and grey channel (Phase contrast) imaging. The software ImageJ was used to overlay both channel images. The position of the central region of the *S. lividans* chromosome is indicated by the red spots.

3.1.4 Measuring fluorescence intensity as an indication of TetRmcherry binding efficiency to *tetO* arrays located on plasmid and chromosome:

In the FROS system, *tetO* array (n=120 copies) is bound by an optimized TetR-mCherry fusion protein, resulting in red fluorescent foci, which can be visualized with fluorescence microscopy Images were processed by using the software FIJI or ImageJ. The fluorescence intensity was then quantified and measured within the living hyphae. The data were further analyzed and plotted using GraphPad Prism software. The significance was determined via one-way ANOVA

The software ImageJ or FIJI generates a graph showing fluorescence intensity along the selected region of the plasmid (Figure 3.4) and chromosome (Figure 3.7) with peaks, indicating areas of TetRmCherry binding to *tetO*-arrays. This type of analysis can be used to characterize the relative locations of plasmids and chromosomes within the living mycelium and to quantify the intensity of TetRmcherry binding to *tetO-arrays*.

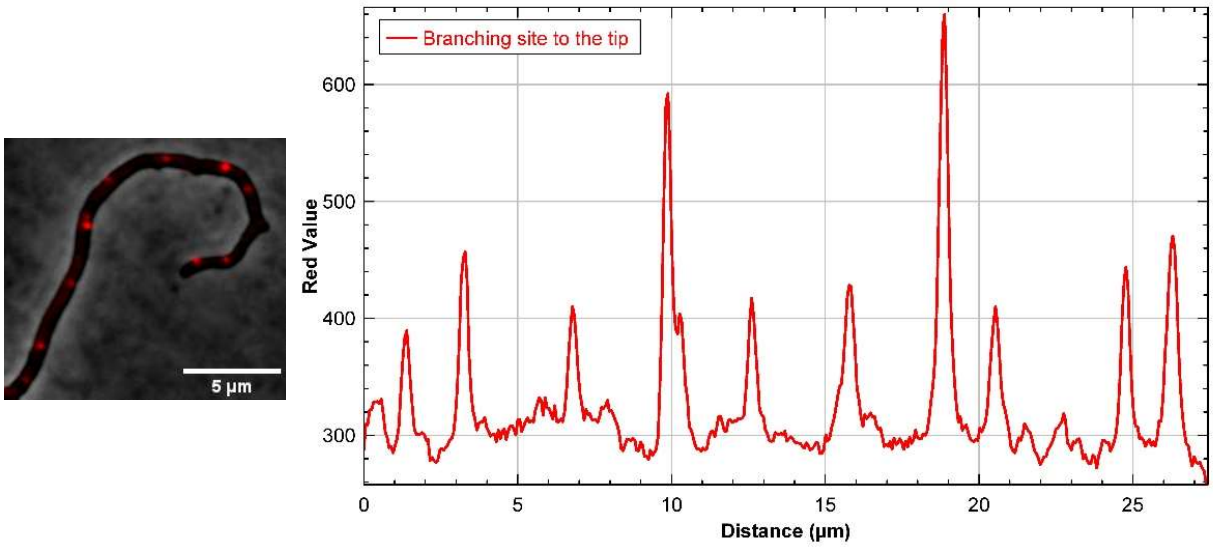

Figure 3.8: The graph plot profile indicating the intensity of red fluorescence spots from the plasmid visualization image (Figure 3.4) The intensity is measured from the selected region, in the direction of the branching site to the tip. The hyphal regions that do not contain a *tetO* array have an intensity value of <300, whereas the TetRmcherry binding to the *tetO* array has an intensity value of >350.

Similarly, the chromosome localization image (Figure 3.7) was used to determine the intensity of the red fluorescence spots (Figure 3.9). The binding of TetRmcherry to chromosome-localized *tetO* array had an intensity of >350 (-450), very similar to that caused by the binding to the SCP2tetO-localized *tetO* array.

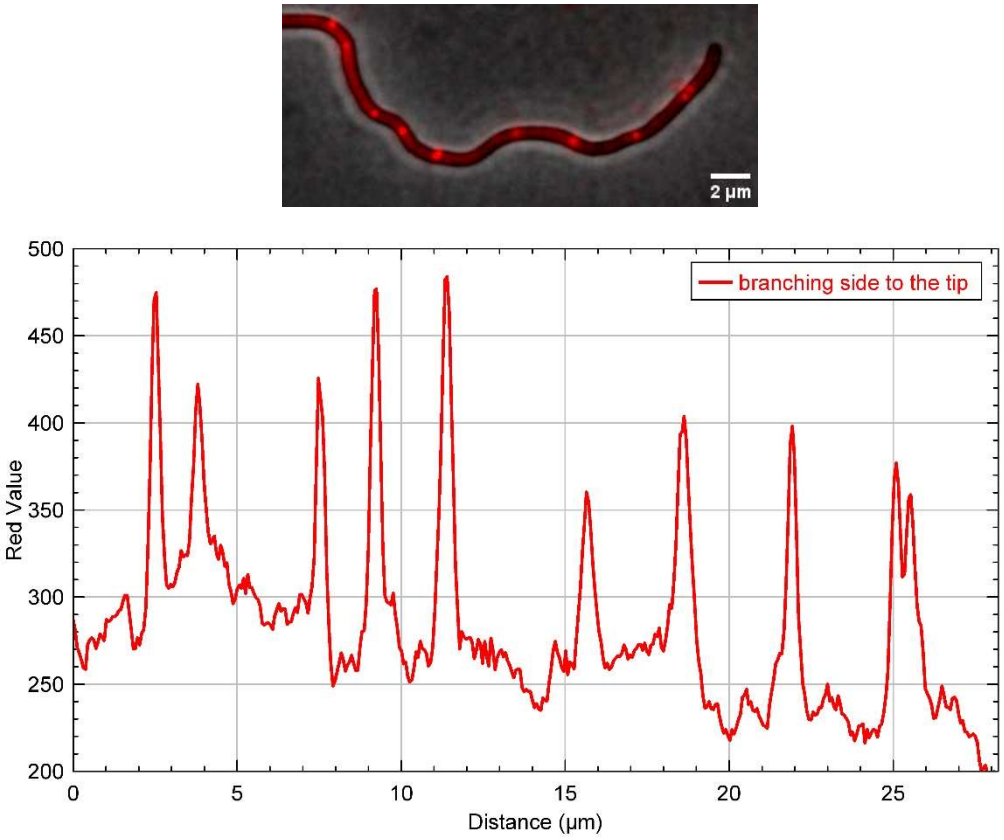

Figure 3.9: The graph plot profile displaying the red-spot intensity values generated from the chromosomal localization image shown in Figure 3.7. Each spot represents the peak of the graph, where the intensity of the red spot value is measured over 350. Intensity is measured from the branching site to the tip (left to right). At the tip region, two red spots are visible; it looks like the chromosome is replicated and has an almost similar intensity. Like as previous plot profile, without binding of *tetO* to the TetRmcherry, giving an intensity value of less than 250.

3.2. Localization of SCP2tetO in substrate mycelium in comparison to the chromosome

In contrast to unicellular bacteria, which divide by binary fission producing two nearly identical daughter cells, filamentous *Streptomyces* grows by apical tip extension and branching. It possesses two distinct modes of cell division: the formation of cross-walls in vegetative hyphae and the formation of sporulation septa in aerial hyphae. One could imagine that the position of a plasmid molecule and the chromosome might be influenced by these processes affecting the localization in different parts of the mycelium.

Therefore, SCP2tetO and the chromosome were localized by fluorescence microscopy in tips, at branches, in short-branched hyphae and long-branched hyphae. Strains were grown overnight at 29°C on R5 agar supplemented with respective antibiotics. Images were grouped into different classes according to the type of hyphal shape. For each hypha, the position of the plasmid and chromosome, respectively was detected, and its distance to the originating branch and the tip of the hypha was determined. Thus, the average position of SCP2tetO and that of the chromosome was calculated for each “hyphal class”.

3.2.1. Positions of SCP2tetO and the chromosome in short non-branched hyphae of *S. lividans*

The positions of plasmid SCP2tetO was determined in 37 short non-branched hyphae (table 3.1) and those of the chromosome in 34 hyphae (Figure 3.10, table 3.2). Based on the statistical analysis, the localization of plasmid SCP2tetO differed only slightly from that of the chromosome. The distance of plasmid SCP2tetO to the tip was 2.21 µm (± 0.99 µm), while the chromosome localized at a distance of 3.69 µm (± 2.86 µm) to the tip (Figure 3.10). Similarly, the distance between SCP2tetO and the branching site was 1.25 µm (± 1.01 µm) and 2.56 µm (± 1.85 µm) for the chromosome.

In summary, there were no significant differences in the localization pattern between the plasmid and the chromosome except at the tip, where the plasmid located closer to the tip than the chromosome.

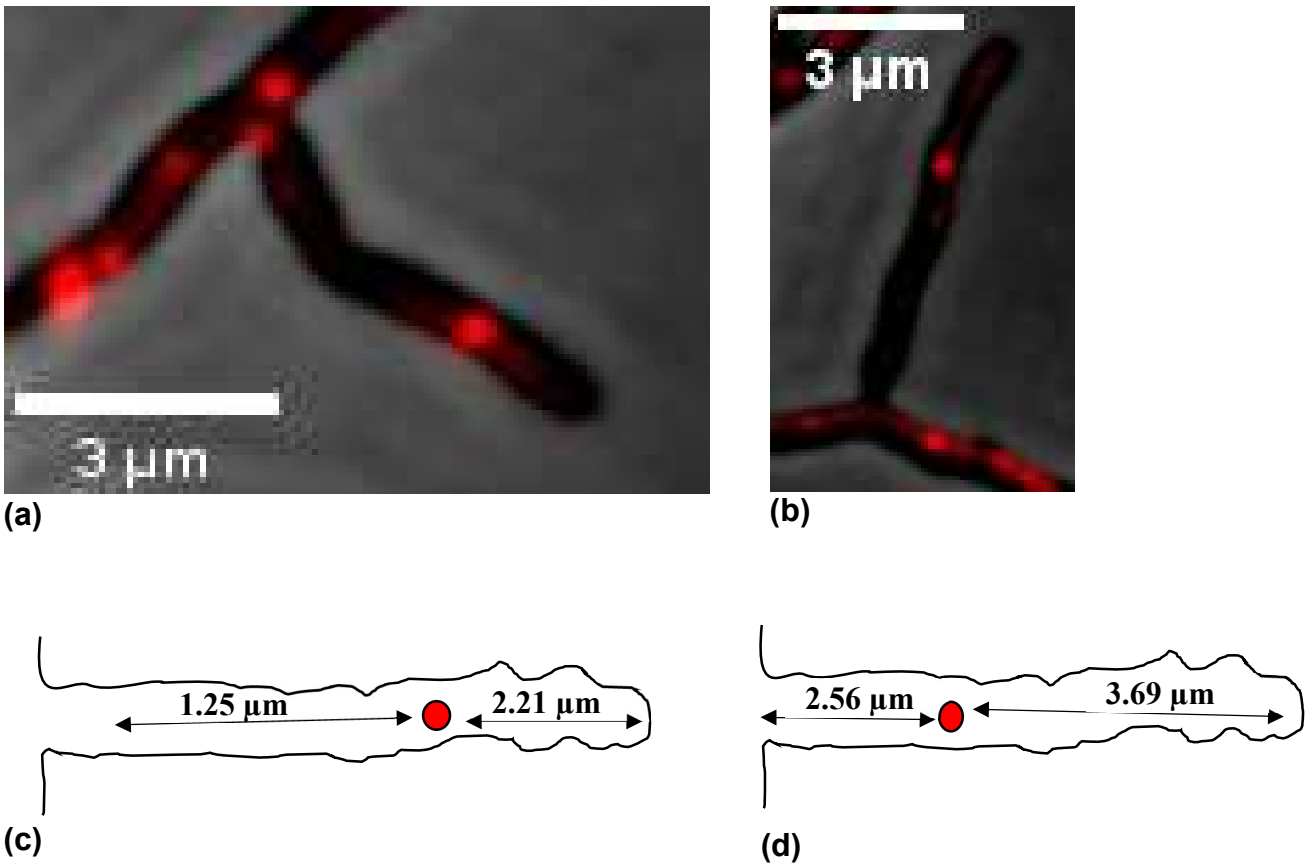

Figure 3.10: Localization of the single copy number plasmid SCP2tetO (a) and the chromosome (b) in short non-branched hyphae of *S. lividans* JT46::pTetRmcherry. (c) A schematic diagram illustrating the position (n=37) of plasmid SCP2tetO (d) and the chromosome (d, n=34).

Table 3.1: Position of the single copy plasmid SCP2tetO in non-branched hyphae of *S. lividans* JT46::ptetRmcherry

	tip to plasmid (µm)	plasmid to branching site (µm)	total length (µm)
Minimum	0.43	0	1.12
25% Percentile	1.38	0.51	2.45
Median	2.10	1.02	3.29
75% Percentile	**2.84**	**1.93**	**4.34**
Maximum	4.85	3.62	6.75
Mean	**2.21**	**1.25**	**3.46**
Std. Deviation	**0.99**	**1.01**	**1.40**
Std. Error of Mean	0.16	0.17	0.23
Lower 95% CI of mean	1.88	0.91	2.99
Upper 95% CI of mean	**2.55**	**1.58**	**3.93**

Table 3.2: Position of the chromosome in non-branched hyphae of *S. lividans* JT46::ptetRmcherry

	tip to chromosome spot (µm)	spot to branching site (µm)	total length (µm)
Minimum	0.91	0.34	1.89
25% Percentile	1.97	1.07	3.87
Median	2.80	2.19	5.18
75% Percentile	**4.29**	**3.36**	**7.75**
Maximum	12.32	8.35	18.34
Mean	**3.69**	**2.56**	**6.24**
Std. Deviation	**2.86**	**1.85**	**3.68**
Std. Error of Mean	0.49	0.32	0.63
Lower 95% CI of mean	2.69	1.91	4.96
Upper 95% CI of mean	4.68	3.20	7.53

3.2.2. Positions of SCP2tetO and the chromosome, when two copies were present in short non-branched hyphae of *S. lividans*

Next, I analyzed short hyphae containing two copies of SCP2 or the chromosome (Figure 3.11). The positions of SCP2tetO were determined in 28 non-branched hyphae (table 3.3) and that of the chromosomes in 16 hyphae (table 3.4).

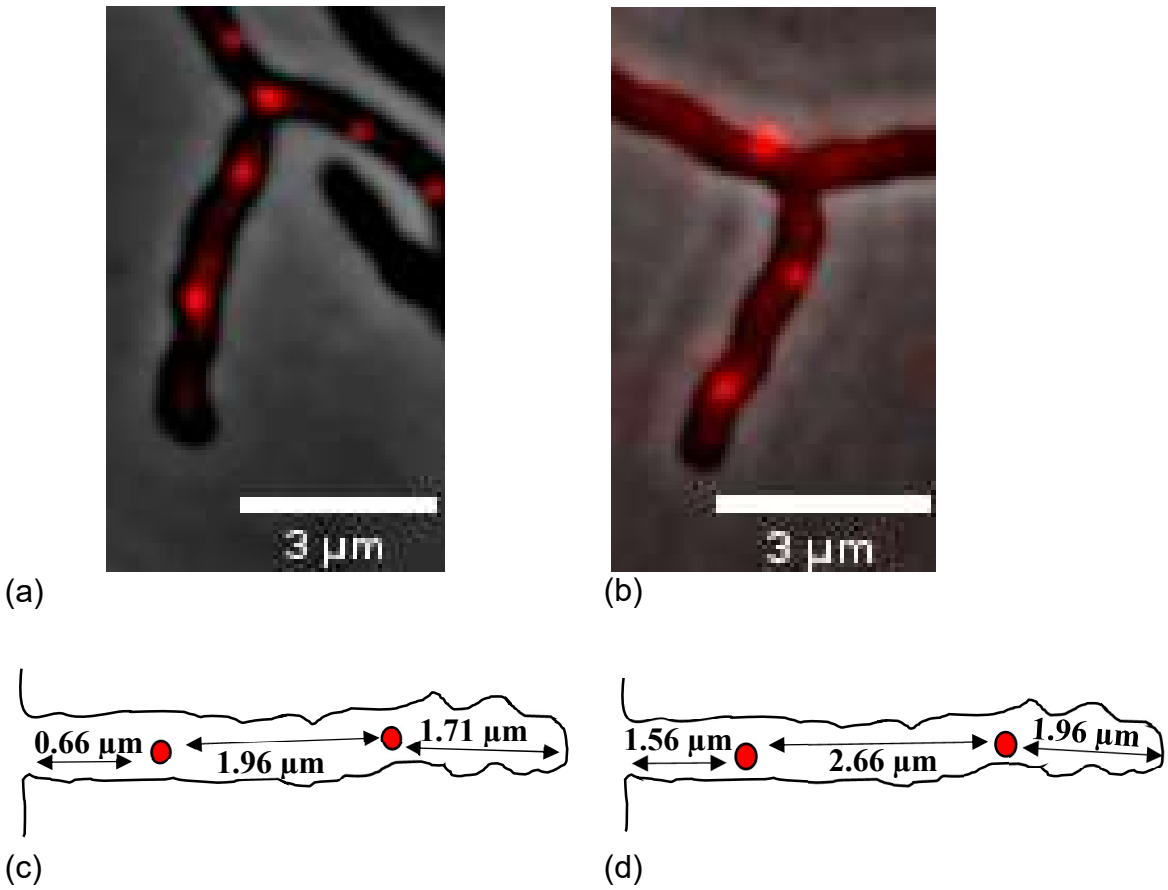

Figure 3.11: Distribution pattern of two copies of plasmid SCP2tetO (a) and two chromosome copies (b) in non-branched *Streptomyces lividans* hyphae. A schematic diagram showing plasmids positions (c) (n=28) (**Table 3.3**) and illustration of chromosomes distribution (d) in the hyphae (n=16) (**Table 3.4**)

Table 3.3: Positions of two copies of SCP2tetO in non-branched hyphae of *S. lividans* JT46::ptetRmcherry

	tip to plasmid1 (µm)	plasmid1 to plasmid2 (µm)	plasmid2 to branching site (µm)	total length (µm)
Minimum	0.48	0.38	0	0.89
25% Percentile	0.91	0.84	0	2.86
Median	1.49	1.68	0.55	3.81
75% Percentile	**2.08**	**3.09**	**1.00**	**5.26**
Maximum	4.75	4.65	4.16	13.56
Mean	**1.71**	**1.96**	**0.66**	**4.33**
Std. Deviation	**1.09**	**1.28**	**0.86**	**2.49**
Std. Error of Mean	0.21	0.24	0.16	0.47
Lower 95% CI of mean	1.29	1.47	0.33	3.36
Upper 95% CI of mean	**2.13**	**2.46**	**0.98**	**5.29**

Table 3.4: Positions of two chromosome copies in non-branched hyphae of *S. lividans* JT46::ptetRmcherry

	tip to spot1 (µm)	spot1 to spot2 (µm)	spot2 to elongation site (µm)	total length (µm)
Minimum	**0.80**	**0.72**	**0.23**	**3.46**
25% Percentile	1.14	1.67	0.59	4.18
Median	1.75	2.41	1.33	5.57
75% Percentile	2.67	3.24	1.95	8.01
Maximum	**3.92**	**7.22**	**5.85**	**11.31**
Mean	**1.96**	**2.66**	**1.56**	**6.18**
Std. Deviation	**0.96**	**1.66**	**1.35**	**2.41**
Std. Error of Mean	0.24	0.41	0.34	0.60
Lower 95% CI of mean	1.44	1.78	0.84	4.89
Upper 95% CI of mean	2.47	3.55	2.28	7.46

The plasmid SCP2tetO position was determined in 28 short non-branched hyphae (table 3.3), while the chromosome position was determined in 16 hyphae (table 3.4). The statistical analysis showed that the distribution of the plasmid SCP2tetO in the mycelium was slightly different from the chromosome's distribution. Specifically, I found that the distance between two SCP2tetO plasmids was 1.96 µm (± 1.28 µm), while the distance between two chromosomes was 2.66 µm (± 1.66 µm). Moreover, the distance from the tip to the first copy of plasmid SCP2tetO was 1.71 µm (± 1.09 µm), while it was for the chromosome 1.96 µm (± 0.96 µm).

The distance of the branching site to the first copy of the plasmid SCP2tetO was 0.66 µm (± 0.86 µm), and that of the chromosome 1.56 µm (± 1.35 µm),

In summary, I did not observe any significant differences in the localization of the plasmid and the chromosome, except at the branching site, where the plasmid was closer to the branching site than the chromosome.

3.2.3. Positions of SCP2tetO and the chromosome, when multiple copies were present in long non-branched hyphae of *S. lividans*

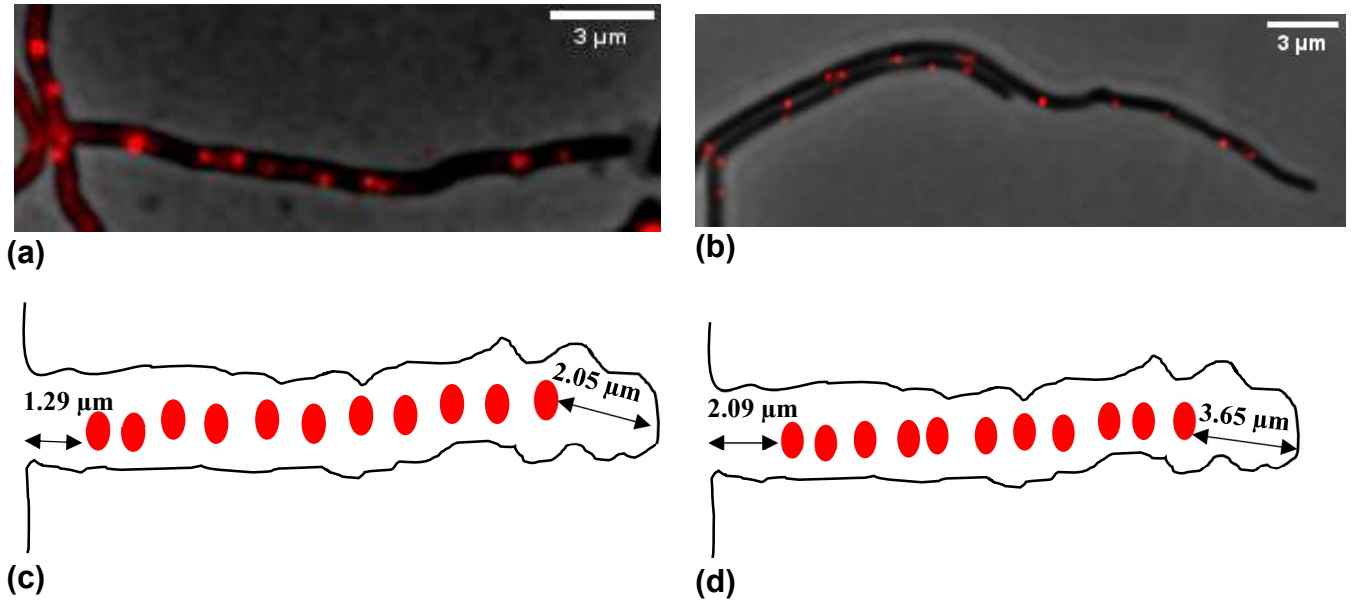

Figure 3.12: Distribution of plasmids (n=13) and chromosomes (n=15) in non-branching hyphae. Each non-branched hyphae contains more than ten localized red spots, chromosomes, or plasmids.

In particular, the distance between the tip and plasmid SCP2tetO (2.05µm; ± 1.38µm) was shorter than the chromosome (3.65µm; ± 1.91µm). Furthermore, the branching site to the FROS complexes was also closer in plasmid SCP2tetO (1.29µm; ± 1.09µm) than in the chromosome (2.09µm; ± 1.22µm).

Table 3.5: Positions of multiple copies of SCP2tetO in long non-branched hyphae of *S. lividans* JT46::ptetRmcherry

	tip to plasmid1	plasmid1 to plasmid2	plasmid2 to plasmid3	plasmid3 to plasmid4	plasmid4 to plasmid5	plasmid5 to plasmid6	plasmid6 to plasmid7	plasmid7 to plasmid8	plasmid8 to plasmid9	plasmid9 to plasmid10	plasmid10 to plasmid11	last plasmid to elongation	total length (µm)
Total number of hyphae	13	13	13	13	12	8	6	3	2	2	1		
Minimum	0.39	0.47	0.44	0.45	0.49	0.29	0.54	0.54	0.65	2.12	1.52	0	4.26
25% Percentile	0.95	0.59	0.64	0.66	0.67	0.59	1.14	0.54	0.65	2.12	1.52	0.65	6.42
Median	1.35	1.25	1.12	0.94	1.81	2.05	1.96	1.45	1.05	2.36	1.52	0.99	15.31
75% Percentile	3.54	1.73	2.29	1.58	3.63	3.21	3.41	1.75	1.44	2.60	1.52	2.04	20.15
Maximum	4.16	3.71	4.47	3.45	4.66	8.75	3.94	1.75	1.44	2.60	1.52	3.61	24.15
Mean	**2.05**	**1.37**	**1.69**	**1.25**	**2.18**	**2.58**	**2.16**	**1.25**	**1.05**	**2.36**	**1.52**	**1.29**	**13.18**
Std. Deviation	1.38	0.92	1.31	0.83	1.56	2.71	1.28	0.63	0.56	0.34	0	1.09	6.98
Std. Error of Mean	0.38	0.26	0.36	0.23	0.45	0.96	0.52	0.36	0.39	0.24	0	0.30	1.94
Lower 95% CI of mean	1.22	0.81	0.89	0.75	1.19	0.32	0.82	-0.32	-4.03	-0.71		0.63	8.96
Upper 95% CI of mean	2.89	1.93	2.49	1.75	3.17	4.85	3.51	2.82	6.12	5.43		1.95	17.40

Table 3.6: Positions of multiple chromosome copies in long non-branched hyphae of *S. lividans* JT46::ptetRmcherry

											Total number of hyphae
tip to spot1	**3,65**	1,91	0,49	2,59	4,71	8,45	4,18	3,34	2,64	0,55	15
spot1 to spot2	**2,27**	1,83	0,47	1,26	3,28	7,71	3,26	1,55	1,32	0,51	15
spot2 to spot3	**4,07**	2,85	0,74	2,49	5,65	9,12	7,62	3,1	1,53	1,38	15
spot3 to spot4	**2,89**	1,66	0,43	1,96	3,81	7,51	3,54	2,96	1,80	0,45	15
spot4 to spot5	**2,09**	1,56	0,47	1,04	3,14	5,07	3,06	1,31	1,08	0,78	11
spot5 to spot6	**2,94**	1,56	0,55	1,64	4,25	5,4	4,13	3,16	1,29	0,88	8
spot6 to spot7	**2,44**	1,36	0,48	1,30	3,57	4,04	3,83	2,55	0,98	0,77	8
spot7 to spot8	**2,47**	1,53	0,58	1,06	3,89	4,55	3,67	2,69	0,79	0,54	7
spot8 to spot9	**1,65**	1,048	0,39	0,68	2,62	3,69	2,421	1,255	1,076	0,674	7
spot9 to spot10	**1,72**	1,45	0,65	-0,079	3,52	4,27	2,834	1,142	0,8925	0,709	5
spot10 to spot11	**4,60**	4,85	2,79	-7,44	16,64	10,19	10,196	2,004	1,61	1,61	3
spot11 to spot12	**2,26**	1,49	0,86	-1,44	5,96	3,77	3,767	2,217	0,79	0,79	3
spot12 to spot13	**1,99**	1,36	0,78	-1,38	5,36	3,01	3,005	2,511	0,448	0,448	3
spot13 to spot14	**1,97**	1,60	0,93	-2,01	5,95	3,65	3,645	1,816	0,448	0,448	3
spot14 to spot15	**2,04**	0,35	0,24	-1,08	5,16	2,29	2,285	2,0395	1,794	1,794	2
spot15 to spot16	**1,57**	0,90	0,64	-6,53	9,67	2,21	2,21	1,57	0,94	0,94	2
spot16 to spot17	**5,45**	0	0			5,45	5,45	5,45	5,45	5,45	1
spot17 to spot18	**1,94**	0	0			1,93	1,93	1,93	1,93	1,93	1
spot18 to spot19	**1,97**	0	0			1,97	1,97	1,97	1,97	1,97	1
spot19 to spot20	**3,05**	0	0			3,05	3,05	3,05	3,05	3,05	1
last spot to elongation	**2,09**	1,22	0,31	1,42	2,77	4,09	3,32	2,31	1,03	0	
total length (µm)	**25,3**	13,26	3,42	17,99	32,68	52,90	32,19	23,77	13,05	10,98	

The results suggest that mycelial growth may influence the distribution of plasmids and chromosomes in *Streptomyces lividans*. The plasmid may be more mobile and capable of moving towards areas of mycelial growth.

3.3. Localization of SCP2tetO by time-lapse imaging

The still images shown above only show the momentary positions of SCP2tetO (or that of the chromosome) in the mycelium but cannot reveal the kinetics of movement and its dependence on growth, in particular, a possible correlation with the rate of tip elongation and branching. To follow SCP2tetO in real-time, the mycelium of *S. lividans* JT46::ptetRmcherry (SCP2tetO) was grown on a coverslip, inserted into R5 agar for 16-20 hours.

The homemade imaging chamber consists of a microscope-slide-sized piece of stainless steel with a 1.3 cm diameter hole in the center. An air-permeable membrane with water-impermeable polymer film covers this hole. The polymer film was fixed to the metallic carrier by using the gene frame. A second gene frame was glued on the top of the polymer film. Within the second gene frame, a thin layer of minimal agarose, supplemented with glucose, asparagine, histidine, proline, leucine, kanamycin, thiostrepton, and apramycin was poured in, flattened with a sterilized glass slide, and allowed to cool down for 15 min at 4°C. Subsequently, the glass slide was removed from the agar layer and the coverslip was glued on the second gene frame with the attached mycelium facing to the minimal agarose and the cleaned side of the coverslip facing to the outside of the imaging chamber. This experimental setup is described in chapter 2.2.10.4. Before applying the slides for time-lapse imaging under the fluorescence microscope, samples were incubated for 4-6 hours at 29°C to stimulate mycelium growth. Samples were observed via brightfield and fluorescence microscopy in a Zeiss Axio Observer Z1 automated microscope LSM800 at a λ_{ex} of 353 nm and a λ_{em} of 465 nm. Images were acquired using an Orca Flash 4.0 V2 camera (Hamamatsu) and an α Plan-Apo 100×/1.46 Oil Ph3 objective (Zeiss). The fluorescence filter was Texas Red excitation 540 nm, emission 668 nm (described in material and method chapter). Images were processed using the Zen 2.3 (blue edition) software package (Zeiss).

Alternatively, the samples were also analysed under the Nikon Eclipse Ti automated microscope with a Perfect Focus system, an Orca Flash 4.0 camera or a Prime BSI

camera, and CFI Plan-Apo DM 100×/1.45 Oil Ph3 objective or CFI Apo TIRF 100×/1.49 Oil objective with the external Phase Contrast. The HC Filter sets used were EGFP excitation of 472 nm, emission of 520 nm, and Texas Red excitation of 555 nm, emission of 617 nm (Figure 3.13).

Images were taken more than 8 hours, at intervals of 5 – 20 minutes. The individual images were combined into a movie by FIJI software. The selected labeling intensity was then quantified and measured within the living hyphae. The data were further analysed and plotted using GraphPad Prism software. The significance or not was determined via one-way ANOVA.

3.3.1. Tip association of SCP2tetO in fast-growing hyphae

When incubated on the slide, some hyphae grew faster than others and did not branch. An example video of such hyphae, showing the position of SCP2tetO at 5 min intervals for about 3.95 hours (from 5 min – 235 min), is shown below (Figure 3.13). SCP2tetO followed the extending tip at a nearly constant distance. After 90-100 minutes, when the hyphae had a length of approximately 15.5 µm (95min) -16.01 µm (100min), the plasmid spot was duplicated, most likely indicating replication of SCP2tetO.

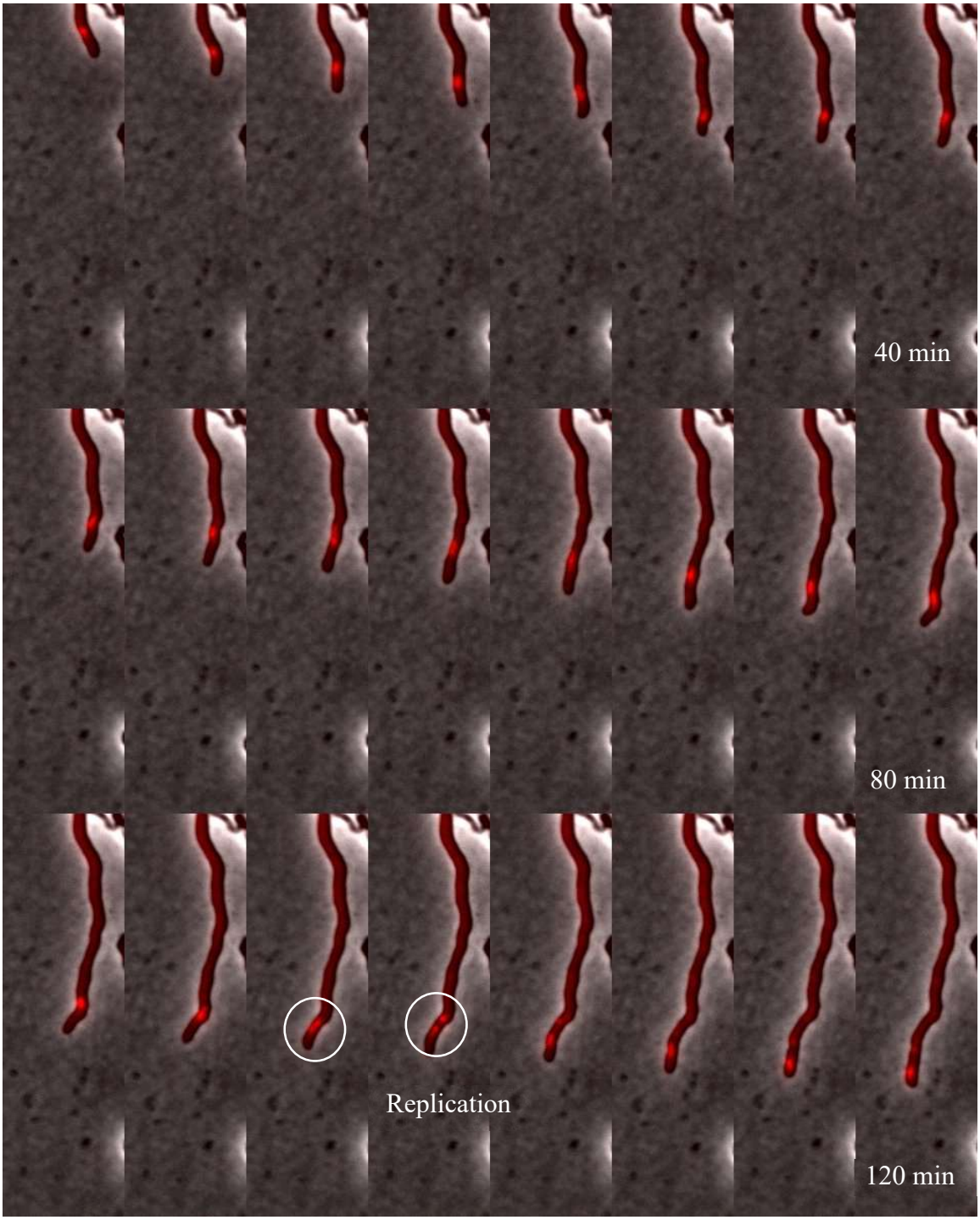
40 min
80 min
Replication
120 min

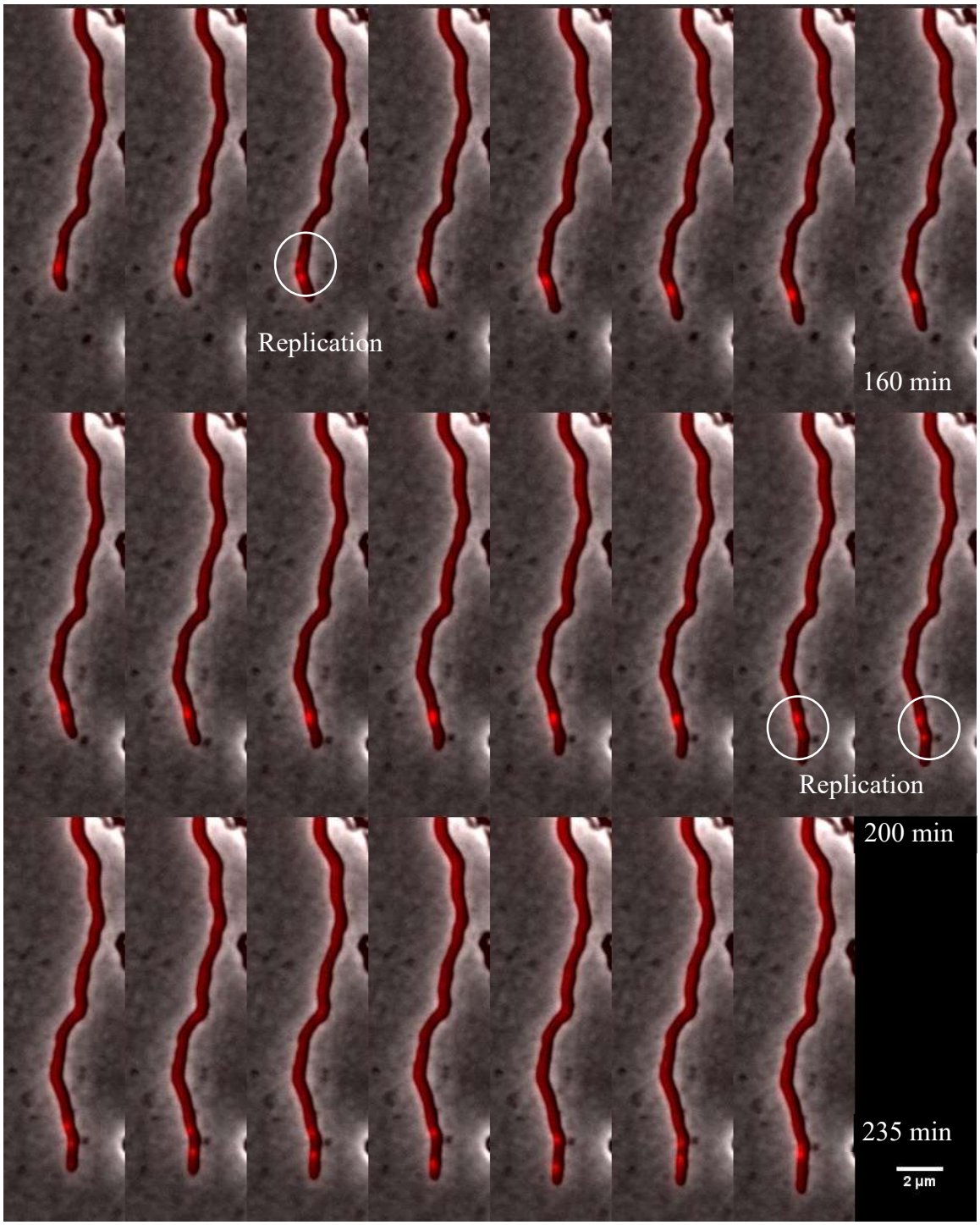

Figure 3.13: Time-lapse imaging of plasmid migration in extending *S. lividans* hyphae. Plasmid SCP2tetO was visualized (overlay of phase contrast image with the red channel; Nikon Eclipse fluorescence microscope) by FROS in 5 min intervals. The plasmid did not have a static position but followed the extending tip. Duplication of the red fluorescence spot, probably indicating replication of SCP2tetO (highlighted by the dashed circle), occurred close to the tip.

Other time-lapse videos are shown in the supplementary data (Figure 6.2, 6.3). In most videos, the plasmid localized close to the tip of fast-growing unbranched hyphae and followed the tip during elongation, as shown in Figure 3.13. The elongation speed was 0.09 µm per minute and the total length of the hypha was 21.48 µm.

3.3.2. Impact of hyphal branching on plasmid migration and replication.

In other time-lapse images evidence was observed that branching not only influences plasmid migration, but might also induce replication of the plasmid. An example of such a time-lapse video is given in Figure. 3.14.

The first image displays two plasmids marked by white arrows, while the yellow arrow indicates the direction of hypha elongation. After a quarter of an hour, a fresh branch emerged (indicated by a white circle), and three plasmids are visible next to the branching site (pointed out by white arrows). One plasmid entered into the extending tip, while another remained close to the point of branching, and the other one followed the elongating hyphae that had left the lens coverage. After 35 minutes, the plasmid that was marked beforehand entered the newly generated hypha at the branch (2.303 µm). Upon entering, the plasmid divided into three distinct red spots, denoting its replication within 40 minutes, as illustrated by three white arrows. After that, the newly replicated plasmid followed the elongating tip. After 1.55 hours, this hypha started to branch again, as indicated by a white circle. When the hypha had reached a length of 4.82 µm at the time point of 2.25 hours, a plasmid spot was visible. This plasmid replicated at time point 3.4 hours of time-lapse images frame. Furthermore, the plasmid that had previously been labelled by a blue arrow, remained at the branching site of the hyphae.

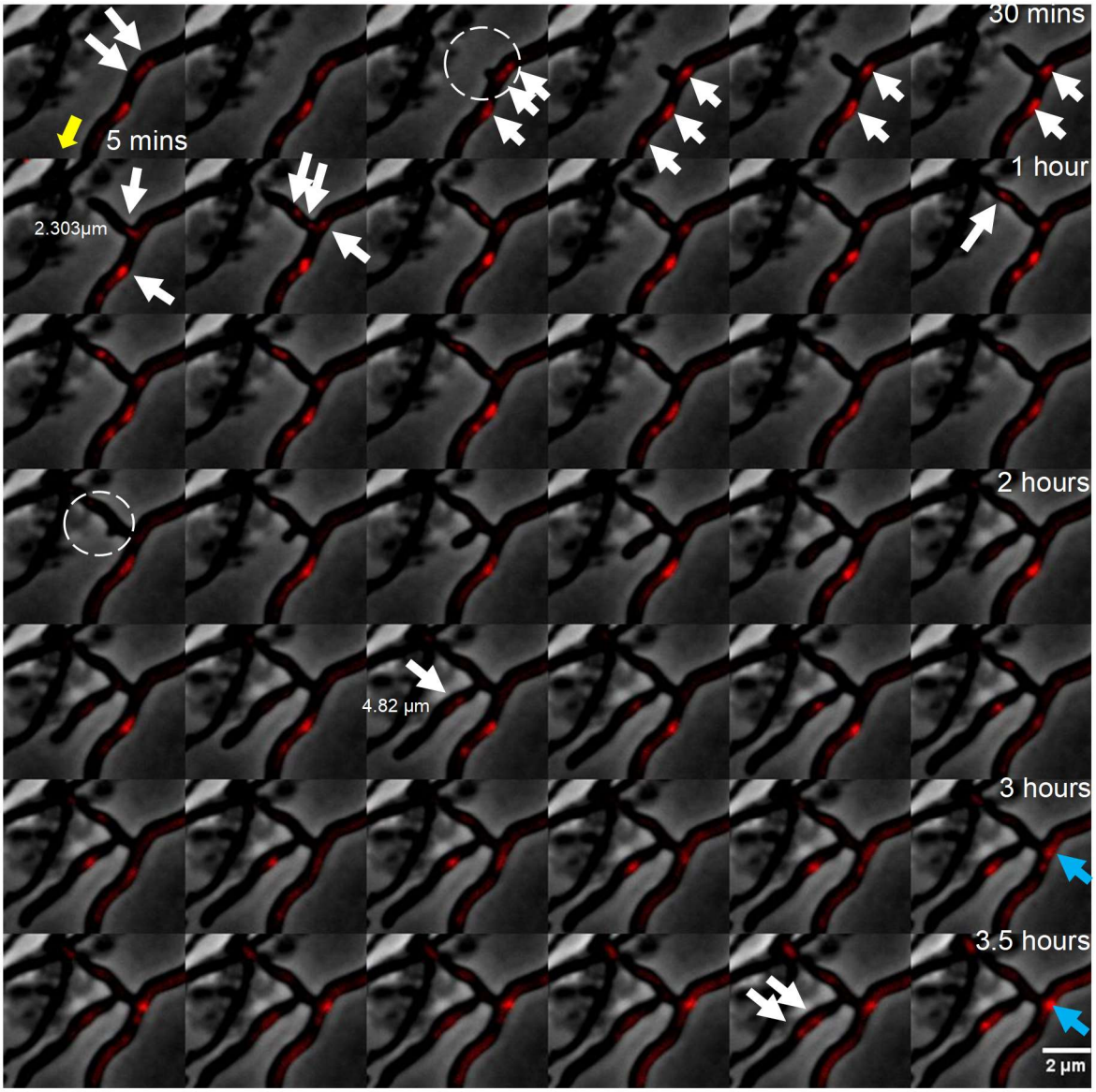

Figure 3.14: Branching hyphae have an effect on plasmid replication and movement. The following images at 5 minutes of interval, show the kinetics of plasmid localization and replication within growing hyphae over 210 mins (3.5 hours). The first image depicts two plasmids (marked as white arrows) and the yellow arrow represents the direction of hyphal elongation. After 15 minutes a new branch is generated (marked as a white circle), and a couple of plasmids remain next to the branching site (white arrows). One of the plasmids followed the elongating new tip, while the other remained very close to the branching site. At 35 mins, the previously marked plasmid entered at the branch into the new hypha, which had a length of 2.303 µm. As the plasmid entered into the new hypha, it splits into 3 red spots, indicating replication (in 40 min, shown as three white arrows). The replicated plasmids then follow the tip of

elongated hyphae. The hyphae branched again at the 95 mins, indicated by the white circle. 40 mins later, the plasmid is visible into the new hypha (length 4.82 µm) and started to replicate (3.4 hours). Also, the previously marked plasmid replicates again, which is indicated by a blue arrow.

3.4. Localization of the *S. lividans* chromosome by time-lapse imaging

To better understand the biology of plasmid movement within the mycelium, it has to be compared with the movements of the chromosome. Previously a TetR-FROS system was used to localize the *oriC* region (sco3879-3878) of *Streptomyces coelicolor*. In these experiments, evidence was reported that the chromosome is associated with the tip localized polarisome, which directs elongation growth (Kois-Ostrowska et al., 2016).

In my experiments with the optimized tetRmcherry, fluorescence images were captured using a Zeiss LSM 800 microscope with both mCherry channel and phase contrast. Due to the availability of technical support, superior optical quality, advanced imaging software for data acquisition and processing, alternatively I used Zeiss LSM over Nikon fluorescence microscope. The sample was prepared as described before in R5 media containing the antibiotic Apramycin$^{50mg/ml}$. The cover slide was then transferred to solid MM (minimal media) containing Apramycin$^{25mg/ml}$. After 3-5 hours of incubation at 29°C, the sample was used for time-lapse imaging.

3.4.1. Localization of the chromosome in non-branching hyphae

Upon incubation of the sample, some hyphae grew faster compared to the others and did not branch. An example time-lapse image of such hyphae is shown in Figure 3.15. This elongating hypha grew up to a total length of 26.209 µm, with an elongation speed of 0.06 µm per minute. The chromosome copies appear as red fluorescence foci in the mycelium. Similar to the observed plasmid movement close to the elongating tip (Figure 3.13), the chromosome also followed the tip (Figure 3.15, marked by white arrows). Over the 8 hours of growth the chromosome was localized in close to the tip elongation site and at certain intervals the chromosome seemed to replicate (indicated by a white circle).

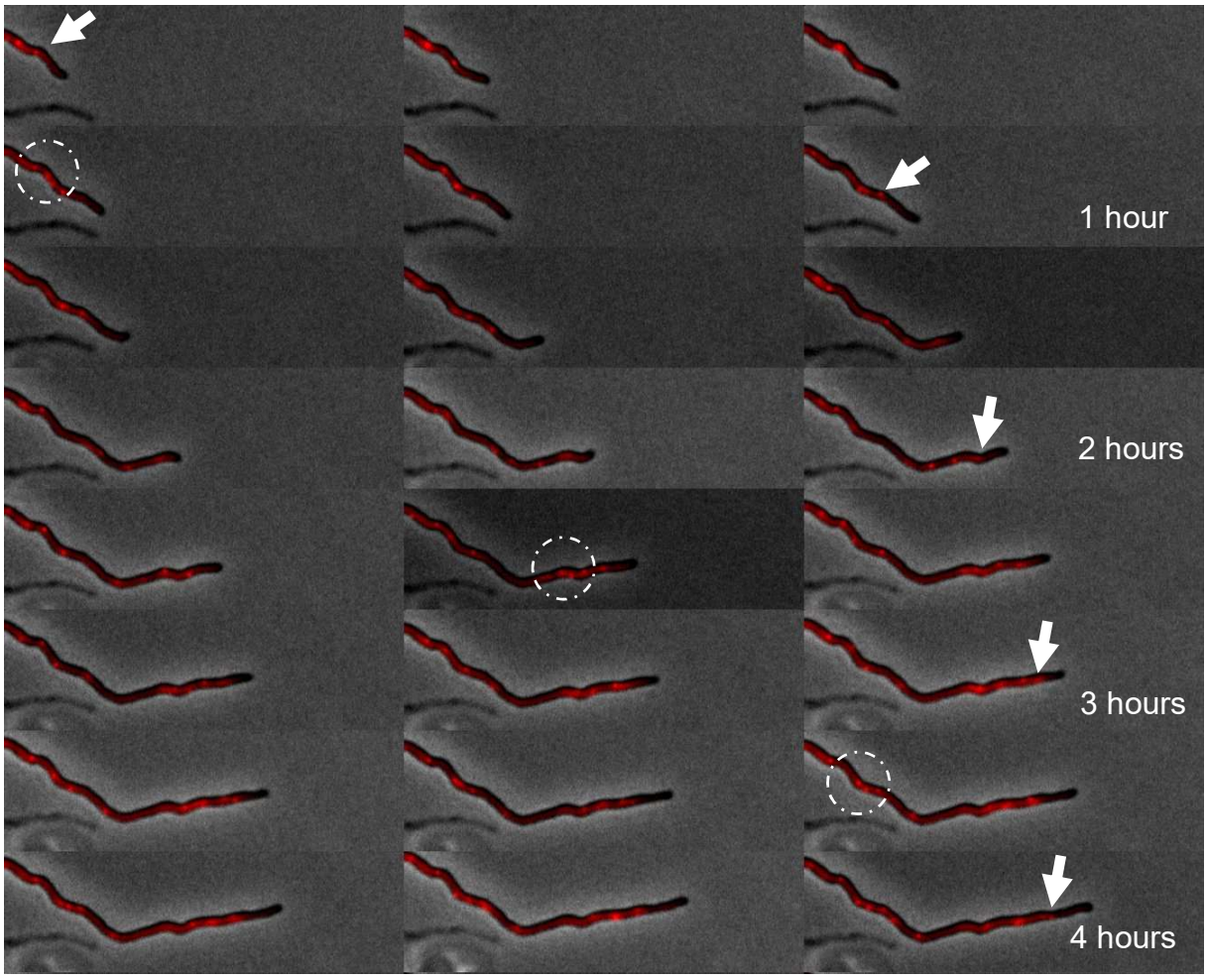

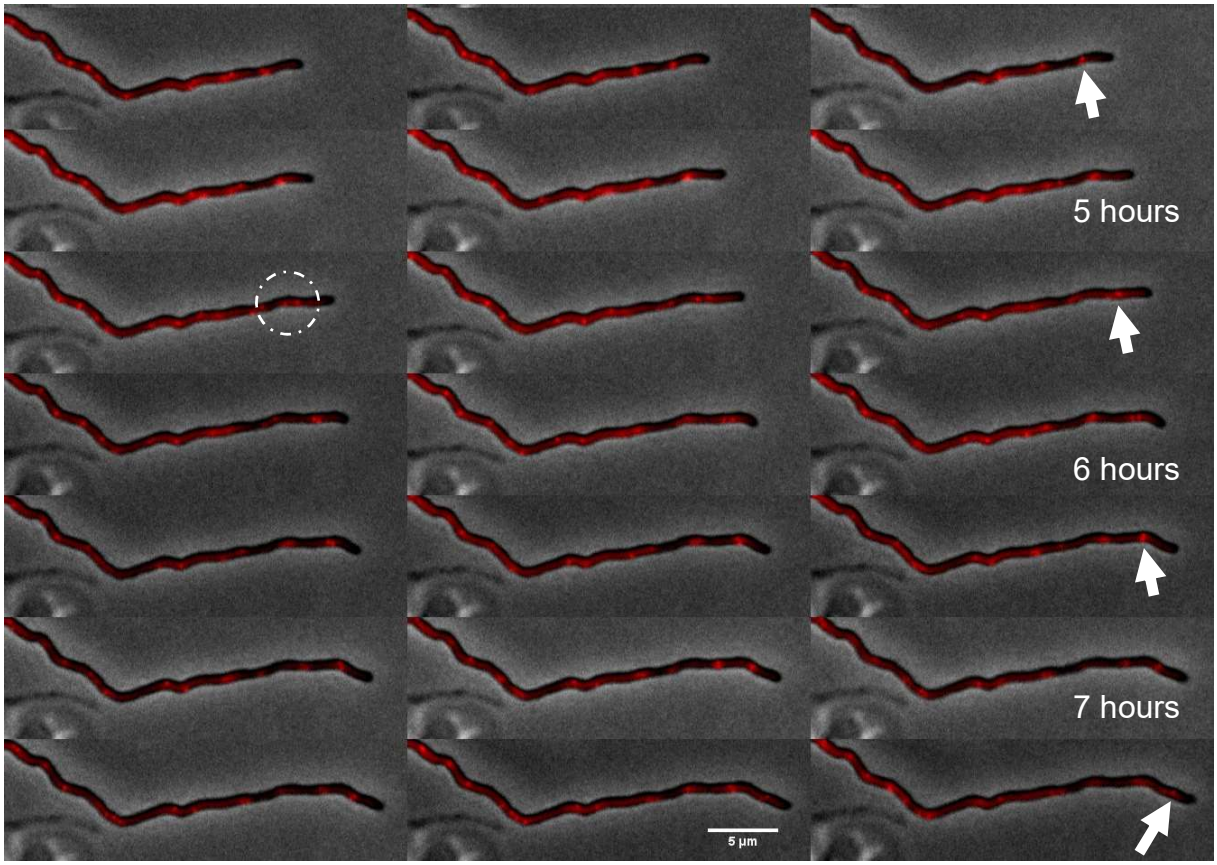

Figure 3.15: Visualizing chromosome localization in extending *S. lividans* JT46::tetRmcherry hyphae. The localization of chromosome copies (integrated pIJ12507tetO) is visualized (overlay of phase contrast image with the red channel) by FROS in the time-lapse image, with the chromosomes appearing as red-spots in the mycelium. As the hypha elongates, the spot moves with the tip (marked by a white arrow). The images were taken at 10-minute intervals. At several time periods (for example 30 min, 2.20 hours, 5.10 hours) a chromosome seemed to replicate, resulting in the appearance of two fluorescence spots close-by (indicated by white circles).

This time-lapse analysis showed that the chromosome followed the extending hyphal tip in a similar pattern as observed for plasmid SCP2tetO. (More time-lapse images are attached in the supplementary data Figure 6.4, 6.5))

3.4.2. Localization of the chromosome during hyphal branching

Next, I analysed the influence of branch formation on chromosome localization (Figure 3.16). Growth was observed for 120 minutes, images were taken at 10 minutes intervals. At the starting point, 4 copies of the chromosome were visible in the non-branched mycelium. After 10-20 mins a new branch is formed (highlighted by a dashed white circle). Simultaneously, one chromosome (yellow arrow) replicates and subsequently moves into the newly extending hyphae, where it undergoes further rounds of replication (white arrows). The other chromosome copies (blue arrow) in the "old" mycelium continue their movement following the hyphal tip (not visible).

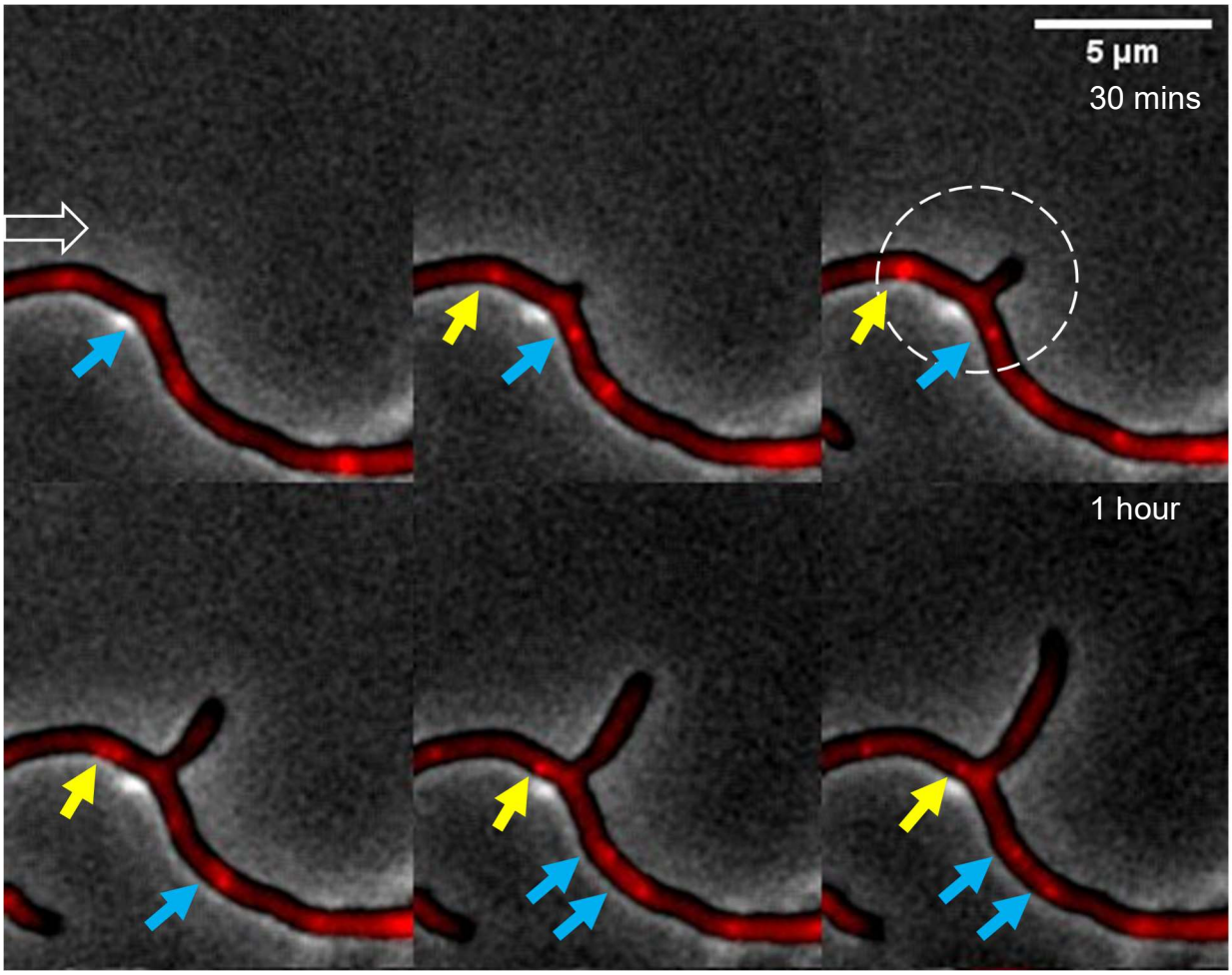

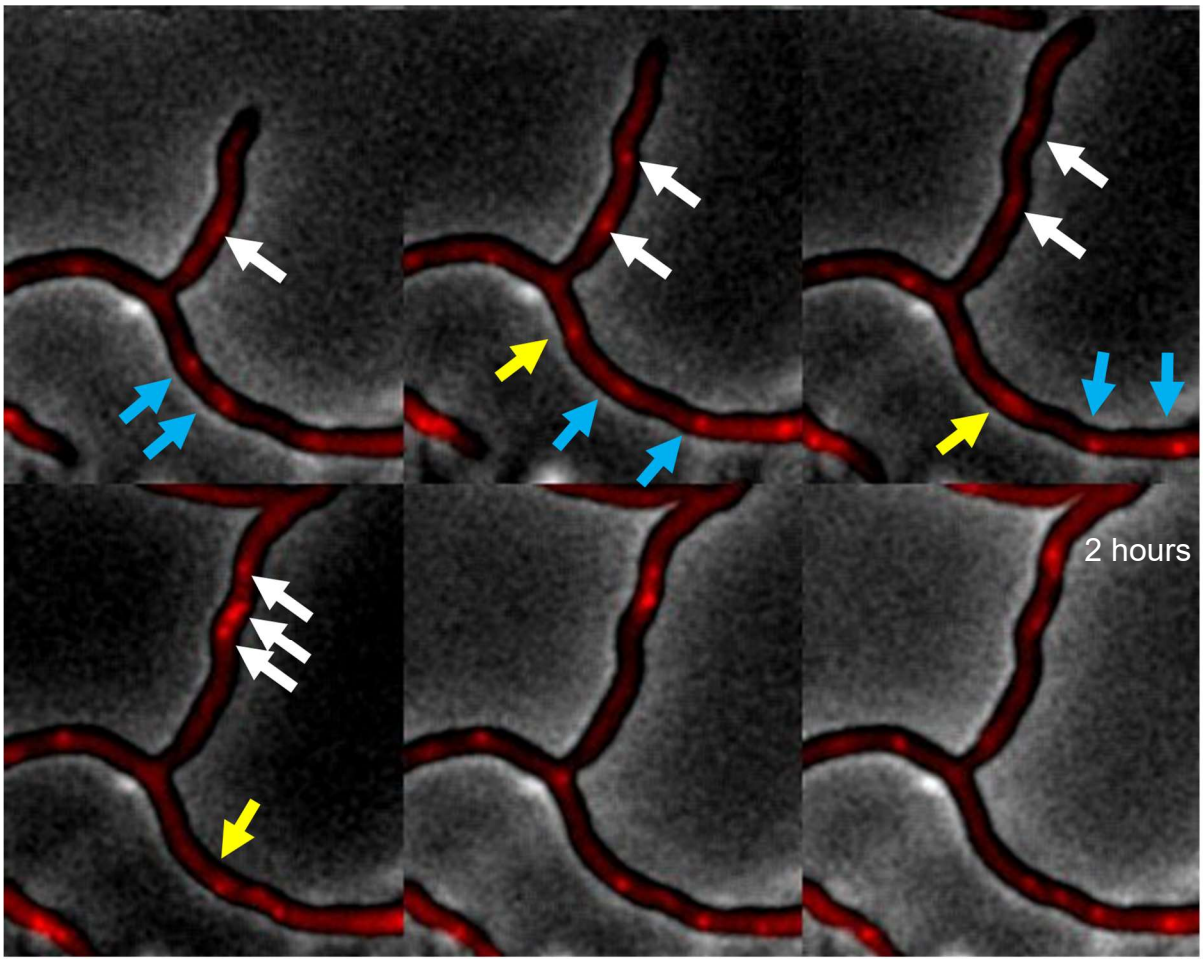

Figure 3.16: A series of time-lapse images illustrating FROS complexes (red spots) of chromosome localization during hyphal branching. Snapshots were taken at 10 minutes intervals. The non-filled white arrow in the first snapshot image indicates the direction of hyphal growth. The chromosome positions are marked by yellow and blue arrows, respectively. When branching occurred (marked by a white circle) the chromosome (yellow arrow) on the left site of the developing hyphae replicates and enters the new hyphae, where it replicates again (white arrows). Blue arrows mark chromosomes in the “old” hyphae, continuing their movement in the direction of hyphal growth.

3.4.3. Influence of *parA*$_{SCP2}$ deletion on SCP2tetO localization

To analyse, whether a plasmid-encoded cytoskeletal element is involved in plasmid movement, a possible candidate, the ParAB$_{SCP2}$ partitioning system of SCP2tetO was inactivated. *parA*$_{SCP2}$, encoding the motor ATPase was completely deleted via Lambda RED mediated recombination. The mutant plasmid was introduced into *S. lividans* JT46::tetRmcherry, and the sample was prepared for microscopy as described above. After 20 hours of incubation at 29°C, the sample was analysed under the fluorescence microscope to detect the plasmid SCP2tetOΔ*parA* (Figure 3.17). Deletion of *parA*$_{SCP2}$ affected the number of visible plasmid spots. Moreover, fluorescence intensity was higher than that of the parental SCP2tetO plasmid (Figure 3.18). As shown in Figure 3.17, the plasmid spots were more widely distributed (distance from the tip: 23.74 µm, 42.58 µm, and 51.71 µm, respectively).

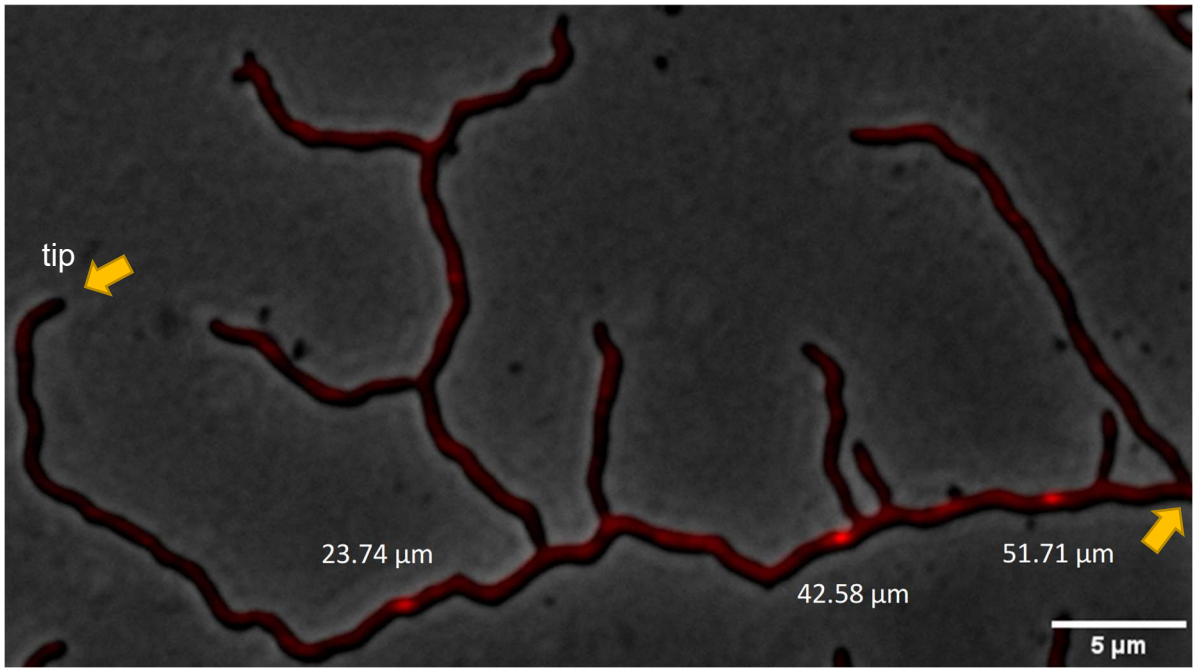

Figure 3.17: Fluorescence image of *S. lividans* JT46::ptetRmcherry (SCP2tetOΔ*parA*), revealing the positions of SCP2tetOΔ*parA*. Overlay of phase contrast image with fluorescence image (red filter, 1000ms exposure time). Yellow arrows mark the start and end of the measured hypha.

3.4.3.1. Intensity profile of SCP2tetOΔ*parA* fluorescence:

Figure 3.17 clearly shows plasmid spots with higher fluorescence intensity. To compare fluorescence intensity with that of SCP2tetO (Figure 3.4) or that of the chromosome (Figure 3.7), the intensity profile was determined for the hypha, marked with yellow arrows (Figure 3.17). The plot profile indicated that the SCP2tetOΔ*parA* plasmids had intensity values of more than 800, about double the fluorescence intensity observed for SCP2tetO (Figure 3.8) or that of the chromosome (Figure 3.9). This suggests that after replication of SCP2tetOΔ*parA,* the *parA* deletion prevented proper separation of the two plasmid copies, resulting in an intertwined plasmid cluster.

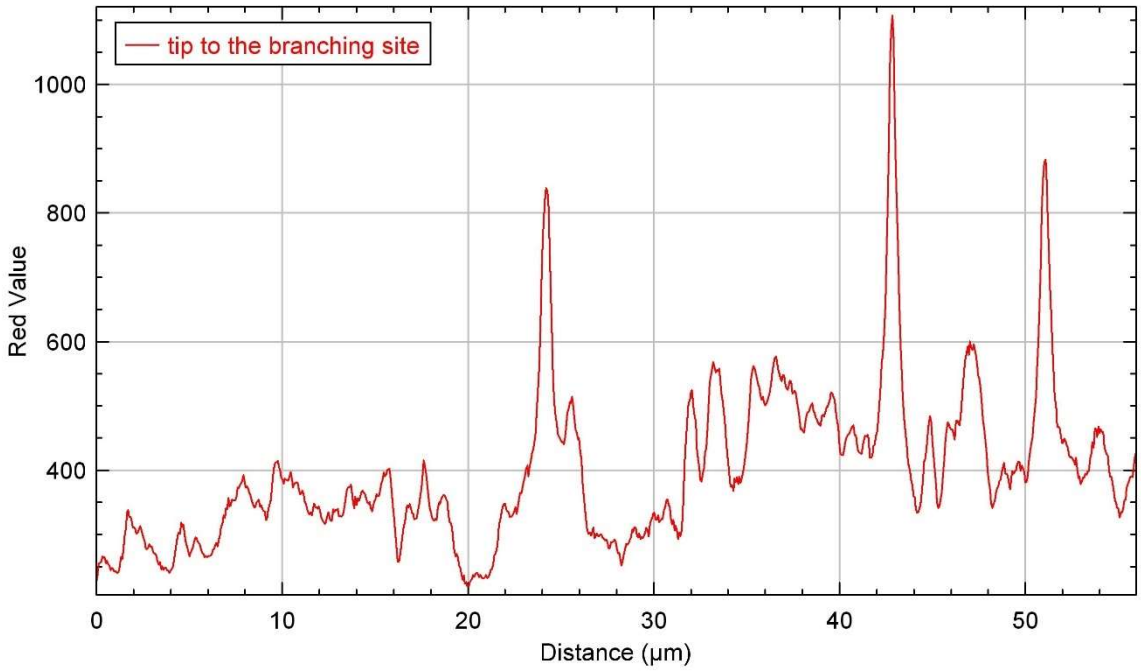

Figure 3.18: The intensity plot profile of the marked hypha from Figure 3.17. The SCP2tetOΔ*parA* spots have a high fluorescence intensity (> 800), suggesting clusters of the plasmid, instead of a single copy.

3.4.3.2. Stability of plasmid SCP2tetOΔ*parA*:

Knowledge of plasmid stability is crucial for correlating the red fluorescence spots with plasmid copies. On the one hand, the highly repetitive *tetO* array is known to affect plasmid stability, resulting in a mixed plasmid population with full or partial deletions of the *tetO* array (M. Arndt, Bachelor thesis). Moreover, one would expect that deletion of the partitioning ATPase gene *parA*$_{SCP2}$ interferes with the segregational stability of the plasmid, as described for SCP2 and many other low-copy number plasmids. Therefore, the stability of SCP2tetOΔ*parA* was analysed following the same procedure as used for the plasmid SCP2tetO stability test (see 3.1.2.1). Here, 100 individual colonies on R5 medium, most likely originating from a single protoplast, were transferred in parallel to both LB-agar and LB_thio25$^{mg/ml}$ agar.

Thiostrepton-supplemented agar allowed the growth of only 28 % of the colonies, which demonstrated that SCP2tetOΔ*parA* was highly unstable. Whereas the parent plasmid SCP2tetO was lost in only 56.5 % of the colonies (Figure 3.5.) deletion of *parA*$_{SCP2}$ increased the instability in vegetative mycelium to 72 % plasmid loss.

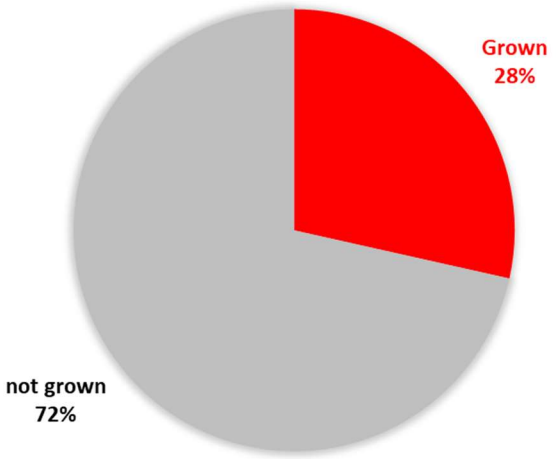

Figure 3.19: Pie chart depicting the percentage of thiostrepton-resistant and -sensitive colonies after protoplast regeneration. The plasmid loss rate in the vegetative mycelium was assessed by transforming the vegetative mycelium it into “single genome”-protoplasts and determining the percentage of plasmid loss. After regeneration on R5 agar without selection, 100 individual colonies, most-likely derived from single protoplasts were picked in parallel onto LB and LB_ thio25$^{mg/ml}$ agar, confirming the presence of SCP2tetOΔ*parA*. The study was performed in duplicate. 72% of JT46::pTetRmcherry colonies had lost the plasmid SCP2tetOΔ*parA*.

3.5. Detection of conjugative plasmid transfer by FROS

Previously, conjugative plasmid transfer in *S. lividans* was detected by fluorescence microscopy (Thoma et al., 2016). This study marked the conjugative multi-copy plasmid pLT303 with *eGFP* and the recipient with *mCherry.* Thus, detection of plasmid transfer was only possible with delay due to the time period required for plasmid establishment in the recipient and expression of *eGFP* in sufficient amounts to detect plasmid-encoded fluorescence.

3.5.1. Microscopic still image analysis for SCP2tetO plasmid transfer

To enable the detection of conjugative plasmid transfer in real time, the FROS system described above was applied. Mycelium of the donor *S. lividans JT46*::ptetR-mCherry (SCP2tetO) (red plasmid spots) was mixed at a ratio of 10:1 with the “green” recipient strain JT46::ptetRmcherry::eGFP(pGM190), (supplementary data Figure 6.6), labelled with eGFP and TetRmcherry, and spotted at the edge between the agar and the inserted coverslip (Figure 2.2.1). The samples were prepared according to the description in the method section (see 2.2.10.2.) After overnight incubation at 29°C, the coverslip with the attached mycelium was removed and observed by fluorescence microscopy. After selecting a specific position, three images were taken with three different channel filters. At first mCherry channel with 1000 ms exposure time to localized plasmid SCP2tetO in the mycelium. Second, with the GFP channel at 500 ms exposure time to observe green mycelium (recipient) and the last one with phase contrast. All three images were overlaid with FIJI software to visualize the SCP2tetO plasmid (red spots) and the plasmid transfer to the recipient (green mycelium). Plasmid transfer could be detected (red spots in green hyphae, Figure 3.20, yellow arrows) when donor and recipient hyphae were in intimate contact at the lateral walls (Figure 3.20, dashed white circles).

(a)

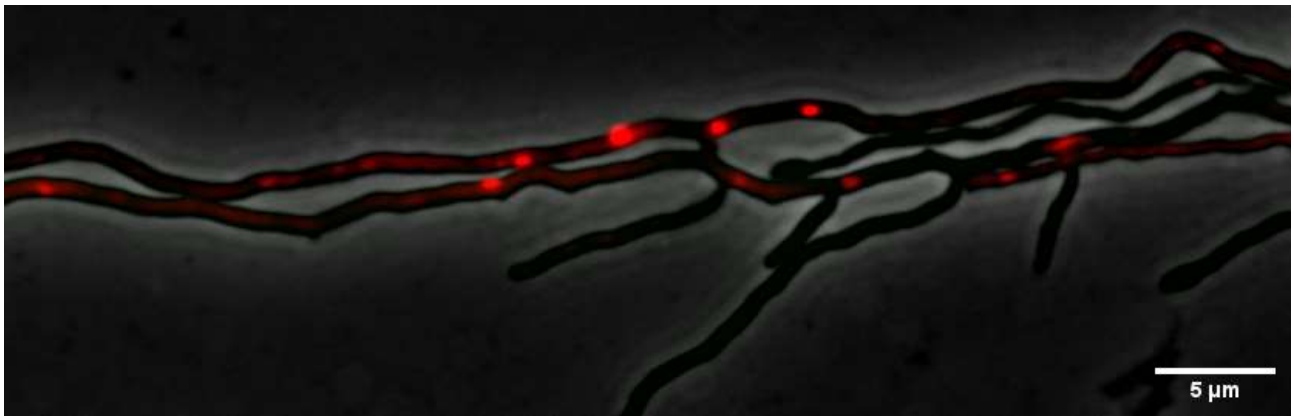

(b)

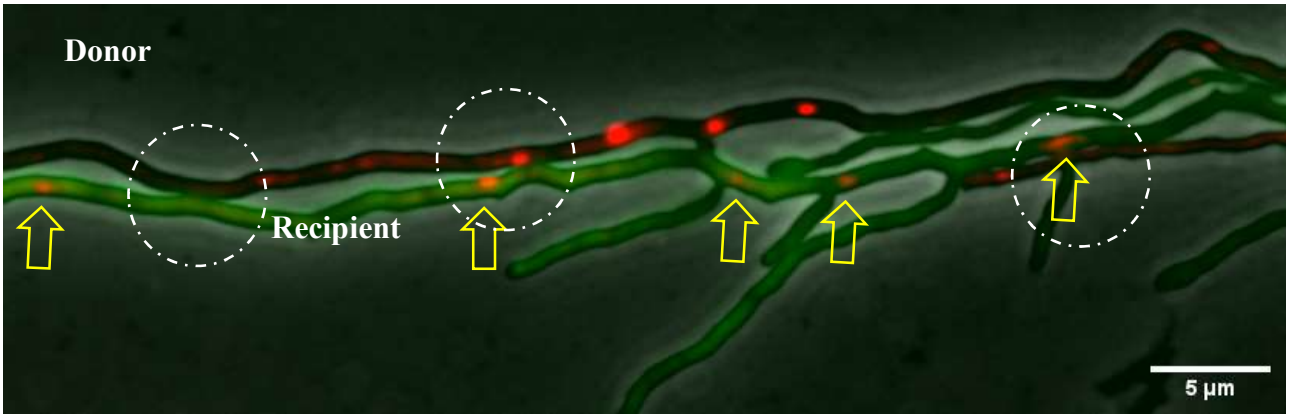

Figure 3.20: Visualization of conjugative plasmid transfer by FROS. **(a)**, overlay of phase contrast with the red channel, **(b)**, overlay of phase contrast with red and green channel. Donor JT46::ptetRmcherry(SCP2tetO) and recipient JT46::ptetR-mcherry::eGFP(pGM190) were mixed and grown on a coverslip inserted into R5 agar supplemented with thiostrepton and kanamycin. Upon contact with the recipient mycelium (green hyphae), the conjugative plasmid (red spots) was transferred from the donor mycelium. The dashed circles indicate the possible contact sites for conjugative DNA transfer. Following the initial transfer, copies of the plasmid spread in the recipient mycelium (yellow arrows).

3.5.2 Time-lapse imaging to visualize conjugative plasmid SCP2tetO transfer from donor to the recipient mycelium in real-time.

Still images do not allow to draw conclusions concerning the kinetics of conjugative plasmid transfer. However, the FROS system described above (see 3.1.) should be ideal to observe conjugative plasmid transfer in real-time. Since TetRmcherry is already present in the recipient in this experimental setup, the plasmid should be detected immediately upon entering the recipient hyphae.

Like as before, the samples were prepared according to the protocol (see 2.2.10.2.). Both donor and recipient were mixed at a ratio of roughly 1:1. Plates were incubated for 16-20 hours at 29°C. Then the coverslip was removed from the R5 agar together with the attached mycelium, cleaned on the bottom side, and assembled to the imaging chamber (illustrated in Figure 2.2.2). This experimental setup is described in chapter 2.2.10.4. The prepared slides were incubated for another 4-6 hours at 29°C, to support growth of the mycelium in the MM agarose medium. After that, the samples were analysed under fluorescence microscopy (ZEISS) for conjugative plasmid transfer.

A series of time lapse images (Figure 3.21a) showed at the beginning mycelial growth without making direct contact. At the time point of 100 minutes (white dotted circle) (Figure 3.21 b), a green recipient hypha made contact to the plasmid-containing (red spots) donor hyphae. Following the contact with the donor hypha at an angle of 74° (Figure 3.23 a) it alters its direction of growth, indicative of a response to the interaction. After 3.3 hours, the plasmid is observed within the recipient hypha, highlighted by a yellow arrow. By the 3.6-hour mark, the plasmid disseminated within the recipient hyphae, characterized by the presence of three red spots (yellow arrows).

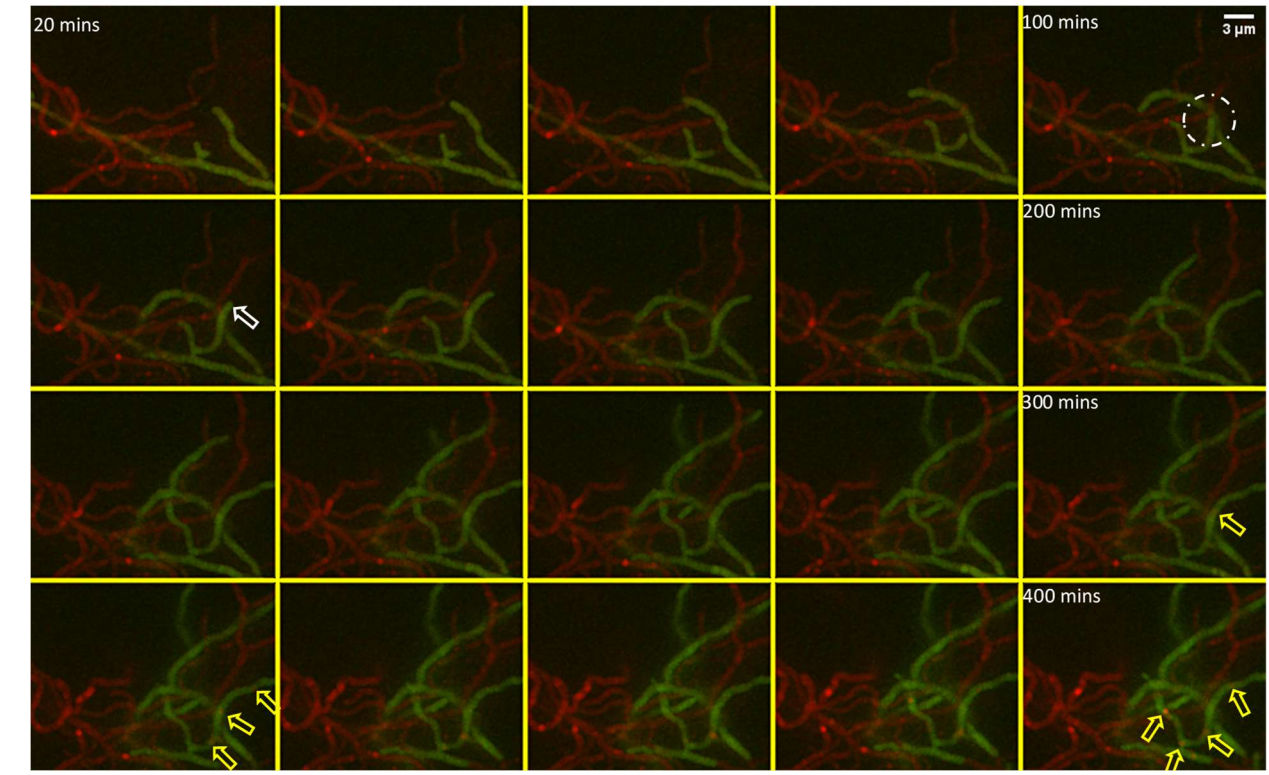

a)

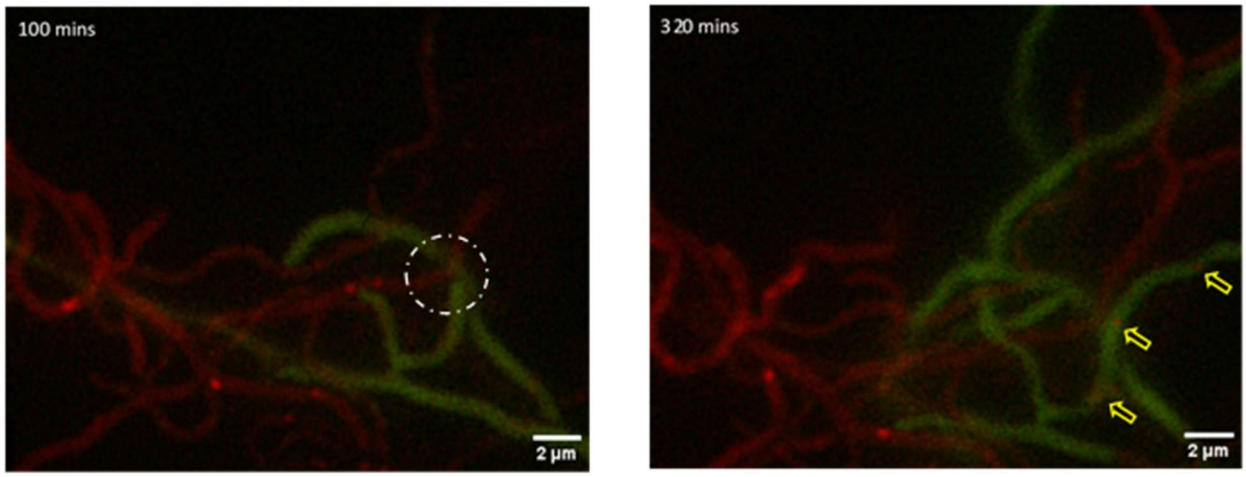

b)

Figure 3.21: Time lapse imaging of conjugative plasmid transfer from donor to the recipient mycelium. (a) *S. lividans* JT46::pTetRmcherry (SCP2tetO) donor (red hyphae) was mixed with the recipient *S. lividans* JT46::pTetRmcherry_eGFP (green hyphae). Images were taken in 20 min intervals. At the time point of 100 minutes, both donor and recipient mycelium make contact as indicated by the white dotted circle. After 200 minutes, a plasmid spot (yellow arrow) is visible in the recipient mycelium as a result of plasmid transfer. Subsequently, the plasmids are spreading in the recipient mycelium (3 spots are indicated as yellow arrows at 320 mins). As a result, several spots are visible in the green mycelium. (b) Left side- the contact location at 100

minutes is visible in the magnified image. The white dot circle represents the contact site for both donor (red) and recipient green hyphae. Right side- the magnified image at 320 minutes shows the plasmid locations in the recipient green hyphae, as indicated by the yellow arrows.

3.5.3 Influence of ParA$_{SCP2}$ on SCP2tetO transfer

Deletion of *parA*$_{SCP2}$ interfered with the proper separation of replicated plasmids from each other, resulting in plasmid clusters. To investigate whether the motor ATPase ParA$_{SCP2}$ also affects conjugative plasmid transfer by preventing the movement to the donor, a mating was set up with the Δ*parA* mutant of plasmid SCP2tetO on a coverslip as described in 2.2.10.2. The coverslips were analysed under the fluorescence microscope after an overnight (16-20 hours) incubation at 29°C.

The appearance of red fluorescence spots, indicating the presence of plasmid SCP2tetOΔ*parA* in the recipient hyphae next to contact sites of donor and recipient (Figure 3.22, red arrows) demonstrated, that conjugative plasmid transfer of plasmid SCP2tetOΔ*parA* was not abolished by the deletion of *parA*$_{SCP2}$.

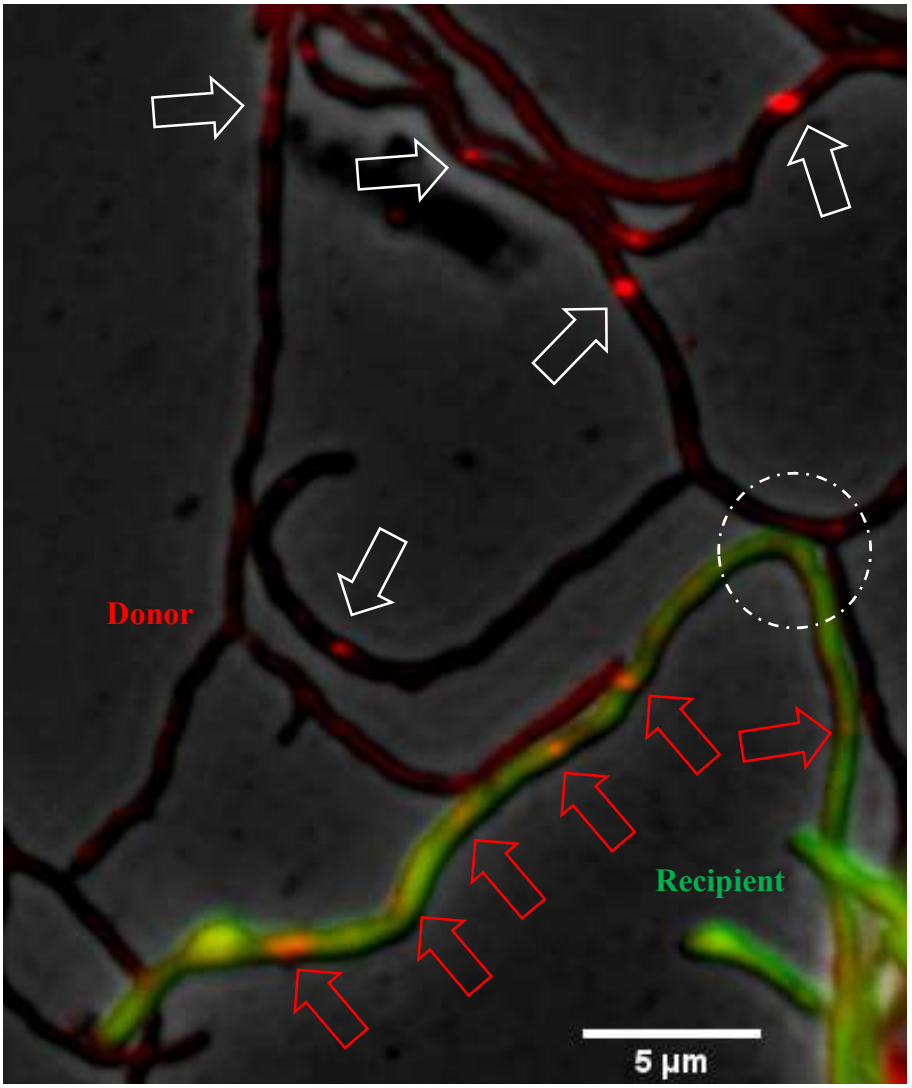

Figure 3.22: Fluorescence imaging of the conjugative transfer of plasmid SCP2tetOΔ*parA*. Bright fluorescence spots of SCP2tetOΔ*parA* in the donor are marked by white arrows. Upon contact (white circles) with recipient mycelium (green hyphae), the mutant plasmid is transferred and several clear red SCP2tetOΔ*parA* spots are visible in the green recipient hyphae.

To confirm the observed transfer of SCP2tetOΔ*parA* and to calculate the efficiency of transfer, genetic crosses were performed. Plasmids SCP2tetO and SCP2tetOΔ*parA* were introduced into *S. lividans* strain TK54 by PEG mediated protoplast transformation. 10^6 spores of the resulting strains were mixed with 10^6 spores of apramycin resistant TK64::pRM43 and plated onto R5 agar and incubated for 5-8 days at 29°C. After that, spores were harvested and the titer was determined to calculate

the number of donors (thio^R/kan^R), recipients (apra^R), and transconjugants (thio^R/apra^R), recipients that have obtained the plasmid.

A transfer rate (mean value of 3 replicates) of approximately 12.2% (± 0.33) (table 3.7) of the conjugative plasmid (thio/apra) was observed for the parental plasmid SCP2tetO. In contrast, the plasmid SCP2tetOΔ*parA* had a reduced transfer rate of only 2.36 % (± 0.15). Apparently, the Δ*parA* deletion reduced the plasmid transfer rate by a factor of about 5.

Table 3.7: Crossing results of the two strains TK54(pSCP2tetO) and TK54(pSCP2tetOΔ*parA*) with TK64::pRM43.

Strain(s)	Thio_Titer (Donor)	Apra_Titer (Recipient)	Thio/Apra_ Titer (Plasmid Transfer)	% Plasmid Transfer (Thio)	Mean	Std. dev.
TK54pSCP2tetO_1 X TK64pRM43	3.07E+09	2.87E+09	3.68E+08	11.98%		
TK54pSCP2tetO_2 X TK64pRM43	2.65E+09	2.23E+09	3.33E+08	12.57%	**12.2%**	**0.33**
TK54pSCP2tetO_3 X TK64pRM43	2.69E+09	2.48E+09	3.24E+08	12.01%		
TK54pSCP2tetOΔ*ParA*_1 X TK64pRM43	2.03E+09	1.61E+09	4.46E+07	2.19%		
TK54pSCP2tetOΔ*ParA*_2 X TK64pRM43	1.58E+09	1.47E+09	3.82E+07	2.42%	**2.36%**	**0.15**
TK54pSCP2tetOΔ*ParA*_3 X TK64pRM43	2.05E+09	1.50E+09	5.08E+07	2.48%		

3.5.4 Importance of the hyphal contact angle for enabling conjugative plasmid transfer

During the extensive attempts to observe conjugative plasmid transfer by time-lapse imaging, it was realized that the donor and recipient frequently made contact, but this contact did not result in the conjugative plasmid transfer. So the question arose, why are some hyphal contacts ineffective in plasmid transfer? A comparison of contact sites resulting in plasmid transfer (e.g. Figure 3.23) and those which did not support subsequent plasmid transfer (e.g. Figure 3.24) suggested that the angle of hyphal contact might be crucial. Thus, the angle of hyphal contact was measured with FIJI (method described in 2.2.11).

Streptomyces grow by apical tip extension, so the tips are the only part of the mycelium that can make contact and most likely areas for initiation of conjugative DNA transfer. When the donor and recipient hyphae had made contact, the angle of the contact site seems to be important for the DNA transfer. No plasmid transfer was observed, when the contact angle is less than 27.5° (Figure 4.26, a-c). But, at 59° and 74° angles, conjugative plasmid transfer and subsequent spreading spreading of the plasmid was observed (Figure 4.25).

(a)

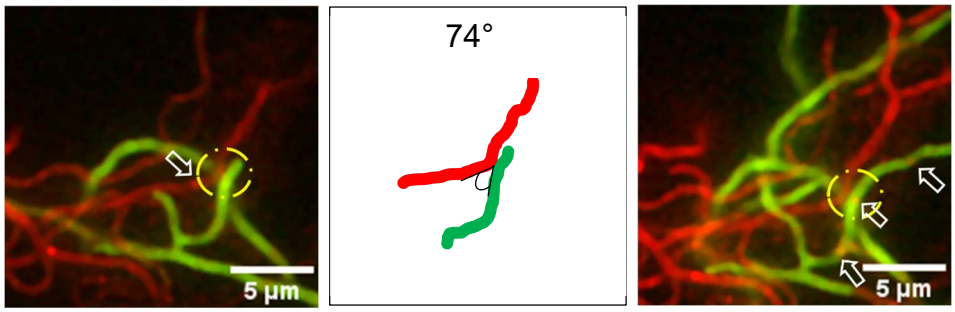

1min 220 mins

(b)

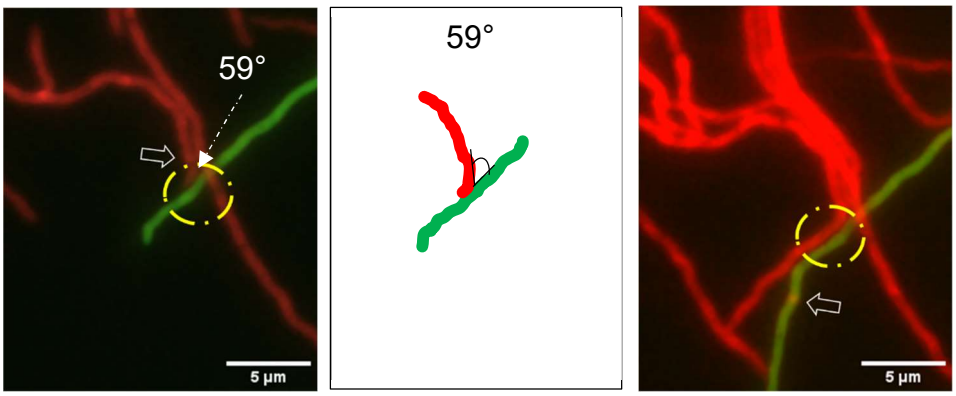

1min 250 mins

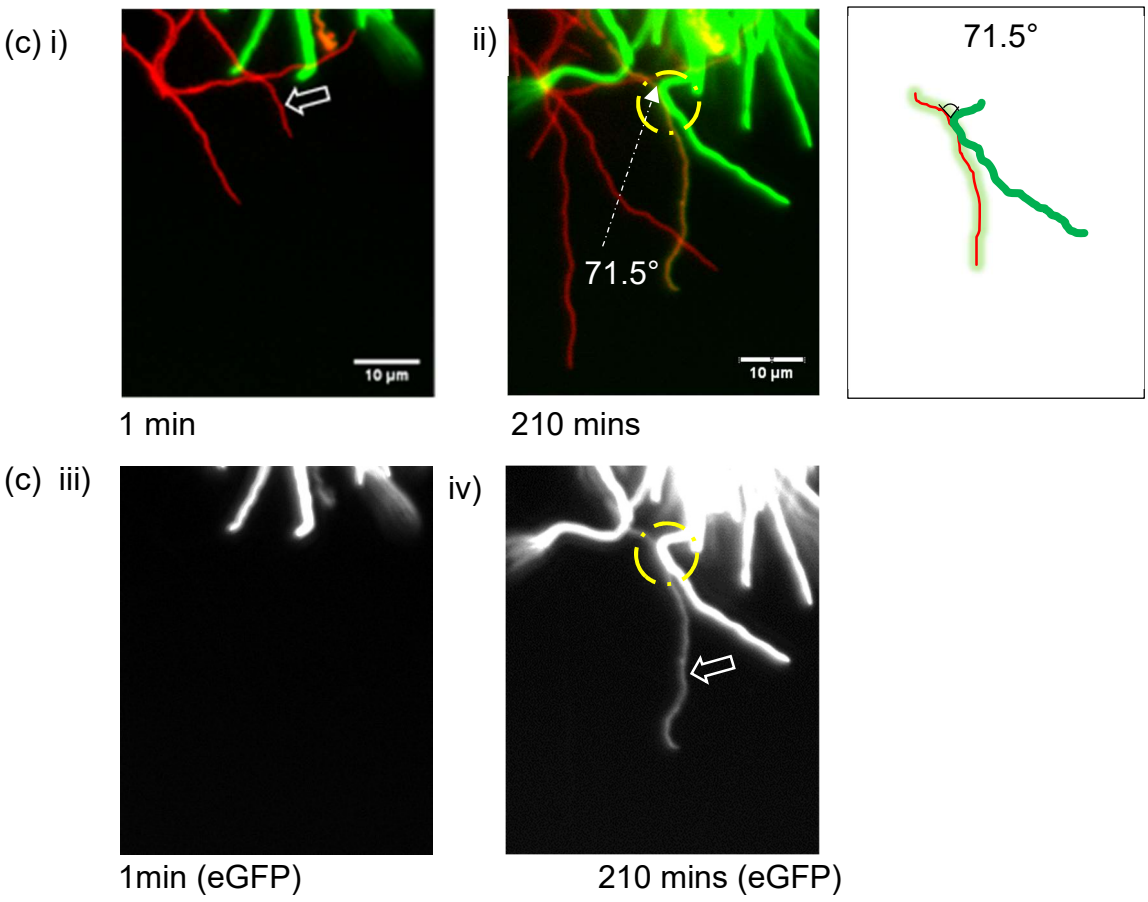

Figure 3.23: Showing effective contact sites with angles. The contact sites of donor (red) and recipient (green) are marked as yellow circles and white arrows represent the location of the plasmid. A schematic diagram shows the contact angle of both hyphae. a) The green recipient hyphae established contact with the conjugative plasmid donor red colour hyphae at a 74° angle. Subsequently, after 220 minutes, the presence of three discernible plasmids were observed within the recipient hyphae. b) The plasmid containing tip of the red donor hyphae-initiated contact with the green recipient hyphae at a 59° angle. The transferred plasmid is visibility in the recipient hyphae 250 minutes after the initial contact. c) These time-lapse images are taken from L. Thoma *et*. al (2019). Upon plasmid transfer (after 210 minutes), the recipient hyphae (red colour) turns into yellow (overlay of green and red). Images on the button (iii, iv) side show the eGFP-channel, while on the top (i, ii), the merged eGFP/mCherry images are displayed.

(a)

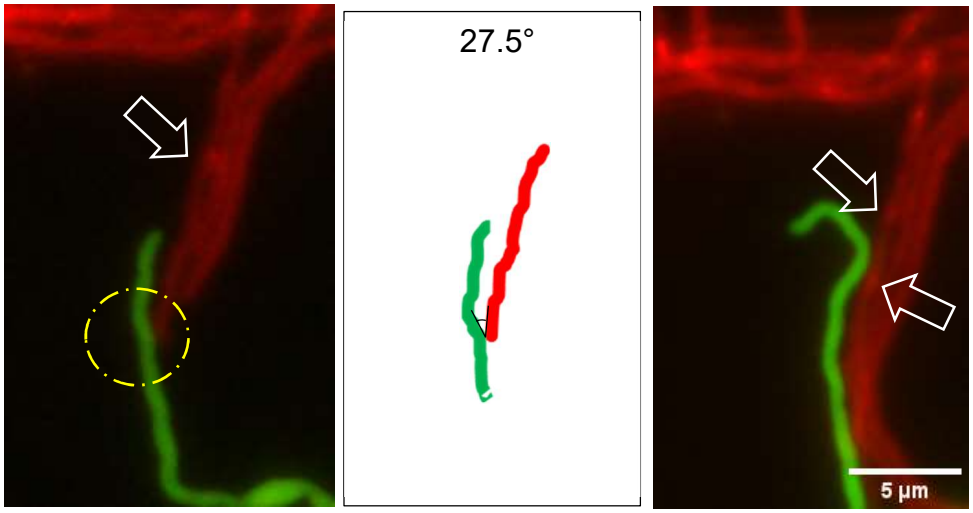

1 min (27.5°) 260 mins

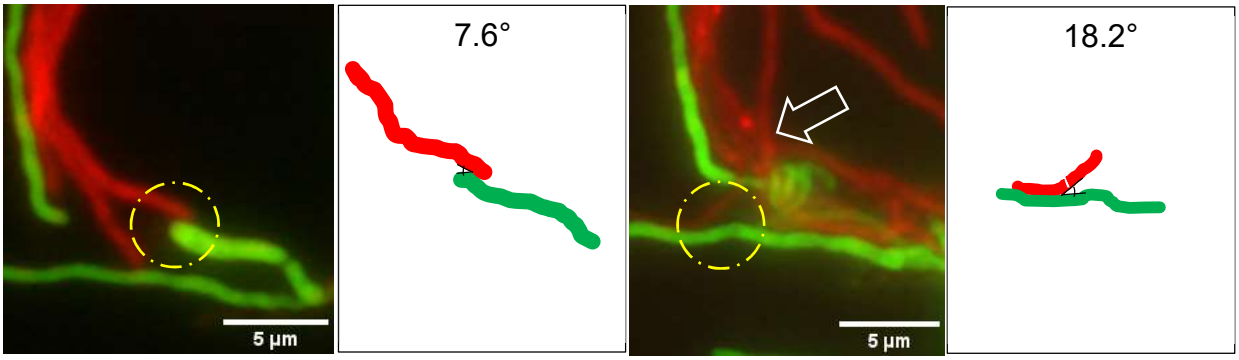

(b) 1 min (7.6°) 560 mins (18.2°)

c)

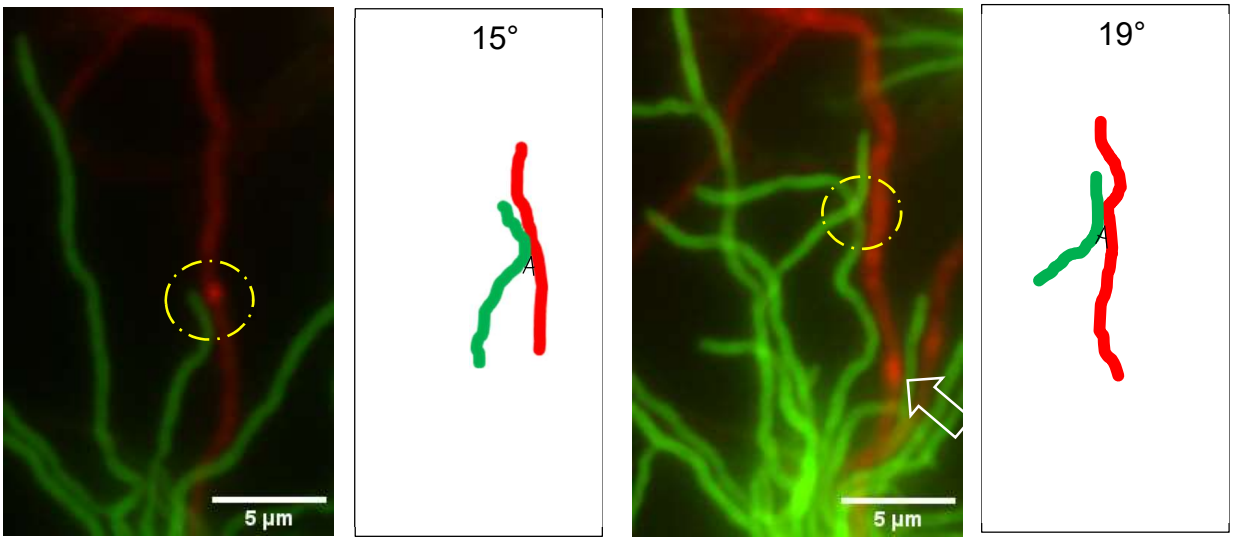

1 min (15°) 700 mins (19°)

Figure 3.24. Showing non-effective contact sites with angles. The contact sites marked as yellow circle and white arrows represent the location of plasmids A schematic diagram shows the contact angle of both hyphae. a) Mycelial tip of donor and recipient find each other on solid medium in the angle of 27.5°. During the subsequent 260 minutes, the donor hyphae extended along the lateral wall of the recipient hyphae, yet no transfer of the plasmid was detected. b) Two different angles, 7.6° and 18.2° are measured in the contact sites and no plasmid transfer occurred, after 580 minutes. c) Also, no plasmid transfer to the recipient occurred even after 700 minutes of incubation, when the two hyphae were in contact at 15° and 19°C angles.

3.5.5 Visualization of chromosome transfer into the recipient mycelium

Conjugative *Streptomyces* plasmids were shown to confer fertility by mobilizing chromosomal markers (Bibb et al., 1981, Kieser et al., 1982). A recent analysis including genetic crosses with multiple-marked *S. coelicolor* strains indicated that each plasmid transfer could be associated with the transfer of the complete chromosome (manuscript in preparation). To visualize the transfer of chromosomal DNA, the FROS system was applied to *S. coelicolor*. Subsequently, pIJ12075-tetO and pTetRmcherry were introduced into *S. coelicolor* M145 by intergeneric conjugation and integrated into the genome, yielding strain M145::pTetRmCherry::pIJ12507tetO. This strain was transformed with the conjugative plasmid pIJ303 by PEG-mediated protoplast transformation. The resulting strain was used as the donor and mated with *S. coelicolor* M1146::pGFPtetRmCherry as the recipient.

The homogenized mycelia of both samples were mixed and pipetted on the top of the coverslips inserted into R5 agar and incubated at 29°C for 16 hours. In this experimental setup, the chromosomes in the donor hyphae light up as red fluorescent foci (Figure 3.25, yellow arrows), while the recipient hyphae appear green. When the donor and recipient strains made contact (white circles) at the lateral walls, the chromosome was transferred, which is visualized as red spots in the green hyphae (white arrows). This is the first report, demonstrating the transfer of chromosomal DNA by fluorescence microscopy.

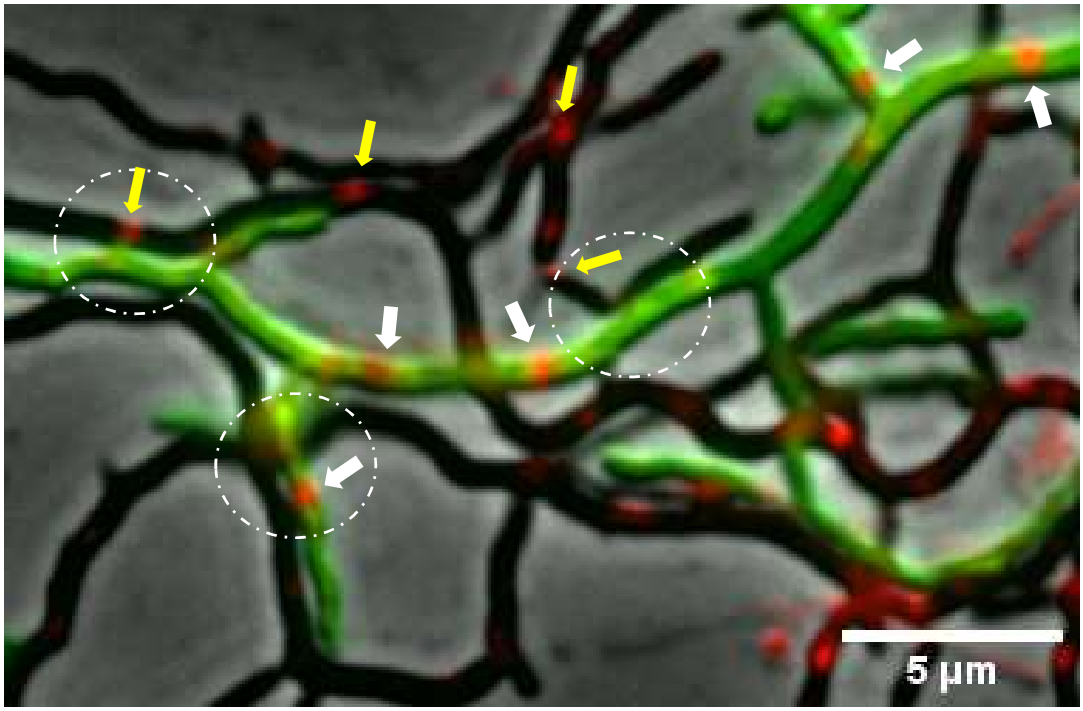

Figure 3.25: Visualization of chromosome transfer by FROS. The positions of several chromosome spots in the donor mycelium are indicated by yellow arrows and possible contact sites for conjugative DNA transfer by white circles. Chromosomes that have been transferred to the recipient appear as red fluorescent foci in green hyphae (white arrows).

4. Discussion

A crucial factor of bacterial growth is to ensure proper segregation of the genetic material during cell division. This process is a particular challenge in mycelial *Streptomycetes*, since they grow by apical tip extension forming a multiple-branched mycelium that penetrates the substrate (Flärdh & Buttner, 2009). This unusual mode of growth does not include classical cell division, although the hyphae are structured into compartments by septal cross walls that are formed at irregular distances by the SepX protein (Bush et al., 2022). This raises the question, how *Streptomyces* manages the distribution of the genetic material, plasmids, and the chromosome, within the hyphal compartments of the branching mycelium. This question was addressed in this thesis by the localization of the single copy number plasmid SCP2 (Bibb et al., 1977; Haug et al., 2003) in *S. lividans* by time lapse imaging.

4.1 FROS technology to localize specific DNA sequences in living cells

A well-known technique for fluorescently tagging specific DNA (e.g. chromosomal) sequences is called Fluorescence In Situ Hybridization (FISH) (Langer-Safer et al., 1982). In this method, fluorescently labelled DNA fragment probes were created by nick translation or PCR-mediated incorporation of fluorescent nucleotide analogs (Rigby et al., 1977). The fluorescent DNA fragment probes are in situ hybridized to the genomic DNA after the cells have been made permeable. FISH's main drawback is that the method cannot be used for live cell imaging since the cells must be fixed, permeabilized, and treated to denature the DNA to allow hybridization of the fluorescent DNA probes with the genomic DNA. Additionally, the fixing procedure could theoretically cause artifacts. However, this technique is still employed for calculating loci distances at the molecular level (Iwasaki et al., 2015; Kim et al., 2016).

Fluorescent repressor-operator systems (FROS) are based on the interaction of a bacterial operator sequence and a repressor protein fused to a fluorescent protein. To improve sensitivity, an array ($n_{120\text{-}240}$) of operator sequences is integrated into the target locus of the genome to support binding of multiple fluorescent repressor proteins. There are two common types of FROS: one is based on the repressor and the operator of the lactose operon (*lacO*/LacR) proposed in 1996 (Straight et al., 1996), and the other is based on the repressor and the operator of the tetracycline

resistance operon of *Escherichia coli* (*tetO*/TetR) proposed a year later (Michaelis et al., 1997).

Combination of both systems enabled the simultaneous visualization of two different loci in cells. Chromosome condensation was measured in living *Saccharomyces cerevisiae* cells, by the use of two fluorescent repressor operator systems (FROS) labelled loci (Vas et al., 2007). The fraction of cells in which fluorescent FROS foci could be distinguished or overlapped was used to quantify chromosomal condensation rather than locus distance. Petrova et al., improved this system in *S. pombe* by tracking the FROS foci positions over time and using the distance between them to calculate chromosomal condensation (Petrova et al., 2013).

By using the tetO/TetR FROS system in *S*. *coelicolor*, Kois-Ostrowska et al., showed that the chromosome remains closely associated with the extending hyphal tip (Kois-Ostrowska et al., 2016). Mutant strains of *S*. *coelicolor* lacking ParA showed delocalization of the chromosome, since ParA was shown to anchor the oriC region of the tip-proximal chromosome copy to the hyphal tip through interaction with the apical polarisome (Kois-Ostrowska et al., 2016). The polarisome is composed of the cytoskeletal elements DivIVA and FilP and directs growth by apical tip extension and branching (Ausmees, 2013; Fuchino et al., 2013). In addition to the established FROS systems, alternative loci tagging systems based on inactivate Cas9-FP have recently been established, also in conjunction with the expression of GFP-tagged nanobodies (SunTag) (Chen et al., 2013; Tanenbaum et al., 2014). Most FROS studies mainly report on the localization of chromosomal loci (Robinett et al., 1996; Viushkov et al., 2022) and only in few studies FROS was also applied for the visualization of plasmid DNA in growing cells. FROS studies revealed that RK2 in *Caulobacter crescentus* is unevenly distributed between the cell compartments and is inherited by progeny cells in an asymmetrical manner (Wegrzyn et al., 2013).

In addition, the conjugative plasmid transfer in living mycelium has been observed by classical time-lapse fluorescence microscopy. (Thoma et al., 2019). Here, the conjugative plasmid encoded a soluble eGFP protein and the recipient was marked by the integration of the mCherry gene into the chromosomal PhiC31 attachment site. Thus, conjugative plasmid transfer was detected, when certain hyphae showed fluorescence in both channels (green and red). However, plasmid transfer into the

recipient was detectable only with delay, due to the time period required for establishment of the plasmid and expression of eGFP in sufficient amounts. This drawback should be eliminated by using the FROS method to localize the chromosome, plasmid movement, and conjugative plasmid transfer.

4.2 The single copy number plasmid SCP2tetO moves within the growing mycelium

After the development of the FROS system for SCP2tetO detection in *S. lividans*, still images of fluorescence microscopy were analysed to elucidate whether SCP2 occupies a specific position in the mycelium. Plasmid position was calculated for 37 short non-branched hyphae (1.12 - 6.75µm length) (table 3.1), which contained a single SCP2tetO fluorescence spot.

At a certain length, the hyphae contained more than two plasmids. A hypha of 4.26 µm length contained four plasmids. The longest hypha had a length of 24.15 µm and contained eleven plasmids. The first plasmid copy localized close (**1.29 µm ± 1.09)** to the branching site, while the tip-proximal copy had a distance of **2.05µm (± 1.38)** to the tip. The average plasmid to plasmid distance was determined to be 1.37 **µm (±0.92**) (table 3.5). These values from the localization of a single copy plasmid in a growing mycelium indicates that one plasmid copy follows the extending tip, while one copy localized very close to the branching site (Figure 3.13).

4.3 Movement of SCP2tetO resembles that of the chromosome

Localization of SCP2tetO close to the tip resembled localization data of the *S. coelicolor* chromosome. By labelling of the chromosomal replication initiation region (*oriC*) and time-lapse microscopy, it was shown that the chromosomes were anchored to the tips of vegetative hyphae via interaction with the polarisome (Kois-Ostrowska et al., 2016).

To directly compare SCP2tetO localization with the localization of the chromosome, the same FROS system was applied for determining the positions of the chromosomes (n=34) (table 3.2). The *tetO* array was integrated into the chromosome of *S. lividans* upstream of SLI_5122, approximately 973 kbp downstream of the *oriC*. Fluorescence

microscope imaging of short hyphae, which contained a single chromosome, revealed that the chromosome was placed in an average distance of **2.56 µm (± 1.85)** to the branching site and **3.93 (± 2.86)** µm to the tip. In comparison, the position of SCPtetO was 1.25 µm (±1.01) to the branch and 2.21 µm (± 0.99) to the tip.

In longer hyphae (n=16) of 3.46 µm - 11.31 µm length (table 3.4), two chromosome copies were observed. One chromosome was located at an average distance of **1.56 µm** (± 1.35) from the branching site, the other copy **1.96 µm** (± 0.96) from the tip. This is similar to the plasmid distribution pattern, where one copy of SCP2tetO located close (0.66 µm ± 0.86 µm) to the branching site and the second copy close (1.71 µm ± 1.09 µm) to the tip. The average distance between two chromosome copies was 2.66 µm ± 1.66, again very similar to the distance (1.96 µm ± 1.28) of the SCP2tetO copies.

Also, in the very long hyphae (10.98 – 52.90 µm, n=15) that contained multiple chromosome copies, the localization pattern was similar to that of plasmid SCP2tetO. The first chromosome localized 2. 09 µm ± 1.22 (SCP2tetO: 1.29 µm ± 1.09; n=13) from the branching site and the tip-proximal chromosome in a distance of 3.65 µm ± 1.91 (SCP2tetO: 2.05 µm ± 1.38; n=13) to the tip. The distance between two chromosome spots was about 2. 27 µm ± 1.83 µm on average, that of SCP2tetO was **1.37 µm (±0.92)**.

Time lapse imaging of SCP2tetO localization and that of the chromosome revealed that the tip proximal copy always followed the extending tip at a constant distance. At certain time points the chromosomes replicated as it is indicated by the splitting of the fluorescent spots (e.g. figure 3.15, 40 min, 2.20 hours, 3.3 hours). Both, replication of the plasmid or the chromosome is not restricted to the tip-proximal copy, also other copies undergo replication, preferentially those, which had entered a new hyphae after branching.

These data are therefore consistent with earlier reports that DNA replication takes place throughout the length of the hyphae and is not restricted to the tip (Kummer & Kretschmer, 1986a, 1986b; Yang & Losick, 2001). Observation of the replication factory (replisome), tagged by a DnaN-eGFP fusion, of *S. coelicolor* by time lapse imaging (Wolánski et al., 2011) revealed multiple replisomes throughout the whole

mycelium. Where the tip-proximal replisome was always positioned at a distance of 5.32 (±2.00) µm to the tip.

Tip association of a chromosome copy was mediated by the partitioning ATPase ParA through interaction with the polarisome, the apical protein complex directing peptidoglycan incorporation (Kois-Ostrowska et al., 2016) (Figure 4.1). This complex consists of various proteins and includes cytoskeletal elements, like FilP (Bagchi et al., 2008), DivIVA (Flardh, 2003; Hempel et al., 2008), ParA (Jakimowicz et al., 2007), and ParB (Jakimowicz et al., 2002).

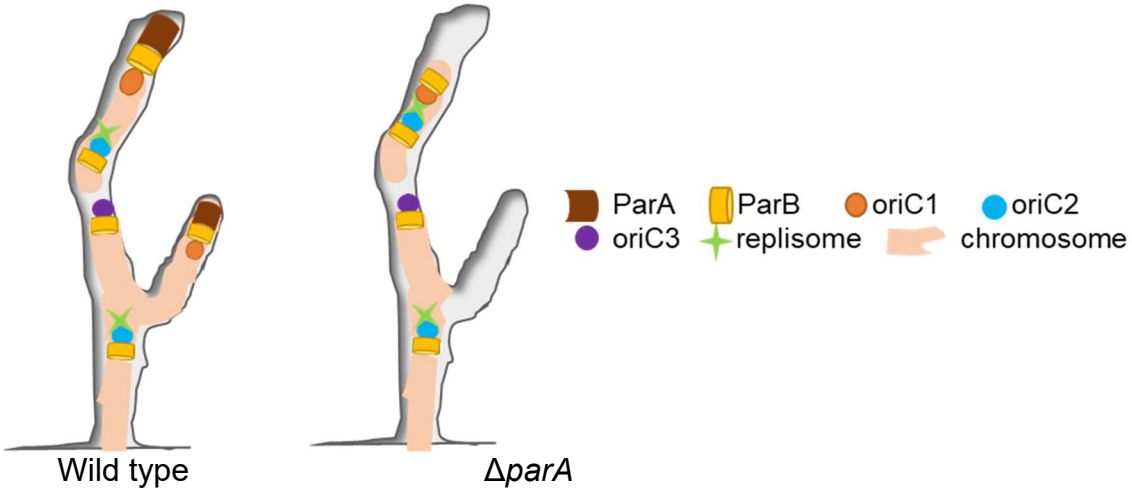

Figure 4.1: Illustrated model of ParA anchorage of the oriC/ParB complex at the tips of extending hyphae (modified from from Kois-Ostrowska et al., 2016). ParA interacts with a polarisome component and binds to one of the multiple *oriC*s associated with ParB on the chromosome. During chromosome replication, ParA captures one daughter *oriC* near the tip and maintains a constant distance, while the other daughter *oriC´s* are left behind, allowing for distal replication. During branching, ParA acts as an anchor by capturing ParB-*oriC* complexes and targeting them to the new hyphal tube, facilitating efficient extension. This interaction with polar proteins is unique to *Streptomyces* and is essential during spore germination and branching.

All in all, the distribution pattern of SCP2tetO resembles that of the chromosome and the tip-proximal copy of SCP2tetO followed the tip in a constant distance like the

chromosome. There are several explanations possibly to explain this localisation pattern:

i. SCP2tetO is somehow associated with the chromosomal DNA.
ii. SCP2tetO (and the chromosome) stay associated with the replisome (which is positioned in the mycelium by unknown factors)
iii. ParA not only anchors the chromosome to the tip but also the plasmid SCP2tetO
iv. The plasmid encoded $ParAB_{SCP2}$ system functions in an analogous way as the chromosomal ParA/B and anchors SCP2tetO to the tips and branching site by the interaction of $ParA_{SCP2}$ with components of the polarisome

4.4 $ParA_{SCP2}$ is required to separate the replicated plasmid copies and to anchor SCP2tetO to hyphal tips and branching points.

Not only chromosomes, but also low-copy-number plasmids like SCP2 (Haug et al., 2003) and linear plasmids like SLP2 (Huang et al., 2003) or SCP1 (Bentley et al., 2004) involve a functional ParAB partitioning system to ensure stable maintenance during vegetative growth and sporulation. ParB is a DNA binding protein, which binds specifically to one or more centromere-like *parS* sites. ParA is an ATPase, which binds non-specifically to DNA and transports the ParB-*parS* complex to distribute the plasmid copies. The *parAB* system of SCP2 has been demonstrated to be important for stable maintenance of SCP2, in particular during sporulation of *S. coelicolor* (Haug et al., 2003).

To study whether the $ParAB_{SCP2}$ system of SCP2tetO affects anchoring of the plasmid to tips and branching sites and the movement of the plasmids within the mycelium, a *parA* mutant of plasmid SCP2tetO was generated. In plasmid SCP2tetOΔ*parA* *parA* was completely deleted by lambda *red* mediated recombination (Datsenko & Wanner, 2000).

Detection of SCP2tetOΔ*parA* by FROS revealed a significantly different localization pattern, compared to SCP2tetO. Fewer and more widely distributed, but very bright SCP2tetOΔ*parA* spots were observed. These spots were only very rarely detected close to the tips or branching sites. The fluorescence intensity (Figure 3.18) of SCP2tetOΔ*parA* was about double compared to SCP2tetO. This suggests that in the

absence of ParA, the replicated plasmid copies could not separate and stayed intertwined. Moreover, proper anchorage of the plasmid to the tips and branching sites was affected. Thus, the $ParAB_{SCP2}$ system of SCP2 seems to have a similar function, as it was reported for the chromosomal ParAB system(Kois-Ostrowska et al., 2016).

The localization defect of SCP2tetOΔ*parA* is also in agreement with the increased instability of SCP2tetOΔ*parA* in vegetative mycelium, causing plasmid loss in 72 % of the colonies derived from regenerated protoplasts.

The ParAB system of SCP2tetOΔ*parA* is not essential for conjugative plasmid transfer from the donor to the recipient, but it affected the efficiency of plasmid transfer. Whereas, plasmid SCP2tetO was transferred with a rate of 12.2%, the conjugative plasmid transfer of SCP2tetΔ*parA* was reduced to 2.36% (Table 3.7). Transfer of SCP2tetΔ*parA* was also detected by FROS (Figure 3.22).

4.5 FROS allows detection of conjugative plasmid transfer by life cell imaging

Mycelial growth by apical tip extension implies that peptidoglycan (PG) remodelling mainly takes place at the hyphal tip and that only the tip compartments of donor and recipient mycelium are able to make contacts. Nevertheless, conjugative plasmid transfer was detected via the lateral walls (Thoma et al., 2016; Thoma & Muth, 2016). This suggests that transfer involves a conjugation bridge via new branching sites developing at the lateral wall. Alternatively, the contacting tip might generate a fusion and simultaneously a new tip is generated, which continues growth along the lateral wall of the mating partner. By conventional fluorescence microscopy the alternative route of transfer cannot be distinguished, since the resolution is not sufficient.

Therefore, it was attempted to use FROS to observe the conjugative plasmid transfer in real time. Still images of mating hyphae (Figure 3.20) demonstrated the suitability of FROS to detect conjugative plasmid transfer. In this study, donor and recipient hyphae were grown on coverslips inserted into R5 agar.

However, observation of conjugative plasmid transfer by time lapse imaging was much trickier. Donor and recipient hyphae had to grow in the microscopic chamber on an air permeable membrane. Under these conditions the mycelium did not show reproducible growth and it could not be predicted which tips elongated properly and

which tips didn´t continue growth. Moreover, the irradiation with UV light affected viability of the mycelium and simultaneously bleached the fluorescence of TetRmcherry. Thus, conjugative DNA transfer in the microscopic chamber was a rare and hardly detectable event, compared to the ~ 100 % efficient plasmid transfer on agar plates.

Although the quality of the time lapse videos was not satisfying, conjugative plasmid transfer could be observed. However, the transferred plasmid was detectable only about 4 hours after hyphal contact. Since conjugative plasmid transfer is mediated by the FtsK-like DNA translocase TraB, the transfer should require only seconds. For FtsK from *P. aeruginosa* the speed of DNA-translocation was determined to be 17,5 kbp/ sec (Jean et al., 2020). If TraB of SCP2tetO works with a similar efficiency, the transfer of SCP2tetO would require only two seconds, and not 4 hours. But it is not known, how long it takes to build up a translocation pore spanning the cell envelopes of donor and recipient before DNA translocation can take place.

In PG binding assays, it was demonstrated that the DNA-translocase TraB of plasmid pSVH1 can interact with PG of *S. lividans* (Vogelmann et al., 2011). Since *Streptomyces* plasmids typically do not encode a PG-hydrolase (Thoma & Muth, 2015), transfer at the tips or branching sites would enable TraB to recruit PG-hydrolases involved in apical tip extension that are chromosomally encoded (Flärdh et al., 2012). This would allow formation of a mating channel that penetrates the PG-sacculi (Thoma & Muth, 2012). This mating channel does not constitute a simple hyphal fusion that would allow free diffusion of proteins, nucleic acids, and other cellular components, but is specific for the specific conjugative plasmid, that is recognized by TraB (Grohmann et al., 2017; Thoma et al., 2016).

When a tip approaches the mating partner it seems to bend (or generates a new tip, if the original tip fuses with the mating partner) and grows for a while next to the mating partner. I had found that the angle of hyphal contact between donor and recipient hyphae was crucial for conjugative plasmid transfer to occur. Several events of contact angles up to 27.5° (donor tip-recipient lateral wall; 27.5°, 7.6°, 18.2°, 20°and recipient tip-donor lateral wall; 21.2°, 19°, 24°, 15°, 19°) did not support transfer of the plasmid. In contrast, plasmid transfer into the recipient was observed, when the contact angle was higher than 59° (Figure 3.23).

Demonstration of chromosomal DNA transfer by FROS.

Conjugative *Streptomyces* plasmids were shown to transfer(mobilize) chromosomal markers with high efficiency. Recently it was shown that in certain matings frequency of the transfer of megabase sized chromosomal DNA fragments (or the complete chromosome) can achieve nearly 100 %, meaning that each plasmid transfer event is associated with the simultaneous transfer of chromosomal DNA (H. Hirkow, Bachelor thesis, L. Sniegula, Bachelor thesis, Thoma et al., manuscript in preparation). This high frequency chromosomal DNA transfer only occurred, if the donor was proficient for antibiotic production and the recipient lacked the respective biosynthetic gene clusters (BGCs). This suggested that BGCs have a stimulatory effect on chromosome transfer, probably by acting as non-conventional toxin-antitoxin systems, selecting for the preferential survival of those recipients, which obtained the BGCs (including the resistance determinant as “antitoxin”) by conjugation (Thoma et al., manuscript in preparation).

To support these findings with an independent technique, the FROS system was transferred to *S. coelicolor*. Plasmids pTetRmcherry and pIJ12507tetO were integrated into the respective chromosomal attachment sites of the wildtype *S. coelicolor* M145. Subsequently the conjugative multi copy plasmid pIJ303 (Kieser et al., 1982) was introduced. As a recipient, the so-called super host *S. coelicolor* M1146, where all four BGCs of *S. coelicolor* had been deleted (Gomez-Escribano & Bibb, 2011) was labelled by the integration of pTetRmcherry_eGFP.

When both strains were mated on a cover slide inserted into R5 agar, the transfer of the (central part) of the donor chromosome and its subsequent spreading in the recipient mycelium was observed (Figure 3.25). This is the first report of visualization of conjugative transfer of chromosomal DNA independent of any previous selection process.

5. References

Amado, E., Muth, G., Arechaga, I., & Cabezón, E. (2019). The FtsK-like motor TraB is a DNA-dependent ATPase that forms higher-order assemblies. Journal of Biological Chemistry, 294(13), 5050–5059. https://doi.org/10.1074/jbc.RA119.007459

Ausmees, N. (2013). Coiled coil cytoskeletons collaborate in polar growth of *Streptomyces*. BioArchitecture, 3(4), 110–112. https://doi.org/10.4161/bioa.26194

Bagchi, S., Tomenius, H., Belova, L. M., & Ausmees, N. (2008). Intermediate filament-like proteins in bacteria and a cytoskeletal function in *Streptomyces*. Molecular Microbiology, 70(4), 1037–1050. https://doi.org/10.1111/j.1365-2958.2008.06473.x

Barka, E. A., Vatsa, P., Sanchez, L., Gaveau-Vaillant, N., Jacquard, C., Klenk, H.-P., Clément, C., Ouhdouch, Y., & van Wezel, G. P. (2015). Taxonomy, Physiology, and Natural Products of Actinobacteria. Microbiology and Molecular Biology Reviews, 80(1), 1–43. https://doi.org/10.1128/mmbr.00019-15

Becker, E., Herrera, N. C., Gunderson, F. Q., Derman, A. I., Dance, A. L., Sims, J., Larsen, R. A., & Pogliano, J. (2006). DNA segregation by the bacterial actin AlfA during *Bacillus subtilis* growth and development. The EMBO Journal, 25(24), 5919–5931. https://doi.org/10.1038/sj.emboj.7601443

Begg, K. J., Dewar, S. J., & Donachie, W. D. (1995). A new *Escherichia coli* cell division gene, *ftsK*. Journal of Bacteriology, 177(21), 6211–6222.

Bentley, S. D., Brown, S., Murphy, L. D., Harris, D. E., Quail, M. A., Parkhill, J., Barrell, B. G., McCormick, J. R., Santamaria, R. I., Losick, R., Yamasaki, M., Kinashi, H., Chen, C. W., Chandra, G., Jakimowicz, D., Kieser, H. M., Kieser, T., & Chater, K. F. (2004). SCP1, a 356 023 bp linear plasmid adapted to the ecology and developmental biology of its host, *Streptomyces coelicolor* A3(2). Molecular Microbiology, 51(6), 1615–1628. https://doi.org/10.1111/j.1365-2958.2003.03949.x

Bentley, S. D., Chater, K. F., Cerdeño-Tárraga, A.-M., Challis, G. L., Thomson, N. R., James, K. D., Harris, D. E., Quail, M. A., Kieser, H., Harper, D., Bateman, A., Brown, S., Chandra, G., Chen, C. W., Collins, M., Cronin, A., Fraser, A., Goble, A., Hidalgo, J., Hopwood, D. A. (2002). Complete genome sequence of the model actinomycete

Streptomyces coelicolor A3(2). Nature, 417(6885), Article 6885. https://doi.org/10.1038/417141a

Bérdy, J. (2005). Bioactive microbial metabolites. The Journal of Antibiotics, 58(1), 1–26. https://doi.org/10.1038/ja.2005.1

Bérdy, J. (2012). Thoughts and facts about antibiotics: Where we are now and where we are heading. The Journal of Antibiotics, 65(8), 385–395. https://doi.org/10.1038/ja.2012.27

Bibb, M. J., Freeman, R. F., & Hopwood, D. A. (1977). Physical and genetical characterisation of a second sex factor, SCP2, for *Streptomyces coelicolor* A3(2). Molecular and General Genetics MGG, 154(2), 155–166. https://doi.org/10.1007/BF00330831

Bibb, M. J., & Hopwood, D. A. (1981). Genetic Studies of the Fertility Plasmid SCP2 and its SCP2* Variants in *Streptomyces coelicolor* A3(2). Microbiology, 126(2), 427–442. https://doi.org/10.1099/00221287-126-2-427

Bibb, M. J., Ward, J. M., Kieser, T., Cohen, S. N., & Hopwood, D. A. (1981). Excision of chromosomal DNA sequences from *Streptomyces coelicolor* forms a novel family of plasmids detectable in *Streptomyces lividans*. Molecular and General Genetics MGG, 184(2), 230–240. https://doi.org/10.1007/BF00272910

Bibb, M., Schottel, J. L., & Cohen, S. N. (1980). A DNA cloning system for interspecies gene transfer in antibiotic-producing *Streptomyces*. Nature, 284(5756), 526–531.

Birnboim, H. C., & Doly, J. (1979). A rapid alkaline extraction procedure for screening recombinant plasmid DNA. Nucleic Acids Research, 7(6), 1513–1523. https://doi.org/10.1093/nar/7.6.1513

Brock, T. D. (1961). Chloramphenicol. Bacteriological Reviews, 25(1), 32–48. https://doi.org/10.1128/br.25.1.32-48.1961

Brooks, A. C., & Hwang, L. C. (2017). Reconstitutions of plasmid partition systems and their mechanisms. Plasmid, 91, 37–41. https://doi.org/10.1016/j.plasmid.2017.03.004

Bush, M. J., Gallagher, K. A., Chandra, G., Findlay, K. C., & Schlimpert, S. (2022). Hyphal compartmentalization and sporulation in *Streptomyces* require the conserved

cell division protein SepX. Nature Communications, 13(1), 71. https://doi.org/10.1038/s41467-021-27638-1

Carraro, N., & Burrus, V. (2015). The dualistic nature of integrative and conjugative elements. Mobile Genetic Elements, 5(6), 98–102. https://doi.org/10.1080/2159256X.2015.1102796

Champness, W. C. (1994). Regulation and integration of antibiotic production and morphological differentiation in *Streptomyces spp*. Regulation of Bacterial Differentiation, 61–93.

Chang, P.-C., & Cohen, S. N. (1994). Bidirectional replication from an internal origin in a linear *Streptomyces* plasmid. Science, 265(5174), 952–954.

Chater, K. F. (1984). Morphological and physiological differentiation in *Streptomyces*. Microbial Development, 89–115.

Chater, K. F. (1993). Genetics of differentiation in *Streptomyces*. Annual Review of Microbiology, 47, 685–713. https://doi.org/10.1146/annurev.mi.47.100193.003345

Chater, K. F., & Chandra, G. (2006). The evolution of development in *Streptomyces* analysed by genome comparisons. FEMS Microbiology Reviews, 30(5), 651–672.

Chater, K. F., & Losick, R. (1997). Mycelial life style of *Streptomyces coelicolor* A3 (2) and its relatives. Bacteria as Multicellular Organisms, 149–182.

Chen, B., Gilbert, L. A., Cimini, B. A., Schnitzbauer, J., Zhang, W., Li, G.-W., Park, J., Blackburn, E. H., Weissman, J. S., Qi, L. S., & Huang, B. (2013). Dynamic Imaging of Genomic Loci in Living Human Cells by an Optimized CRISPR/Cas System. Cell, 155(7), 1479–1491. https://doi.org/10.1016/j.cell.2013.12.001

Chen, C. W., Yu, T.-W., Lin, Y.-S., Kieser, H. M., & Hopwood, D. A. (1993). The conjugative plasmid SLP2 of *Streptomyces lividans* is a 50 kb linear molecule. Molecular Microbiology, 7(6), 925–932. https://doi.org/10.1111/j.1365-2958.1993.tb01183.x

Chevillotte, M., Menges, R., Muth, G., Wohlleben, W., & Stegmann, E. (2008). A quick and reliable method for monitoring gene expression in actinomycetes. Journal of Biotechnology, 135(3), 262–265. https://doi.org/10.1016/j.jbiotec.2008.04.008

Cohen, S. N., Chang, A. C. Y., & Hsu, L. (1972). Nonchromosomal Antibiotic Resistance in Bacteria: Genetic Transformation of *Escherichia coli* by R-Factor DNA*. Proceedings of the National Academy of Sciences, 69(8), 2110–2114. https://doi.org/10.1073/pnas.69.8.2110

Cornell, C. R., Marasini, D., & Fakhr, M. K. (2018). Molecular Characterization of Plasmids Harbored by Actinomycetes Isolated From the Great Salt Plains of Oklahoma Using PFGE and Next Generation Whole Genome Sequencing. Frontiers in Microbiology, 9. https://www.frontiersin.org/articles/10.3389/fmicb.2018.02282

Cragg, G. M., Kingston, D. G., & Newman, D. J. (2011). Anticancer agents from natural products. CRC press.

Cummins, C. S., & Harris, H. (1956). J. gen. Microbiol, 14, 583.

Dahm, R. (2005). Friedrich Miescher and the discovery of DNA. Developmental Biology, 278(2), 274–288. https://doi.org/10.1016/j.ydbio.2004.11.028

Datsenko, K. A., & Wanner, B. L. (2000). One-step inactivation of chromosomal genes in *Escherichia coli* K-12 using PCR products. Proceedings of the National Academy of Sciences of the United States of America, 97(12), 6640–6645. https://doi.org/10.1073/pnas.120163297

Encheva-Malinova, M., Stoyanova, M., Avramova, H., Pavlova, Y., Gocheva, B., Ivanova, I., & Moncheva, P. (2014). Antibacterial potential of *streptomycete* strains from Antarctic soils. Biotechnology & Biotechnological Equipment, 28(4), 721–727.

Feeney, M. A., Newitt, J. T., Addington, E., Algora-Gallardo, L., Allan, C., Balis, L., Birke, A. S., Castaño-Espriu, L., Charkoudian, L. K., Devine, R., Gayrard, D., Hamilton, J., Hennrich, O., Hoskisson, P. A., Keith-Baker, M., Klein, J. G., Kruasuwan, W., Mark, D. R., Mast, Y., Hutchings, M. I. (2022). ActinoBase: Tools and protocols for researchers working on *Streptomyces* and other filamentous actinobacteria. Microbial Genomics, 8(7), mgen000824. https://doi.org/10.1099/mgen.0.000824

Flardh, K. (2003). Essential role of DivIVA in polar growth and morphogenesis in *Streptomyces coelicolor* A3(2). Molecular Microbiology, 49(6), 1523–1536. https://doi.org/10.1046/j.1365-2958.2003.03660.x

Flärdh, K., & Buttner, M. J. (2009). *Streptomyces* morphogenetics: Dissecting differentiation in a filamentous bacterium. Nature Reviews Microbiology, 7(1), 36–49. https://doi.org/10.1038/nrmicro1968

Flärdh, K., Richards, D. M., Hempel, A. M., Howard, M., & Buttner, M. J. (2012). Regulation of apical growth and hyphal branching in *Streptomyces.* Current Opinion in Microbiology, 15(6), 737–743. https://doi.org/10.1016/j.mib.2012.10.012

Franco, B., González-Cerón, G., & Servín-González, L. (2003). Direct repeat sequences are essential for function of the cis-acting locus of transfer (*clt*) of *Streptomyces phaeochromogenes* plasmid pJV1. Plasmid, 50(3), 242–247. https://doi.org/10.1016/s0147-619x(03)00063-5

Fuchino, K., Bagchi, S., Cantlay, S., Sandblad, L., Wu, D., Bergman, J., Kamali-Moghaddam, M., Flärdh, K., & Ausmees, N. (2013). Dynamic gradients of an intermediate filament-like cytoskeleton are recruited by a polarity landmark during apical growth. Proceedings of the National Academy of Sciences, 110(21), E1889–E1897. https://doi.org/10.1073/pnas.1305358110

Geraci, J. E., Heilman, F. R., Nichols, D. R., Ross, G. T., & Wellman, W. E. (1956). Some laboratory and clinical experiences with a new antibiotic, vancomycin. Proceedings of the Staff Meetings. Mayo Clinic, 31(21), 564–582.

Gomez-Escribano, J. P., & Bibb, M. J. (2011). Engineering *Streptomyces coelicolor* for heterologous expression of secondary metabolite gene clusters. Microbial Biotechnology, 4(2), 207–215. https://doi.org/10.1111/j.1751-7915.2010.00219.x

Grohmann, E., Keller, W., & Muth, G. (2017). Mechanisms of Conjugative Transfer and Type IV Secretion-Mediated Effector Transport in Gram-Positive Bacteria. In S. Backert & E. Grohmann (Eds.), Type IV Secretion in Gram-Negative and Gram-Positive Bacteria (pp. 115–141). Springer International Publishing. https://doi.org/10.1007/978-3-319-75241-9_5

Gust, B., Challis, G. L., Fowler, K., Kieser, T., & Chater, K. F. (2003). PCR-targeted *Streptomyces* gene replacement identifies a protein domain needed for biosynthesis of the sesquiterpene soil odor geosmin. Proceedings of the National Academy of Sciences, 100(4), 1541–1546. https://doi.org/10.1073/pnas.0337542100

Guynet, C., Cuevas, A., Moncalián, G., & Cruz, F. de la. (2011). The *stb* Operon Balances the Requirements for Vegetative Stability and Conjugative Transfer of Plasmid R388. PLOS Genetics, 7(5), e1002073. https://doi.org/10.1371/journal.pgen.1002073

Haug, I., Weissenborn, A., Brolle, D., Bentley, S., Kieser, T., & Altenbuchner, J. (2003). *Streptomyces coelicolor* A3(2) plasmid SCP2*: Deductions from the complete sequence. Microbiology-Sgm, 149, 505–513. https://doi.org/10.1099/mic.0.25751-0

Hazen, E. L., & Brown, R. (1950). Two antifungal agents produced by a soil actinomycete. Science (New York, N.Y.), 112(2911), 423.

Hempel, A. M., Wang, S., Letek, M., Gil, J. A., & Flardh, K. (2008). Assemblies of DivIVA Mark Sites for Hyphal Branching and Can Establish New Zones of Cell Wall Growth in *Streptomyces coelicolor*. Journal of Bacteriology, 190(22), 7579–7583. https://doi.org/10.1128/JB.00839-08

Hodgson, D. A., Mohan, S., Dow, C., & Cole, J. A. (1992). Prokaryotic Structure and Function: A New Perspective.

Hopwood, D. A. (2006). Soil to genomics: The *Streptomyces* chromosome. Annu. Rev. Genet., 40, 1–23.

Hopwood, D. A., Malpartida, F., Kieser, H. M., Ikeda, H., Duncan, J., Fujii, I., Rudd, B. a. M., Floss, H. G., & Ōmura, S. (1985). Production of 'hybrid' antibiotics by genetic engineering. Nature, 314 (6012), Article 6012. https://doi.org/10.1038/314642a0

Hopwood, D. A., & Sermonti, G. (1963). The Genetics of *Streptomyces coelicolor*. In E. W. Caspari & J. M. Thoday (Eds.), Advances in Genetics (Vol. 11, pp. 273–342). Academic Press. https://doi.org/10.1016/S0065-2660(08)60289-8

Hotta, K., Saito, N., & Okami, Y. (1980). Studies on new aminoglycoside antibiotics, istamycins, from an actinomycete isolated from a marine environment. I. The use of plasmid profiles in screening antibiotic-producing *streptomycetes*. The Journal of Antibiotics, 33(12), 1502–1509.

Hsu, C.-C., & Chen, C. W. (2010). Linear Plasmid SLP2 Is Maintained by Partitioning, Intrahyphal Spread, and Conjugal Transfer in *Streptomyces*. Journal of Bacteriology, 192(1), 307–315. https://doi.org/10.1128/jb.01192-09

Huang, C. H., Chen, C. Y., Tsai, H. H., Chen, C., Lin, Y. S., & Chen, C. W. (2003). Linear plasmid SLP2 of *Streptomyces lividans* is a composite replicon. Molecular Microbiology, 47(6), 1563–1576. https://doi.org/10.1046/j.1365-2958.2003.03403.x

Itoh, Y., Kawase, T., Nikaidou, N., Fukada, H., Mitsutomi, M., Watanabe, T., & Itoh, Y. (2002). Functional Analysis of the Chitin-binding Domain of a Family 19 Chitinase from *Streptomyces griseus* HUT6037: Substrate-binding Affinity and cis-Dominant Increase of Antifungal Function. Bioscience, Biotechnology, and Biochemistry, 66(5), 1084–1092. https://doi.org/10.1271/bbb.66.1084

Iwasaki, O., Tanizawa, H., Kim, K.-D., Yokoyama, Y., Corcoran, C. J., Tanaka, A., Skordalakes, E., Showe, L. C., & Noma, K. (2015). Interaction between TBP and Condensin Drives the Organization and Faithful Segregation of Mitotic Chromosomes. Molecular Cell, 59(5), 755–767. https://doi.org/10.1016/j.molcel.2015.07.007

Jakimowicz, D., Chater, K., & Zakrzewska-Czerwinska, J. (2002). The ParB protein of *Streptomyces coelicolor* A3(2) recognizes a cluster of *parS* sequences within the origin-proximal region of the linear chromosome. Molecular Microbiology, 45(5), 1365–1377. https://doi.org/10.1046/j.1365-2958.2002.03102.x

Jakimowicz, D., Zydek, P., Kois, A., Zakrzewska-Czerwinska, J., & Chater, K. F. (2007). Alignment of multiple chromosomes along helical ParA scaffolding in sporulating *Streptomyces* hyphae. Molecular Microbiology, 65(3), 625–641. https://doi.org/10.1111/j.1365-2958.2007.05815.x

Jean, N. L., Rutherford, T. J., & Löwe, J. (2020). FtsK in motion reveals its mechanism for double-stranded DNA translocation. Proceedings of the National Academy of Sciences, 117(25), 14202–14208. https://doi.org/10.1073/pnas.2001324117

Jones, S. E., & Elliot, M. A. (2017). *Streptomyces* Exploration: Competition, Volatile Communication and New Bacterial Behaviours. Trends in Microbiology, 25(7), 522–531. https://doi.org/10.1016/j.tim.2017.02.001

Kataoka, M., Seki, T., & Yoshida, T. (1991). Five genes involved in self-transmission of pSN22, a *Streptomyces* plasmid. Journal of Bacteriology, 173(13), 4220–4228.

Kendall, K. J., & Cohen, S. N. (1988). Complete nucleotide sequence of the *Streptomyces lividans* plasmid pIJ101 and correlation of the sequence with genetic properties. Journal of Bacteriology, 170(10), 4634–4651.

Khan, S. A., Adler, G. K., & Novick, R. P. (1982). Functional origin of replication of pT181 plasmid DNA is contained within a 168-base-pair segment. Proceedings of the National Academy of Sciences, 79(15), 4580–4584. https://doi.org/10.1073/pnas.79.15.4580

Kieser, T., Hopwood, D. A., Wright, H. M., & Thompson, C. J. (1982). pIJ101, a multi-copy broad host-range *Streptomyces* plasmid: Functional analysis and development of DNA cloning vectors. Molecular and General Genetics MGG, 185(2), 223–238. https://doi.org/10.1007/BF00330791

Kim, K.-D., Tanizawa, H., Iwasaki, O., & Noma, K. (2016). Transcription factors mediate condensin recruitment and global chromosomal organization in fission yeast. Nature Genetics, 48(10), Article 10. https://doi.org/10.1038/ng.3647

Kinashi, H. (2011). Giant linear plasmids in *Streptomyces*: A treasure trove of antibiotic biosynthetic clusters. The Journal of Antibiotics, 64(1), 19–25. https://doi.org/10.1038/ja.2010.146

Kinashi, H., Shimaji, M., & Sakai, A. (1987). Giant linear plasmids in *Streptomyces* which code for antibiotic biosynthesis genes. Nature, 328(6129), Article 6129. https://doi.org/10.1038/328454a0

Kois-Ostrowska, A., Strzałka, A., Lipietta, N., Tilley, E., Zakrzewska-Czerwińska, J., Herron, P., & Jakimowicz, D. (2016). Unique Function of the Bacterial Chromosome Segregation Machinery in Apically Growing *Streptomyces*—Targeting the Chromosome to New Hyphal Tubes and its Anchorage at the Tips. PLOS Genetics, 12(12), e1006488. https://doi.org/10.1371/journal.pgen.1006488

Kong, J., Yi, L., Xiong, Y., Huang, Y., Yang, D., Yan, X., Shen, B., Duan, Y., & Zhu, X. (2018). The discovery and development of microbial bleomycin analogues. Applied Microbiology and Biotechnology, 102(16), 6791–6798. https://doi.org/10.1007/s00253-018-9129-8

Kummer, C., & Kretschmer, S. (1986). Dna-Replication Behavior of Individual Nucleoids of 2 *Streptomyces* Strains. Journal of Basic Microbiology, 26(4), 219–223. https://doi.org/10.1002/jobm.3620260409

Lam, K. S. (2006). Discovery of novel metabolites from marine actinomycetes. Current Opinion in Microbiology, 9(3), 245–251.

Langer-Safer, P. R., Levine, M., & Ward, D. C. (1982). Immunological method for mapping genes on *Drosophila polytene* chromosomes. Proceedings of the National Academy of Sciences of the United States of America, 79(14), 4381–4385. https://doi.org/10.1073/pnas.79.14.4381

Lassadi, I., Kamgoué, A., Goiffon, I., Tanguy-le-Gac, N., & Bystricky, K. (2015). Differential Chromosome Conformations as Hallmarks of Cellular Identity Revealed by Mathematical Polymer Modeling. PLOS Computational Biology, 11(6), e1004306. https://doi.org/10.1371/journal.pcbi.1004306

Lau, I. F., Filipe, S. R., Søballe, B., Økstad, O.-A., Barre, F.-X., & Sherratt, D. J. (2003). Spatial and temporal organization of replicating *Escherichia coli* chromosomes. Molecular Microbiology, 49(3), 731–743. https://doi.org/10.1046/j.1365-2958.2003.03640.x

Lederberg, J., & Tatum, E. L. (1946). Gene recombination in *Escherichia coli*. Nature, 158(4016), 558.

Lee, H.-H., Hsu, C.-C., Lin, Y.-L., & Chen, C. W. (2011). Linear plasmids mobilize linear but not circular chromosomes in *Streptomyces*: Support for the ‘end first’ model of conjugal transfer. Microbiology (Reading, England), 157(Pt 9), 2556–2568. https://doi.org/10.1099/mic.0.051441-0

Li, Y., & Austin, S. (2002). The P1 plasmid is segregated to daughter cells by a ‘capture and ejection’ mechanism coordinated with *Escherichia coli* cell division. Molecular Microbiology, 46(1), 63–74. https://doi.org/10.1046/j.1365-2958.2002.03156.x

Li, Y., Sergueev, K., & Austin, S. (2002). The segregation of the *Escherichia coli* origin and terminus of replication. Molecular Microbiology, 46(4), 985–996. https://doi.org/10.1046/j.1365-2958.2002.03234.x

Lydiate, D. J., Malpartida, F., & Hopwood, D. A. (1985). The *Streptomyces* plasmid SCP2∗: Its functional analysis and development into useful cloning vectors. Gene, 35(3), 223–235.

Mann, J. (2001). Natural products as immunosuppressive agents. Natural Product Reports, 18(4), 417–430. https://doi.org/10.1039/b001720p

Mearini, G., Nielsen, P. E., & Fackelmayer, F. O. (2004). Localization and dynamics of small circular DNA in live mammalian nuclei. Nucleic Acids Research, 32(8), 2642–2651. https://doi.org/10.1093/nar/gkh587

Menges, R., Muth, G., Wohlleben, W., & Stegmann, E. (2007). The ABC transporter Tba of *Amycolatopsis balhimycina* is required for efficient export of the glycopeptide antibiotic balhimycin. Applied Microbiology and Biotechnology, 77(1), 125–134. https://doi.org/10.1007/s00253-007-1139-x

Michaelis, C., Ciosk, R., & Nasmyth, K. (1997). Cohesins: Chromosomal Proteins that Prevent Premature Separation of Sister Chromatids. Cell, 91(1), 35–45. https://doi.org/10.1016/S0092-8674(01)80007-6

Milbredt, S., & Waldminghaus, T. (2017). BiFCROS: A Low-Background Fluorescence Repressor Operator System for Labeling of Genomic Loci. G3 Genes|Genomes|Genetics, 7(6), 1969–1977. https://doi.org/10.1534/g3.117.040782

Morrison, D. A. (1979). Transformation and preservation of competent bacterial cells by freezing. In Methods in Enzymology (Vol. 68, pp. 326–331). Academic Press. https://doi.org/10.1016/0076-6879(79)68023-0

Muth, G. (2018). The pSG5-based thermosensitive vector family for genome editing and gene expression in actinomycetes. Applied Microbiology and Biotechnology, 102(21), 9067–9080. https://doi.org/10.1007/s00253-018-9334-5

Nett, M., Ikeda, H., & Moore, B. S. (2009). Genomic basis for natural product biosynthetic diversity in the actinomycetes. Natural Product Reports, 26(11), 1362–1384.

Pernodet, J.-L., & Guerineau, M. (1981). Isolation and physical characterization of *streptomycete* plasmids. Molecular and General Genetics MGG, 182(1), 53–59. https://doi.org/10.1007/BF00422766

Petković, H., Cullum, J., Hranueli, D., Hunter, I. S., Perić-Concha, N., Pigac, J., Thamchaipenet, A., Vujaklija, D., & Long, P. F. (2006). Genetics of *Streptomyces rimosus*, the oxytetracycline producer. Microbiology and Molecular Biology Reviews: MMBR, 70(3), 704–728. https://doi.org/10.1128/MMBR.00004-06

Petrova, B., Dehler, S., Kruitwagen, T., Hériché, J.-K., Miura, K., & Haering, C. H. (2013). Quantitative Analysis of Chromosome Condensation in Fission Yeast. Molecular and Cellular Biology, 33(5), 984–998. https://doi.org/10.1128/MCB.01400-12

Possoz, C., Ribard, C., Gagnat, J., Pernodet, J. L., & Guérineau, M. (2001). The integrative element pSAM2 from *Streptomyces*: Kinetics and mode of conjugal transfer. Molecular Microbiology, 42(1), 159–166. https://doi.org/10.1046/j.1365-2958.2001.02618.x

Possoz, C., Ribard, C., Gagnat, J., Pernodet, J.-L., & Guérineau, M. (2008). The integrative element pSAM2 from *Streptomyces*: Kinetics and mode of conjugal transfer: pSAM2 transfer in *Streptomyces*. Molecular Microbiology, 42(1), 159–166. https://doi.org/10.1046/j.1365-2958.2001.02618.x

Quinn, G. A., Banat, A. M., Abdelhameed, A. M., & Banat, I. M. (2020). *Streptomyces* from traditional medicine: Sources of new innovations in antibiotic discovery. Journal of Medical Microbiology, 69(8), 1040–1048. https://doi.org/10.1099/jmm.0.001232

Reuther, J., Wohlleben, W., & Muth, G. (2006). Modular architecture of the conjugative plasmid pSVH1 from *Streptomyces venezuelae*. Plasmid, 55(3), 201–209.

Ribeiro da Cunha, B., Fonseca, L. P., & Calado, C. R. C. (2019). Antibiotic Discovery: Where Have We Come from, Where Do We Go? Antibiotics (Basel, Switzerland), 8(2), 45. https://doi.org/10.3390/antibiotics8020045

Rigby, P. W., Dieckmann, M., Rhodes, C., & Berg, P. (1977). Labeling deoxyribonucleic acid to high specific activity in vitro by nick translation with DNA polymerase I. Journal of Molecular Biology, 113(1), 237–251. https://doi.org/10.1016/0022-2836(77)90052-3

Robinett, C. C., Straight, A., Li, G., Willhelm, C., Sudlow, G., Murray, A., & Belmont, A. S. (1996). In vivo localization of DNA sequences and visualization of large-scale

chromatin organization using lac operator/repressor recognition. Journal of Cell Biology, 135(6), 1685–1700. https://doi.org/10.1083/jcb.135.6.1685

Sarmiento-Vizcaíno, A., Espadas, J., Martín, J., Braña, A. F., Reyes, F., García, L. A., & Blanco, G. (2018). Atmospheric Precipitations, Hailstone and Rainwater, as a Novel Source of *Streptomyces* Producing Bioactive Natural Products. Frontiers in Microbiology, 9, 773. https://doi.org/10.3389/fmicb.2018.00773

Sermonti, G., & Spada-Sermonti, I. (1955). Genetic recombination in *Streptomyces*. Nature, 176, 121–121.

Sermonti, G., & Spada-Sermonti, I. (1956). Gene recombination in *Streptomyces coelicolor*. Microbiology, 15(3), 609–616.

Servn-Gonzlez, L., Sampieri III, A., Cabello, J., Galvn, L., Jurez, V., & Castro, C. (1995). Sequence and functional analysis of the *Streptomyces phaeochromogenes* plasmid pJV1 reveals a modular organization of *Streptomyces* plasmids that replicate by rolling circle. Microbiology, 141(10), 2499–2510.

Sherratt, D. (2013). Plasmid partition: Sisters drifting apart. The EMBO Journal, 32(9), 1208–1210. https://doi.org/10.1038/emboj.2013.84

Sherratt, D. J., Arciszewska, L. K., Crozat, E., Graham, J. E., & Grainge, I. (2010). The *Escherichia coli* DNA translocase FtsK. Biochemical Society Transactions, 38(2), 395–398.

Shintani, M., Sanchez, Z. K., & Kimbara, K. (2015). Genomics of microbial plasmids: Classification and identification based on replication and transfer systems and host taxonomy. Frontiers in Microbiology, 6, 242.

Straight, A. F., Belmont, A. S., Robinett, C. C., & Murray, A. W. (1996). GFP tagging of budding yeast chromosomes reveals that protein–protein interactions can mediate sister chromatid cohesion. Current Biology, 6(12), 1599–1608. https://doi.org/10.1016/S0960-9822(02)70783-5

Strohl, W. R. (2004). Microbial diversity and bioprospecting. AT Bull, Ed, 336–355.

Tan, S. C., & Yiap, B. C. (2009). DNA, RNA, and protein extraction: The past and the present. Journal of Biomedicine & Biotechnology, 2009, 574398. https://doi.org/10.1155/2009/574398

Tanenbaum, M. E., Gilbert, L. A., Qi, L. S., Weissman, J. S., & Vale, R. D. (2014). A Protein-Tagging System for Signal Amplification in Gene Expression and Fluorescence Imaging. Cell, 159(3), 635–646. https://doi.org/10.1016/j.cell.2014.09.039

Thoma, L., Dobrowinski, H., Finger, C., Guezguez, J., Linke, D., Sepulveda, E., & Muth, G. (2015). A Multiprotein DNA Translocation Complex Directs Intramycelial Plasmid Spreading during *Streptomyces* Conjugation. mBio, 6(3), e02559-14. https://doi.org/10.1128/mBio.02559-14

Thoma, L., & Muth, G. (2012). Conjugative DNA transfer in *Streptomyces* by TraB: Is one protein enough? FEMS Microbiology Letters, 337(2), 81–88. https://doi.org/10.1111/1574-6968.12031

Thoma, L., & Muth, G. (2015). The conjugative DNA-transfer apparatus of *Streptomyces*. International Journal of Medical Microbiology: IJMM, 305(2), 224–229. https://doi.org/10.1016/j.ijmm.2014.12.020

Thoma, L., & Muth, G. (2016). Conjugative DNA-transfer in *Streptomyces*, a mycelial organism. Plasmid, 87–88, 1–9. https://doi.org/10.1016/j.plasmid.2016.09.004

Thoma, L., Vollmer, B., & Muth, G. (2016). Fluorescence microscopy of *Streptomyces* conjugation suggests DNA-transfer at the lateral walls and reveals the spreading of the plasmid in the recipient mycelium. Environmental Microbiology, 18(2), 598–608. https://doi.org/10.1111/1462-2920.13027

Thoma, L., Vollmer, B., Oesterhelt, F., & Muth, G. (2019). Live-cell imaging of *Streptomyces* conjugation. International Journal of Medical Microbiology, 309(5), 338–343. https://doi.org/10.1016/j.ijmm.2019.05.006

Thompson, C. J., Ward, J. M., & Hopwood, D. A. (1980). DNA cloning in *Streptomyces*: Resistance genes from antibiotic-producing species. Nature, 286(5772), 525–527. https://doi.org/10.1038/286525a0

Tsukamoto, T., Hashiguchi, N., Janicki, S. M., Tumbar, T., Belmont, A. S., & Spector, D. L. (2000). Visualization of gene activity in living cells. Nature Cell Biology, 2(12), Article 12. https://doi.org/10.1038/35046510

Vas, A. C. J., Andrews, C. A., Kirkland Matesky, K., & Clarke, D. J. (2007). In Vivo Analysis of Chromosome Condensation in *Saccharomyces cerevisiae*. Molecular Biology of the Cell, 18(2), 557–568. https://doi.org/10.1091/mbc.E06-05-0454

Viushkov, V. S., Lomov, N. A., Rubtsov, M. A., & Vassetzky, Y. S. (2022). Visualizing the Genome: Experimental Approaches for Live-Cell Chromatin Imaging. Cells, 11(24), 4086. https://doi.org/10.3390/cells11244086

Vögtli, M., & Cohen, S. N. (1992). The chromosomal integration site for the *Streptomyces* plasmid SLP1 is a functional tRNATyr gene essential for cell viability. Molecular Microbiology, 6(20), 3041–3050. https://doi.org/10.1111/j.1365-2958.1992.tb01762.x

Waksman, S. A., Schatz, A., & Reynolds, D. M. (2010). Production of antibiotic substances by actinomycetes. Annals of the New York Academy of Sciences, 1213, 112–124. https://doi.org/10.1111/j.1749-6632.2010.05861.x

Washington, J. A., & Wilson, W. R. (1985). Erythromycin: A microbial and clinical perspective after 30 years of clinical use (2). Mayo Clinic Proceedings, 60(4), 271–278. https://doi.org/10.1016/s0025-6196(12)60322-x

Watt, M., Duzeski, J. L., Loomis, A., Machnik, K., Noble, M., Sebestyén, M. G., & Hagstrom, J. (2002). Intracellular Localization and Expression of Labeled Plasmid DNA using Label IT Tracker TM Nucleic Acid Labeling Kits. https://www.semanticscholar.org/paper/Intracellular-Localization-and-Expression-of-DNA-IT-Watt-Duzeski/44310cc39ebbe2e36ba775856ccca6a0353722f5

Watt, V. M. A., Duzeski, J., Loomis, A., Machnik, K., Noble, M., Sebestyen, M., & Hagstrom, J. (2002). Intracellular localization and expression of labeled plasmid DNA using label IT Trackere nucleic acid labeling kits. Mirus Technical Report.

Wegrzyn, K., Witosinska, M., Schweiger, P., Bury, K., Jenal, U., & Konieczny, I. (2013). RK2 plasmid dynamics in *Caulobacter crescentus* cells – two modes of DNA replication initiation. Microbiology, 159(Pt_6), 1010–1022. https://doi.org/10.1099/mic.0.065490-0

Wezel, G. P. van, & McDowall, K. J. (2011). The regulation of the secondary metabolism of *Streptomyces*: New links and experimental advances. Natural Product Reports, 28(7), 1311–1333. https://doi.org/10.1039/C1NP00003A

Wolánski, M., Wali, R., Tilley, E., Jakimowicz, D., Zakrzewska-Czerwińska, J., & Herron, P. (2011). Replisome Trafficking in Growing Vegetative Hyphae of *Streptomyces coelicolor* A3(2). Journal of Bacteriology, 193(5), 1273–1275. https://doi.org/10.1128/jb.01326-10

Woodruff, H. B. (2014). Selman A. Waksman, Winner of the 1952 Nobel Prize for Physiology or Medicine. Applied and Environmental Microbiology, 80(1), 2–8. https://doi.org/10.1128/AEM.01143-13

Wu, L. J., Lewis, P. J., Allmansberger, R., Hauser, P. M., & Errington, J. (1995). A conjugation-like mechanism for prespore chromosome partitioning during sporulation in *Bacillus subtilis*. Genes & Development, 9(11), 1316–1326.

Yang, M. C., & Losick, R. (2001). Cytological evidence for association of the ends of the linear chromosome in *Streptomyces coelicolor*. Journal of Bacteriology, 183(17), 5180–5186. https://doi.org/10.1128/JB.183.17.5180-5186.2001

Youngman, P., Moran, C., & Piggot, P. (1993). Regulation of bacterial differentiation. American Society for Microbiology

6.0 Appendix

6.1 Abbreviations

°C	**degree Celsius**
µm	micrometer
aa	amino acid(s)
AHT	anhydrotetracycline
Apra	apramycin
ATPase	Adenosinetriphosphatase
bp	base pair
clt	cis acting locus of transfer
D	aspartic acid
DNA	deoxyribonucleic acid
ds	double-stranded
dso	double-stranded origin
E. coli	*Escherichia coli*
e.g.	for example
eGFP	enhanced green fluorescent protein
et al.	and others
FISH	Fluorescence in situ hybridization
FROS	Fluorescent repressor operator system
h	hour(s)
HGT	horizontal gene transfer
ICE	integrative and conjugative elements
Kan	kanamycin
kb	kilobase
min	minutes
ml	Milliliter(s)
ms	millisecond(s)
ORF	open reading frame
oriT	origin of transfer
PCR	polymerase chain reaction

PEG	Polyethylene glycol
Rep	replication protein
S.	*Streptomyces*
Spd	Spread protein
ss	single-stranded
T4SS	type IV secretion system
Thio	thiostrepton
TRS	TraB recognition sequence
T-strand	transferred strand
ϕBT1	ϕBT1 phage

6.2 Supplementary data

Figure 6.1: A steel rod-shaped homogenizer for *Streptomyces* mycelium homogenization. It is designed for efficient disruption and mixing, is shown inserted into the Eppendorf tube containing the mycelium sample. Through controlled pressure and swirling motions, the homogenizer aids in breaking down the mycelium, ensuring thorough homogenization.

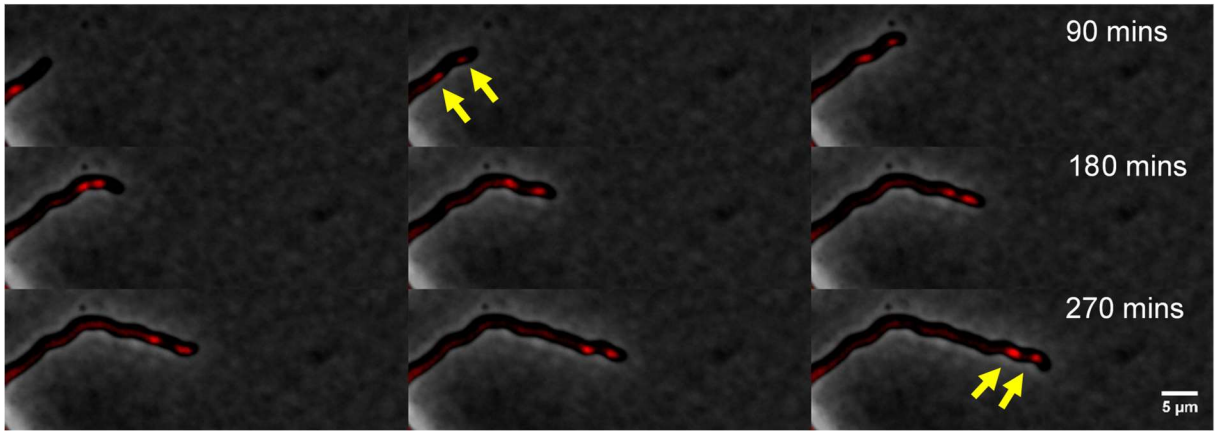

Figure 6.2: Displays a time lapse sequence capturing the movement of the SCP2tetO plasmid within the extending tip of *S. lividans* hyphae. The red spots indicates the presence of the plasmid in the JT46::ptetRmcherry strain, tracking the tip's movement. Each sequential series depicts a 30-minute timeframe, highlighting how the plasmid consistently follows the tip during the elongation of the hyphae.

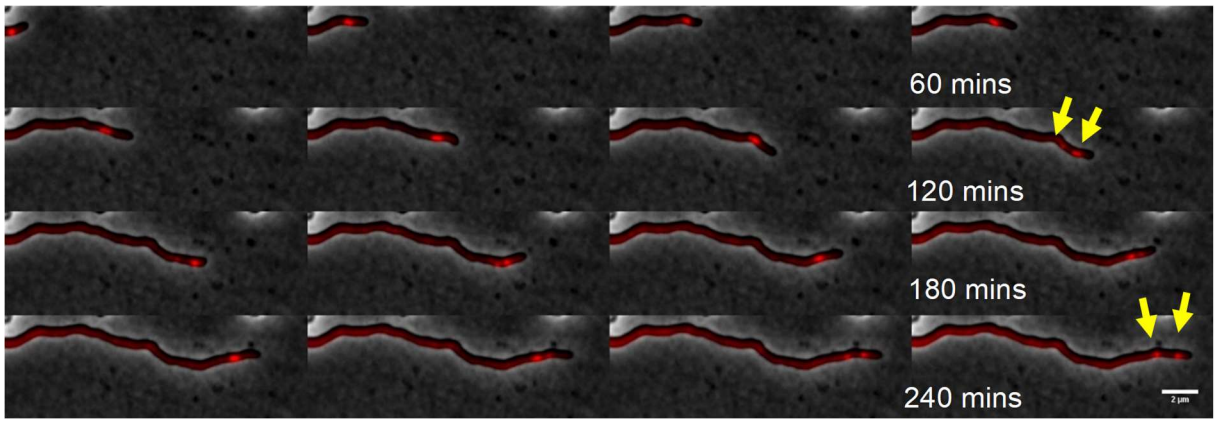

Figure 6.3: Time lapse imaging of plasmid migration in extending *S. lividans* hyphae. Notably, the red spots representing the plasmid SCP2tetO in the JT46::ptetRmcherry strain follow the elongating tip. At 15-minute intervals, the images capture the plasmid seemingly splitting into two entities after 2 hours, which could indicate a replication event, while continuing to follow the elongation of the tip.

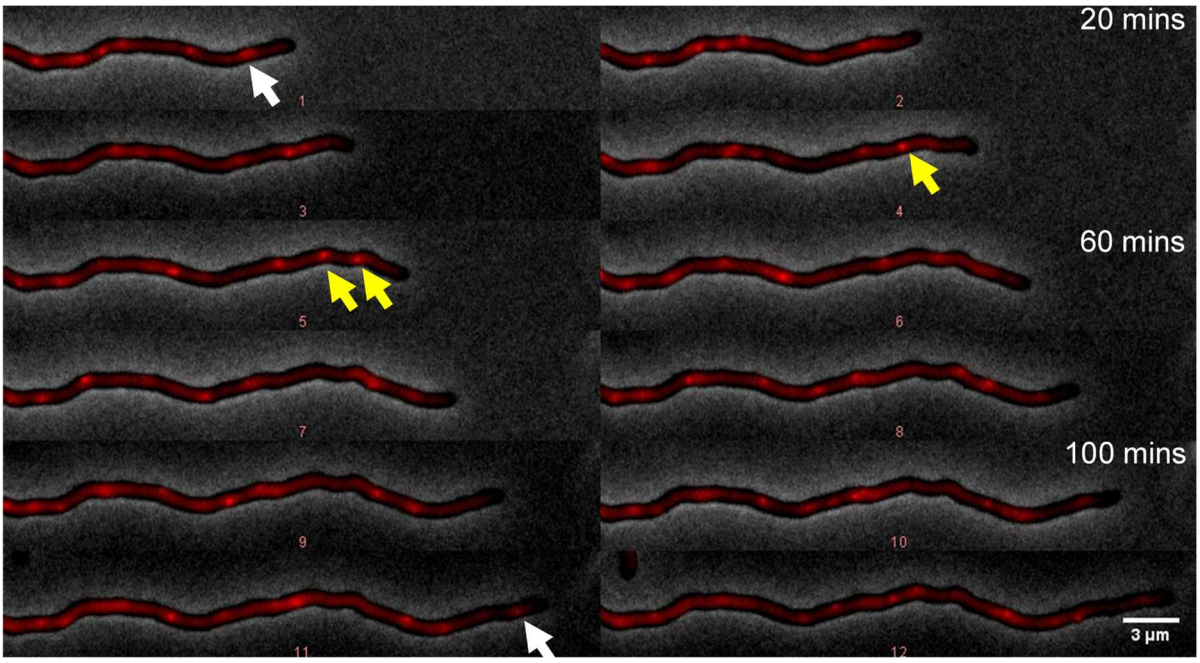

Figure 6.4: Visualizing chromosome localization in extending *S. lividans* JT46::tetRmcherry hyphae. The localization of chromosome copies (integrated pIJ12507tetO) is visualized by FROS in the time-lapse image, wherein an overlay of the phase contrast image with the red channel image, highlights the chromosomes as red spots within the mycelium. During hyphal elongation, the spot moves with the tip (marked by a white arrow). The imaging was conducted at intervals of 10 minutes. Notably, at the 40-minute mark, a chromosome exhibited signs of replication, leading to the emergence of two fluorescence spots in the subsequent image at 50 minutes (as denoted by yellow arrows).

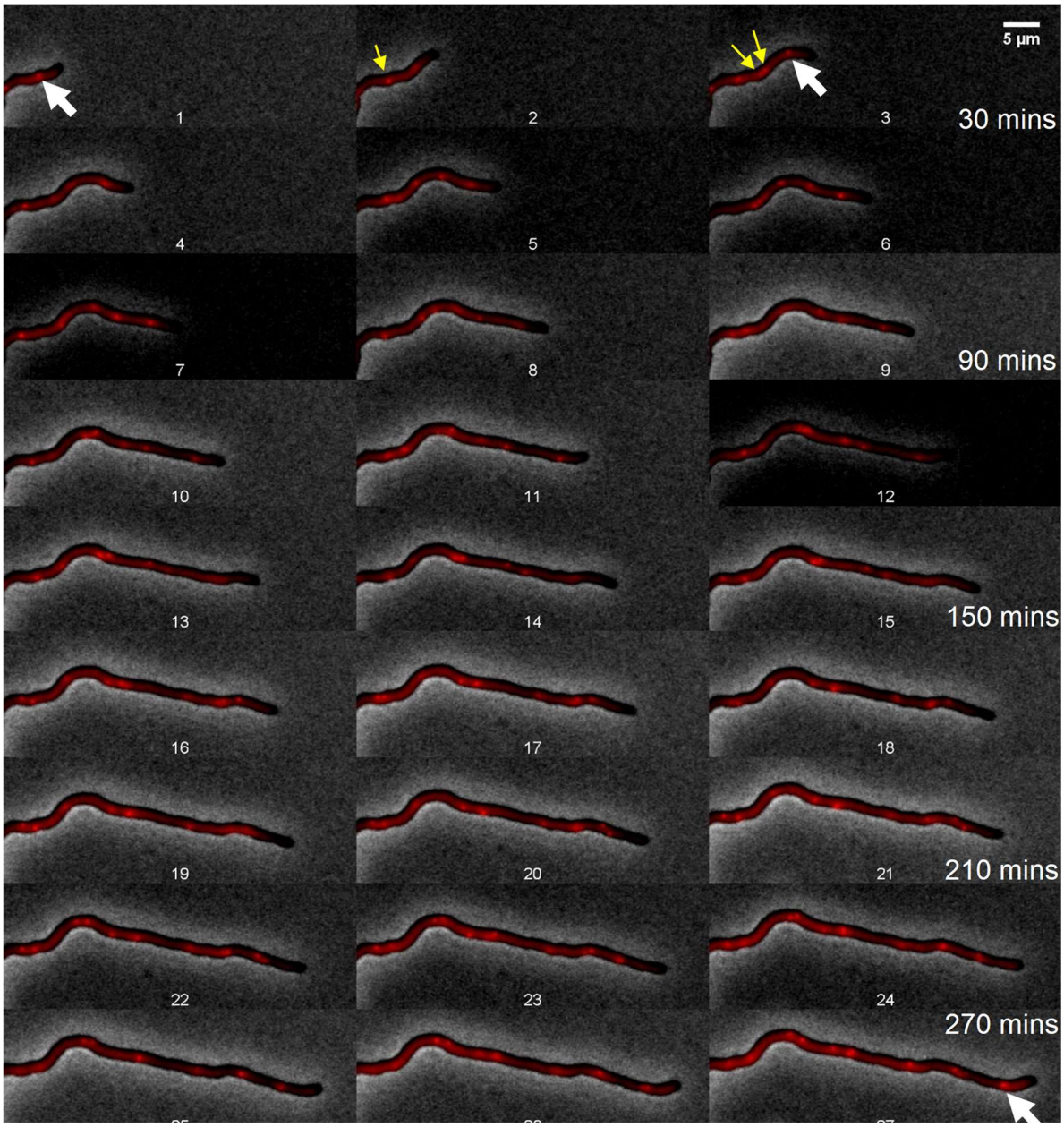

Figure 6.5: Visualizing chromosome localization in extending hyphae of *S. lividans* JT46::tetRmcherry strain using fluorescence imaging . The chromosome localization is visualized in the time-lapse image under the fluorescence microscope, with the chromosome appearing as a red spot in the living mycelium. As the hyphae elongate, the spot moves to the tip compartment (marked as white arrows). The images were taken at 10-minute intervals, and following a 30-minute period, the chromosome is either replicated or segregated, resulting in the appearance of two visible spots (indicated by yellow arrows).

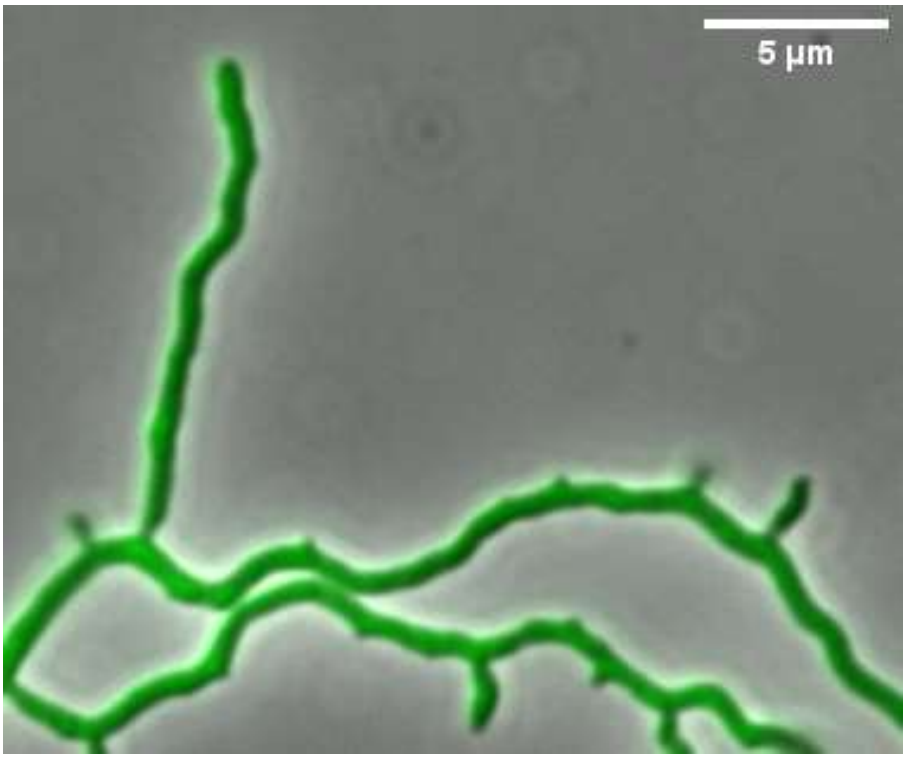

Figure 6.6: Microscopic image of strain JT46::ptetRmcherry::eGFP (pGM190); named as recipient. An overlay image of the phase contrast image with the green fluorescence channel image.

6.3 Table:

6.4 Figure:

7. Acknowledgement

First and foremost, I am extremely grateful to my supervisor, Dr. rer. nat. Günther Muth for his valuable advice, continuous support, and patience during my PhD study. His immense knowledge and plentiful experience on *Streptomyces* and plasmid biology have encouraged me in all the time of my academic research and daily life.

I would like to express my thanks to my thesis advisors, Prof. Dr. Wolfgang Wohlleben and Prof. Dr. rer. nat. Heike Brötz-Oesterhelt for their advice and technical support on my study.

Special thanks go to Dr. rer. nat. Lina Thoma, Dr. rer. nat. Filipp Oestethelt and Dr. rer. nat. Jan Bornikoel who helped me with the use of the microscope and microscopic data analysis.

Thomas Härtner for his quick and uncomplicated help in dealing with everyday problems in the laboratory. Including, Andreas Kulik, Aysun Engelhard, Janina Lemaire and Pierre Lemaire, who make the work so much easier for all of us.

I would like to thank all the members in 10th floor. It is their kind help and support that have made my study and life in Tübingen a wonderful time. Specially, AG Stegmann and AG Wohlleben group's for organizing social events, seminar and AG Hughes group for nice music. Many thanks to my friend Moushumi Purkayastha for her sincere support.

Finally, I would like to express my gratitude to my parents and my brother for their unconditional support from afar. Very Special thanks to my wife and my son. Without their tremendous understanding and encouragement in the past few years, it would be impossible for me to complete my study.